

**Modified *N*-Acyl Homoserine Lactones for the Evaluation
of Plant-Bacteria Interactions**

**Modifizierte *N*-Acyl Homoserin Lactone zur Evaluierung
der Interaktionen von Pflanzen und Bakterien**

Dissertation zur Erlangung des Doktorgrades

an der Fakultät für Mathematik, Informatik und Naturwissenschaften

Fachbereich Chemie

der Universität Hamburg

vorgelegt von Heike Thomanek

Hamburg, 2014

1. Gutachter: Prof. Wolfgang Maison

2. Gutachter: Prof. Wittko Francke

Tag der Disputation: 05.12.2014

Acknowledgements

I would firstly like to thank my supervisor Prof. Dr. Wolfgang Maison for providing me with such an interesting and exciting project and for giving me the support, encouragement and freedom to make it my own. I have gained a lot of invaluable knowledge from him over the last past years and it has been a pleasure working in his group.

I would also like to say huge thank you to Dr. Adam Schikora and his colleagues Sebastian Schenk and Elke Stein at the University of Gießen for their collaboration on this topic. Adam, thank you for your assistance, guidance and continued support throughout this PhD. A big thank you goes to Elke Stein for testing the biological activities of the AHLs in the lab.

A huge thank you goes to all the support staff at the Universities of Gießen and Hamburg for their help with NMR, MS and additional analytical data. I would like to thank Andreas Hensel for measuring the TEM images and all the students who have worked for me in the lab.

Franziska, thank you for sharing the good and the bad times in front of the IR, TGA and BET and for your patience in all things especially nanoparticles.

Thanks to Moritz and Daniel who helped me with their in depth knowledge of Word and computers in general.

I would like to thank Kay, Julie, Isabel, Elisa, Dorith and Faiza for your patience in proof reading and all the helpful suggestions. Kay and Julie, you put so much time and effort into this thesis and enhanced the “britishness” of my English. Thank you so much!

Thank you Elisa, Christian and Kay for being the great friends you are. A big thank you goes to Dorith and Faiza. It was so much fun working in the lab with you!

A final thank you goes to my parents with their eternal support and encouragement and to my fiancé Carsten for sharing good times and bad, for keeping me smiling and making me very happy.

Content

Abstract	6
1 Introduction.....	7
1.1 Quorum Sensing	7
1.2 QS in Gram-negative bacteria	9
1.2.1 QS in <i>V. fischeri</i>	9
1.2.2 <i>N</i> -acyl-L-homoserine lactones	12
1.2.3 Biosynthesis	13
1.3 Quorum Sensing and plants	15
1.3.1 Rhizosphere	16
1.3.2 Plant pathogenic bacteria	16
1.3.3 Plant growth promoting rhizobia (PGPR).....	17
1.4 Quorum Quenching	19
2 Recent experimental studies.....	21
2.1 Interaction of LuxR-type proteins with AHLs	21
2.2 Designed AHL mimics	23
2.3 Effects of native and non-natural AHLs on plants	28
3 Aims and Objectives	31
4 Results and discussion	34
4.1 Preparation of synthetic <i>N</i> -acyl-L-HSLs.....	34
4.2 Synthesis of acyl-chain modified AHLs.....	35
4.3 Synthesis of lactone ring modified <i>N</i> -acyl-L-homoserine lactones	39
4.4 Synthesis of a bifunctional AHL mimic	43
4.5 Synthesis of AHLs for surface applications	54
4.6 Biological evaluation.....	66
4.7 Immobilisation of catechol-AHL derivatives on TiO ₂ nanoparticles.....	73
4.7.1 The catechol-TiO ₂ System	73
4.7.2 Immobilisation of AHL derivative 39 on TiO ₂ (P25) nanoparticles.....	76
4.7.3 Analytics.....	80
5 Summary	86

6	Zusammenfassung.....	88
7	Outlook	90
8	Experimental	92
8.1	Material and Methods	92
8.1.1	Analytics.....	92
8.2	General procedures	94
8.3	Acyl chain modified AHL-derivatives	97
8.4	Lactone ring modified AHL-derivatives	106
8.5	Synthesis of a bifunctional AHL mimic	111
8.6	Catechol derivatives	119
8.7	Phosphonate derivatives	123
8.8	Nanoparticles	127
9	Hazardous Materials	131
10	Curriculum Vitae.....	137
11	Declaration	139
12	Literature	140
13	Appendix	151

List of Abbreviations

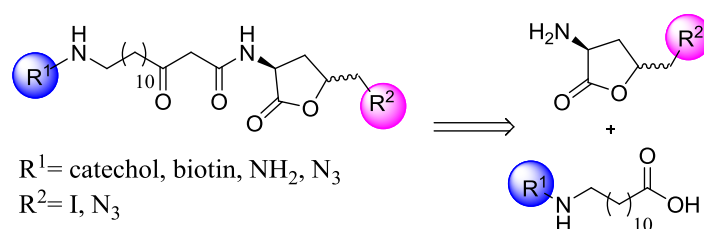
Abb.	Abbildung
ACP	acyl carrier protein
AHL	acyl homoserine lactone
ATR	attenuated total reflection
BET	Brunauer-Emmett-Teller Method
Boc	<i>tert</i> -butoxycarbonyl
Boc ₂ O	di- <i>tert</i> -butyldicarbonate
br	broad
Cbz	benzyloxycarbonyl
COSY	correlated spectroscopy
d	doublet
dd	double doublet
DCC	<i>N,N</i> -dicyclohexylcarbodiimide
DCU	<i>N,N</i> -dicyclohexylurea
DMAP	4-(Dimethylamino)-pyridine
DMF	dimethylformamide
DMSO	dimethylsulfoxide
dt	doublet of a triplet
EDC	<i>N</i> -ethyl- <i>N</i> -(3-dimethylaminopropyl)carbodiimide
ESI	electrospray ionisation
GMP	green fluorescence protein
HMBC	heteronuclear multiple bond coherence
HOBt	hydroxybenzotriazole
HPLC	high performance liquid chromatography
HRMS	high performance liquid chromatography

HSL	homoserine lactone
HSQC	heteronuclear single quantum coherence
IR	infrared
<i>J</i>	coupling constant
LHMDS	lithium bis(trimethylsilyl)amide
m	multiplet
MAP	mussel adhesion protein
Mp	melting point
MS	mass spectrometry
NMR	nuclear magnetic resonance
NOESY	nuclear overhauser effect spectroscopy
NHS-OH	<i>N</i> -hydroxysuccinimide
NP	nanoparticle
PGPR	plant growth promoting rhizobia
ppm	parts per million
q	quartet
QQ	Quorum Quenching
QS	Quorum Sensing
<i>R_f</i>	retention factor
RT	room temperature
s	singulet
SAM	<i>S</i> -adenosyl methionine
SAR	systemic acquired resistance
t	triplet
TEM	transmission electron microscopy

TFA	trifluoroacetic acid
TGA	thermo gravimetric analysis
THF	tetrahydrofuran
TLC	thin liquid chromatography
XRD	X-ray diffraction

Abstract

Bacteria produce signal molecules, also known as autoinducers, of low molecular weight to retrieve information on their local population densities in order to control and coordinate their behaviour. Gram-negative bacteria use *N*-acyl homoserine lactones (AHLs) as signal molecules in a complex cell-to-cell communication process also termed Quorum Sensing (QS). QS plays a key role in both bacterial virulence towards the host and symbiotic interactions with other organisms. This thesis focuses on AHLs of plant associated bacteria and their biological relevance for potential plants. Recent studies have shown that bacteria do not only use AHLs for their communication process but that plants are also able to detect bacterial autoinducers. Moreover they respond to these signal molecules with alterations in gene expression or modification in development, which can be beneficial for the plant. However, the underlying molecular pathways are widely unexplored and plant receptors for AHLs have not been identified so far.



Herein, the synthesis of acyl-chain and lactone-ring modified oxo-C14-AHLs is reported and their biological activity is evaluated in bacteria and plants. It is shown that the new compounds are still recognised by different bacteria and that a novel biotin-tagged AHL derivative interacts with a bacterial AHL receptor. For the isolation, identification and characterisation of new receptors photoaffinity labelling could be the technique of choice. Thus, an AHL mimic containing a photoactive group and a biotin tag was designed which binds irreversibly to the receptor. Biotin used as a tag will allow the isolation of the receptor by affinity chromatography. In addition, several AHLs were prepared containing anchor groups such as catechols and phosphonates for the immobilisation on TiO_2 nanoparticles. These compounds can be utilised for affinity chromatography when the AHL is used as a stationary phase. The coating procedure of the nanoparticles was evaluated and the particles were characterised by different analytical methods.

Keywords: Gram-negative bacteria – Quorum Sensing – AHL – plants – nanoparticles

1 Introduction

For a long time scientists believed that the process of communication between individuals was restricted to higher organisms such as humans or animals. Bacteria on the other hand seemed to be nothing more than blind loners, existing only in a strictly solitary and independent way of life.¹ However, 70 years ago Doudoroff's *et al.* investigations on marine luminous bacteria provided the first evidence of a multicellular bacterial behaviour.² This requires the capability to communicate on a molecular level in order to influence the behaviour of a community of protozoons.^{3,4} Tomasz *et al.*⁵ were the first to describe the cell-to-cell-communication process of Gram-positive bacteria *Streptococcus pneumoniae* while Nealson *et al.* focused on Gram-negative bacteria *Vibrio fischeri* and *Vibrio harveyi*, deciphering the chemical signal molecules necessary for communication.⁶ However, it took another 20 years until these phenomena gained importance, after works on plant and human pathogenic bacteria.⁷⁻⁹ In present days, there are numerous research groups dealing with this topic as the interaction of bacteria with their hosts has often devastating effects on human health and plant crop production,¹⁰⁻¹³ making it crucial to fully understand this extraordinary cell-to-cell communication process.

1.1 Quorum Sensing

Bacteria produce signal molecules of low molecular weight to retrieve information on their local population densities in order to control and coordinate their behaviour. These signal molecules, also known as autoinducers, play a key role in the complex bacterial cell-to-cell communication process.¹⁴ Fuqua *et al.* were one of the first to describe and investigate bacterial communication and defined it as the cell density dependent alternation of gene expression.⁸ The signalling process also termed "Quorum Sensing" (QS) allows the bacteria to sense and respond to their local population densities guaranteeing a fast adaption to environmental changes. The small, hormone-like autoinducers pass the cell membrane and, once a certain threshold concentration is reached, the signal molecules bind to a cognate receptor to form a complex which induces alternation of gene expression.^{3,15} Over 50 species of Gram-negative bacteria have been shown to use AHLs in their QS signalling system.

QS plays a key role in both bacterial virulence towards the host and symbiotic interactions with other organisms. Examples of QS-regulated behaviours are biofilm production,¹⁶⁻²¹ induction of bioluminescence,^{6,22} antibiotic production and virulence factor expression.²³ Figure 1 lists some examples of QS signalling systems, the QS phenotype and the effects on the hosts by different bacterial strains.

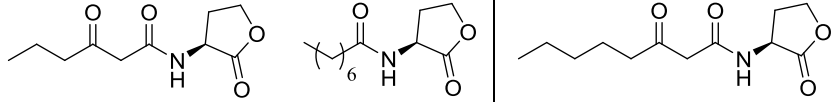
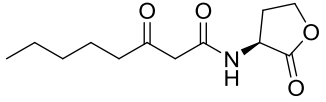
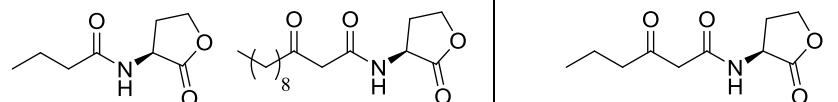
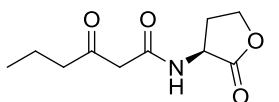
AHL		
bacterium	<i>Vibrio fischeri</i>	<i>Agrobacterium tumefaciens</i>
QS system	LuxI/R	AinS/R
QS phenotype	symbiont	plasmid conjugation
effects on hosts	luminescent bacterium	crown gall tumor
AHL		
bacterium	<i>Pseudomonas aeruginosa</i>	<i>Erwinia carotovora</i>
QS system	RhII/R	LasI/R QscR
QS phenotype	exoenzymes, biofilms	virulence, exoenzymes
effects on hosts	opportunistic pathogen (causes infections)	plant pathogen

Figure 1: Selected examples of different QS signalling systems.²⁴

QS systems can be divided into three classes based on the type of autoinducer and the enzyme used for its detection. Autoinducers either diffuse or are actively transported through the cell membrane.²⁵⁻²⁷ The first class describes Gram-positive bacteria which typically use modified oligopeptides as autoinducers (Figure 2). These signal molecules often contain side-chain modifications such as isoprenyl groups (*Bacillus subtilis*) or thio-lactone rings (*Staphylococcus* spp.).^{28,29} Two-component signal transduction proteins (sensor histidine kinases) detect the extracellular oligopeptides and transfer sensory information by phosphorylation of a response regulator protein. Modification of the response regulator protein alters its DNA binding activity and thus enables control over the transcription of QS-regulated genes.³⁰

The second class of quorum-sensing systems can be found in Gram-negative bacteria which use *N*-acylated-L-homoserine lactones (AHLs) as signal molecules synthesised and modified by the LuxI/R QS system. The LuxI/R system has been identified in over 70 species of Gram-negative bacteria (the detailed mechanism and biosynthesis of AHLs will be explained in chapter 1.2.3).^{10,22,24,31-33} The third QS system describes a combination of the Gram-positive and Gram-negative systems. This hybrid system was first investigated in the bioluminescent marine bacterium *Vibrio harveyi*, which produces and detects two signal molecules AI-1 and AI-2.^{34,35} AI-1 is an AHL **2**, while AI-2 is a borate diester which bears no resemblance to other autoinducers.^{36,37} The alternation of target genes is carried out by a two-component phosphorylation cascade similar to the one in Gram-positive systems.³⁸

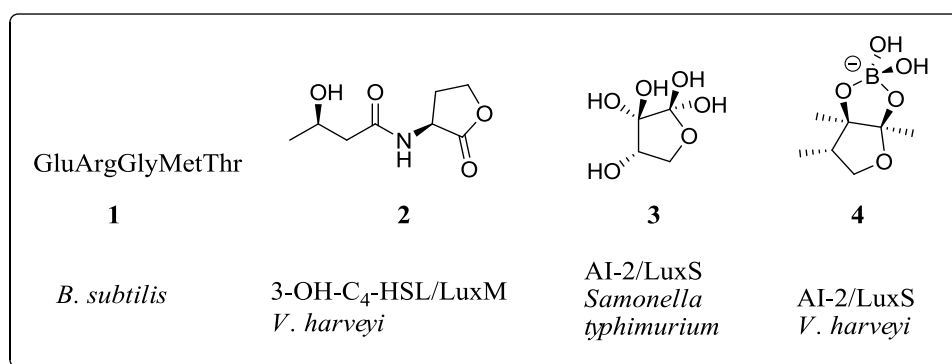


Figure 2: Selected examples for the Gram-positive system **1** and the hybrid system **2 - 4**.²⁷

1.2 QS in Gram-negative bacteria

1.2.1 QS in *V. fischeri*

The process of QS has been best described and investigated in Gram-negative bacteria. It was first discovered in the luminous marine bacterium *Photobacterium fischeri* (*Vibrio fischeri*).³⁹ These bacteria are symbionts of marine fishes and squids but are also capable of a free-living lifestyle at low densities (up to a few hundred cells per mL).¹² Albeit, bioluminescence is only exhibited by *Vibrio fischeri* when the bacterium is living in the symbiotic mode and has reached a high population density (10^{10} - 10^{11} cells/mL). The production of bioluminescence helps the squids or fishes to escape predators while the bacteria gain nutrients from the host.⁴⁰

Based on this information it was hypothesized that these bacteria needed some kind of molecular messenger that was able to enter target cells and to activate the expression of the genes responsible for bioluminescence. Later on the molecular messenger was identified to be a *N*-acyl-L-homoserine lactone.^{6,41}

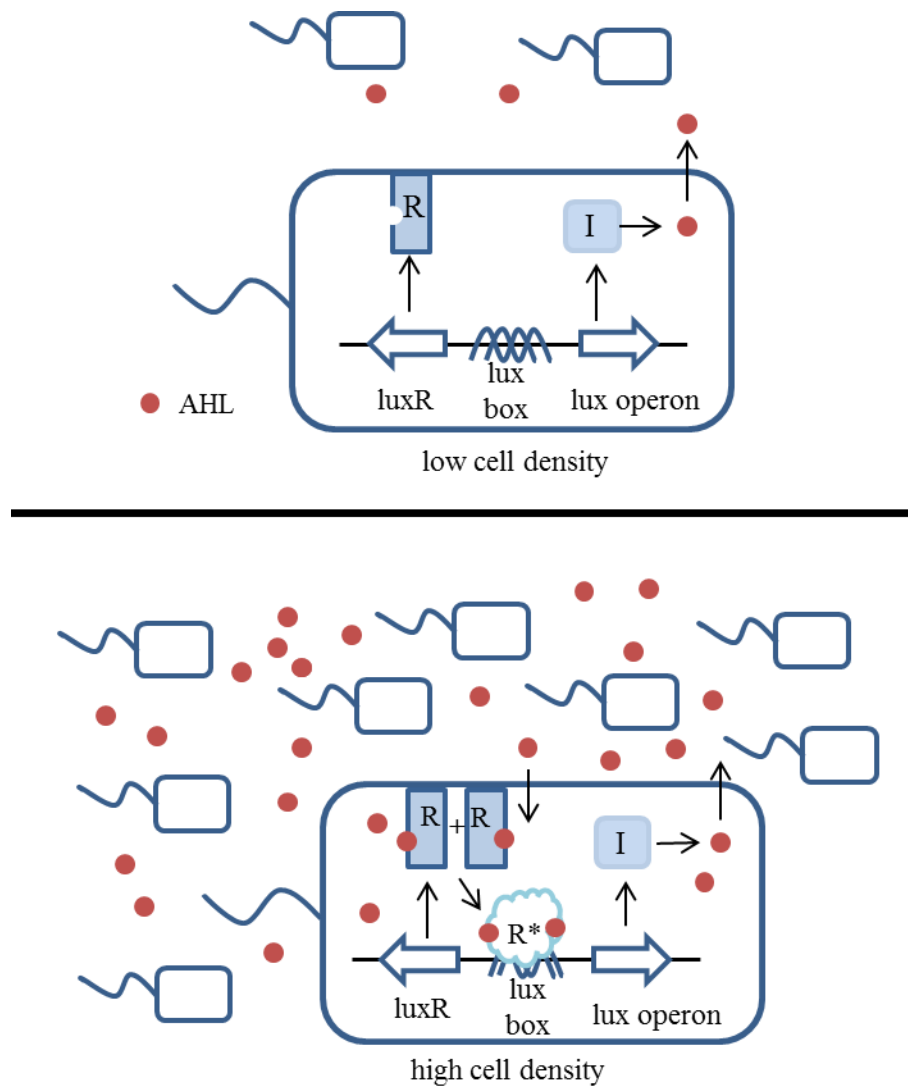


Figure 3: QS in *V. fischeri*. R= LuxR-type protein; I= LuxI synthase; R*= homodimerized LuxR complex; lux operon= *luxICDABEG*⁴²

Therefore, its QS system allows the bacteria to distinguish between low and high population density environments.

In case of a low bacterial population (seawater environment) only a low concentration of the ligand is produced, which is not sufficient to activate the transcription of genes by the operon “*luxICDABEG*” as the bacteria is not able to accumulate.⁴³⁻⁴⁵ The term “*luxI*” at the beginning of the operon “*luxICDABEG*” codes the enzyme “LuxI”, which is the synthase producing AHLs. Taking into account the lack of nutrients in seawater, the bacterium does not expend energy on unnecessary light production. However, this looks different when *V. fischeri* accumulates in the light organ of the squid causing high cell densities.¹²

As stated above AHL ligands are produced by a synthase called “LuxI” and sensed by its cognate receptor (LuxR-type protein). LuxR is a transcriptional activator that is not a transmembrane protein but resides in the cytoplasm.^{46,47} Proteins of the LuxR family can be divided into two functional domains, an amino-terminal and a carboxylic-terminal domain.⁴⁸⁻⁵⁰ The signal molecules can either diffuse freely through cell membranes or are transported by membrane efflux pumps.⁵¹⁻⁵⁴ Especially AHLs with a long, hydrophobic acyl chain need these pump systems to pass the membrane. At high bacterial cell densities the production of AHLs increases until a certain intracellular threshold concentration of the autoinducer is reached.⁵⁵ Subsequently, the AHL binds to the LuxR receptor (through the amino-terminal domain which contains an acyl-HSL-binding region)^{56,57}, which homodimerizes in the next step. Thereafter, the AHL-LuxR-complex binds to the adjacent QS promoter (*i.e.* short palindromic sequence), which is also called “lux box”. In the next step the “*lux* operon” (encodes the genes: *luxICDABEG*) is activated by the “lux box”. The C-terminal domain of the LuxR protein contains a helix-turn-helix motif which is required for DNA binding at the “lux box”. The “*lux* operon” is not only responsible for the transcription of target genes required for bacterial group behaviour but also for coding the LuxI-genes. Therefore, an increased transcription of bioluminescence genes leads to an increased autoinducer production.^{24,46}

Many proteobacteria have homologues of LuxI and LuxR but they regulate different target genes with their AHL autoinducers.^{17,58} In addition, the nomenclature of the synthase and receptor proteins differs from one bacterial species to the other, respectively. One of the most investigated bacterial species is *Pseudomonas aeruginosa*, an opportunistic human pathogen.^{59,60} It causes *i.a.* chronic biofilm infections in the lungs of people suffering from the genetic disease cystic fibrosis.^{9,61}

This bacterium uses two QS systems LasR/LasI and RhlR/RhlI, which are part of the LuxR/LuxI family. Both systems produce two different AHLs, 3-oxo-C12-HSL (Las-system) and C4-HSL (Rhl-system). The Las-system is required for the induction of the Rhl-system and regulates *i.e.* the virulence factor elastase. Mutations of either system reduce the virulence of *P. aeruginosa*.^{62,63}

1.2.2 N-acyl-L-homoserine lactones

To date, a wide range of bacterial autoinducers has been isolated and investigated. The AHL family is the most intensely studied group of QS signal molecules. AHLs are composed of a fatty acid chain ligated to a lactonised homoserine through an amide bond at the α -position (Figure 4).⁶⁴ Generally, the β - and γ -position are unsubstituted.^{45,65,66} The acyl-chain might have various lengths (4C – 18C), saturation levels and/or oxidation states depending on the bacteria producing the AHL.⁶⁷ In most cases the acyl chain consists of an even number of carbons. AHLs with 4 to 8 carbon atoms are called “short-chain AHLs”, while AHLs with a chain of 9 to 18 carbon atoms are classified as “long-chain AHLs”.¹² Additionally, AHLs can be degraded under basic conditions or by degradation enzymes (see chapter 1.4).^{68,69}

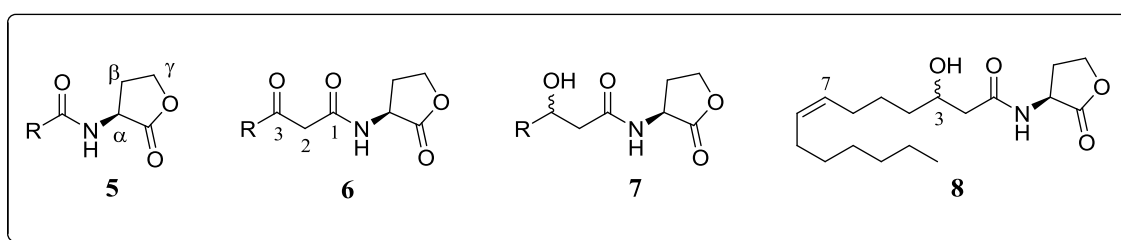


Figure 4: Selected examples of possible AHL modifications.³²

Figure 4 shows some examples of different AHLs identified in Gram-negative bacteria. Substitutions at the C3-position include oxo- or hydroxyl-groups. The third carbon in the acyl chain might also be fully reduced. In addition, some molecules have a double bond at the C7-position with Z stereochemistry in a chain of 14 carbon atoms.^{70,71} The stereochemistry of the α -centre of the homoserine lactone moiety was first investigated for the *Vibrio fischeri* autoinducer *N*-(3-oxo-hexanosyl) homoserine lactone and found to be L.

General analyses have shown that all natural AHLs have the same configuration. Some D-isomers have been synthesised, but they do not show biological activity.^{7,72} Even though AHLs represent the main class of Gram-negative signal molecules some bacteria (*i.e.* *Pseudomonas aeruginosa*, *Pseudomonas putida* WCS 358) were found to produce yet another class of diffusible autoinducers.⁷³ Several examples are shown in Figure 5.

Diketopiperazines like compound **10** have been isolated from different Gram-negative bacteria and their interaction in AHL-dependent QS has been demonstrated.^{73,74} The opportunistic human pathogen *P. aeruginosa* produces PQS **9** next to AHLs, which takes part in the bacterial communication process and plays an important role in regulating virulence gene expression.⁷⁵ Bradyoxetin **10** is produced by *Bradyrhizobium japonicum* to regulate the *nod* genes in a population density dependent fashion. This Gram-negative bacterium is a nitrogen-fixing symbiont of many leguminous plants.⁷⁶⁻⁷⁸

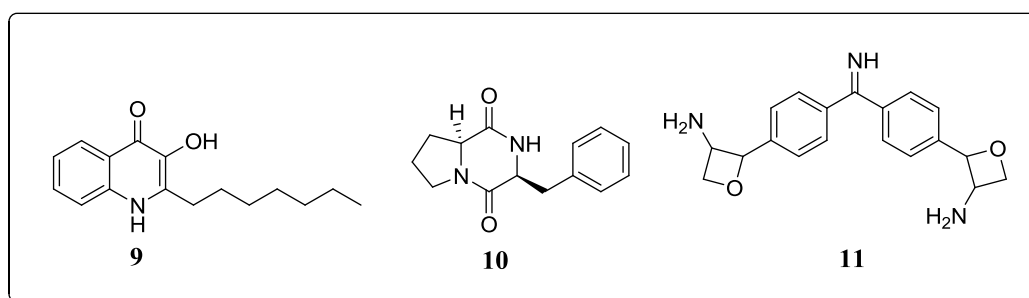


Figure 5: The autoinducers PQS **9**, diketopiperazine **10** and Bradyoxetin **11**. The stereochemistry of Bradyoxetin **11** is still unknown.

1.2.3 Biosynthesis

The production of natural AHLs is catalysed by members of the LuxI family of proteins.⁷⁹ In 1996 Winans *et al.*⁸⁰ and Greenberg *et al.*⁴⁸ showed independently that the acyl moiety of the AHL molecule is derived from fatty acid precursors conjugated to the acyl-carrier-protein (acyl-ACP). Both research groups also demonstrated, by an incubation experiment with the purified synthase, that the homoserine lactone functionality is obtained from *S*-adenosylmethionine (SAM).⁸¹ The genes for AHL synthases from other bacteria are homologous to LuxI.

That suggests that the mechanism for all LuxI homologues is similar.^{82,83} Figure 6 shows the general features of the AHL biosynthesis.

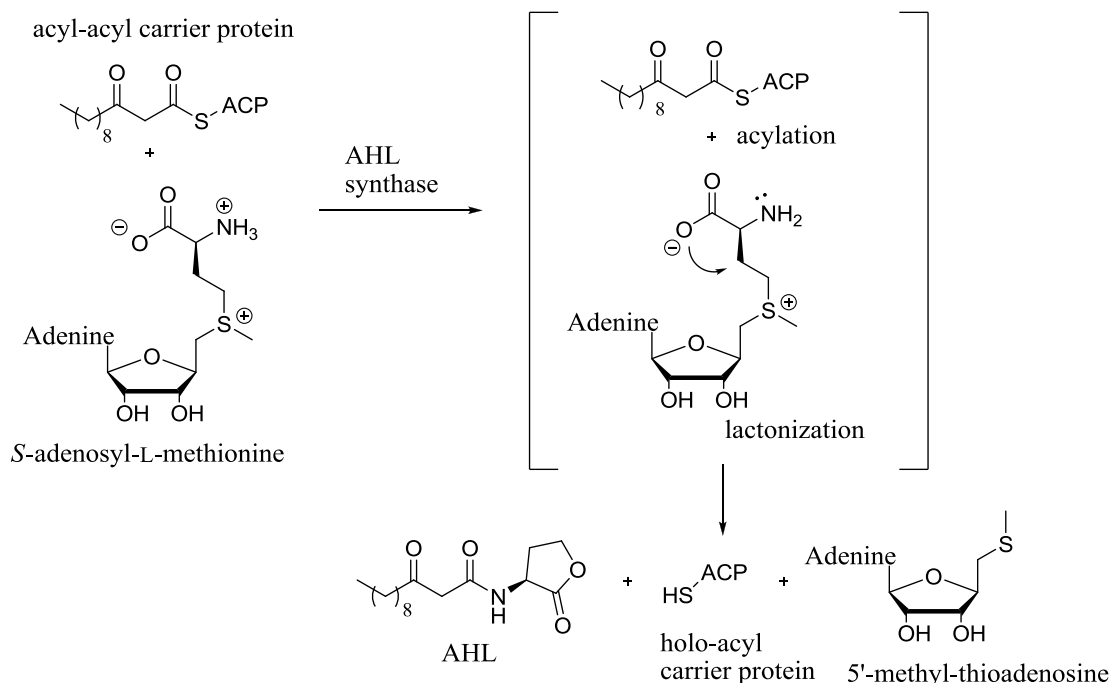


Figure 6: General mechanism of the biosynthesis of AHLs.³

SAM and acyl-ACP bind to the AHL synthase, which is followed subsequently by acylation and lactonization reactions. The signal molecule is then released along with the side products holo-acyl carrier protein and 5'-methylthioadenosine.^{48,81}

SAM is often the source for the supply of acyl groups in different biological pathways. However, the production of AHLs with SAM as a key component is a completely new application of this molecule which bears no resemblance to other SAM dependent reactions.^{40,84} In addition, the AHL synthases share no similarity to other SAM dependent enzymes and might therefore be an interesting target for QS inhibition.⁸⁴ The LuxI-type synthases do not only have the task to recognise SAM but must also be able to specifically identify acyl-ACPs of different chain lengths and reduction states. The specificity of the AHL synthase to a particular chain length varies depending on the bacterial strain.⁸⁵

The amino-terminus of the LuxI-type proteins consists of ten very important amino acid residues. Mutational studies have shown that the residues direct the general aspects of the reaction (*i.e.* recognizing and binding SAM and acyl-ACP) and that seven of them carry charged side chains which are essential to the reaction.^{48,86} The residues of the carboxylic terminus provide the specificity for the appropriate acyl-ACP conjugate, *i.a.* threonine (Thr143) in LuxI which binds specifically to 3-oxo-ACP.⁸⁵ Finally, various AHL types can be produced by the same bacteria. Bacterial strains usually have more than one synthase with each protein being able to synthesise a limited range of signal molecules.^{81,85}

1.3 Quorum Sensing and plants

Bacterial pathogens comprise a large group of species capable of infecting humans, animals and plants alike.⁸⁷ The interactions between bacteria and hosts that determine resistance or susceptibility are not fully understood. Although, there are evolutionary differences between plants and mammals some bacterial strains *i.e.* *Burkholderia cepacia*,⁸⁸ *Pseudomonas aeruginosa*^{88,89} and *Erwinia* spp.^{88,90} are human, animal and plant pathogens. Especially *P. aeruginosa* has been widely investigated as it is one of the most dangerous bacterial pathogens to immunocompromised human patients.⁹¹⁻⁹⁵ Several experiments with microarrays have shown that between 5% and 10% of the *P. aeruginosa* genes are regulated by QS.^{96,97} Different plant pathogenic *Pseudomonas* species have been studied by Dumenyo and contributors. The researchers demonstrated that AHLs were used by the *Pseudomonas* family for the regulation of gene expression and induction of virulence factors.^{98,99} Besides, investigations of this pathogen have stated that they can cause diseases in plants with devastating effects on crop plants.¹² The following chapters of this thesis will focus mainly on the interaction between bacteria and plants - the negative and beneficial effects of the bacterial communication system on the plant.

1.3.1 Rhizosphere

Plants as well as humans and animals are constantly exposed to bacteria. The soil immediately surrounding the roots of a plant is especially rich in microorganisms and called “rhizosphere”.^{100,101} The rhizosphere is divided into two parts, the “endorhizosphere” and the “ectorrhizosphere”. The so called “endorhizosphere” comprises the epidermal layer including root hair, the cortical layer and a mucoid layer of plant as well as bacteria derived polysaccharides.

The “ectorrhizosphere” describes the soil area which expands three millimetres from the root surface. Many microorganisms *i.e.* bacteria use the plants’ exudates as a food source while some metabolites of these microorganisms serve as nutrients for the plant. The development of such a high microbial activity in the root surrounding soil is defined as “rhizosphere effect”.¹⁰² The population density of rhizosphere bacteria surpasses 100 times those densities found in bulk soil.^{103,104} The interaction between rhizosphere bacteria and the plant has a direct effect on the plants’ nutrient supply and their health with either a positive or a negative result. Bacteria inhabiting the rhizosphere use QS and AHLs to communicate and to regulate plant-associated behaviour such as the synthesis of virulence factors, degradation enzymes, regulation of nitrogen fixation genes, plasmid transfer and biofilm production.^{105,106} The plant itself is also able to respond to AHLs inducing either defence or development reactions *i.e.* producing AHL degrading enzymes in the case of a pathogenic bacterium or root hair elongation in the case of a symbiont.⁸⁷

1.3.2 Plant pathogenic bacteria

Gene regulation by AHLs has been extensively studied in plant pathogenic bacteria because of its devastating effects on agriculture.^{66,89} *E. carotovora* causes soft rotting of many vegetable crops including potato, carrot and green pepper. The source of its virulence is the production of a number of exo-enzymes including cellulases and proteases, known for degrading plant cell walls.¹⁰⁷

The plant pathogen *Pantoea ananatis* produces two different AHLs which encode the enzyme that causes rot disease in onions. In 2007 the Ikeda research group was able to inactivate certain genes of the synthase enzyme in order to interrupt the QS process of *P. ananatis*. Biofilm production and infection of the onion leaves was sustainably disrupted.¹⁰⁸ Different *Pseudomonas* species have also been in the centre of attention. Walker *et al.* have shown that pathogenic *Pseudomonas aeruginosa* strains PAO1 and PA14 are capable of infecting the roots of *Arabidopsis thaliana* and sweet basil *in vitro* and in the soil. The strains form a biofilm, which leads to plant mortality seven days after inoculation. When infected with *P. aeruginosa* sweet basil roots produce rosmarinic acid, a compound with antibacterial activity. However, once the biofilm is formed the bacteria are not inhibited by the rosmarinic acid.²¹ *Agrobacterium tumefaciens* is a well investigated standard when it comes to QS and its effect on plants.^{89,109} This bacterium induces the transformation of plant cells by transferring T-DNA from its tumour-inducing plasmid (Ti-plasmid) into the chromosome of a plant cell. This transformation leads to an overproduction of phytohormones by the infected plant cells and to the growth of tumours called “crown galls”. In addition, the transformed DNA (T-DNA) encodes genes that induce the production of opines which serve as nutrients for the pathogen. *A. tumefaciens* is the only bacterium known so far that directs cells to produce nutrients only the colonising bacteria can use.¹¹⁰

1.3.3 Plant growth promoting rhizobia (PGPR)

Besides those negative effects bacteria can have on plants one has to keep in mind that there are also beneficial bacterial species using QS. They belong to the group of “plant growth promoting rhizobia” (PGPR) and are used in agriculture because they induce increased plant growth and plant development.^{98,111-113} Some PGPRs are able to fix nitrogen¹¹⁴ from the atmosphere, can reduce toxic compounds¹¹⁵ and induce plant growth through the production of certain hormones.¹¹⁶⁻¹¹⁸ The suppression of pathogens in the soil by diverse microorganisms without the use of agricultural pesticides is defined by the term “biocontrol”. Microorganisms such as PGPR are able to suppress diseases by plant pathogens and show a certain biocontrol activity. During the last 20 years there have been numerous research groups investigating the mechanisms of biocontrol in order to use microorganisms as plant protective agents instead of toxic chemicals.¹¹⁹

The different mechanisms of biocontrol can be divided into three groups. The first group describes the direct interaction between the rhizosphere bacteria and the pathogen. *Pseudomonas fluorescens* F113 was shown to control the soft rot potato pathogen *E. carotovora* subsp. *atroseptica* by the production of the antibiotic 2,4-diacetylphloroglucinol (DAPG).¹²⁰ Some rhizosphere bacteria can also compete with pathogens for essential nutrients *i.e.* iron.^{121,122}

The second group depicting biocontrol activity characterises the induction of plant defence reactions. Bacterial members of this group increase plant resistance. However, the suppression of the pathogen is executed by the plant itself. One option is the systemic induced resistance (ISR) by the signal molecule salicylic acid which plays an important role in plant defence reactions.¹²³ The *Pseudomonas aeruginosa* 7NSK2 strain induces resistance in barley, tobacco and tomato against *Botrytis cinerea*.¹²⁴⁻¹²⁶ Another possibility is called “induced systemic resistance (ISR)” which is independent from salicylic acid. *P. fluorescens* WCS417r strain induces an increased resistance against fungal and bacterial pathogens.^{123,127}

The third group describes the stimulation of plant growth which can occur by biofertilisation,¹¹⁷ the production of growth hormones (*i.e.* cytokine, auxin)¹²² or by modifications of the ethylene metabolism.¹²⁸ Biofertilisation delineates the supply or availability of nutrients (N₂, P, Fe) to the host plant by microorganisms. Especially bacteria from the family *Rhizobiaecae* are able to bind N₂ from the atmosphere and make it biologically available to the plant. The bacteria *Azospirillum* spp. is not only capable of supplying the plant with N₂ but also produces plant hormones like auxin or cytokine.^{129,130} Another important factor is the ethylene metabolism. Ethylene is a compound that works contrary to auxin. Some rhizosphere bacteria are capable of reducing the ethylene production and therefore stimulate plant growth.^{128,131}

1.4 Quorum Quenching

Not only bacteria can help plants to suppress pathogens, the plants themselves have developed several methods of resistance. The term “Quorum Quenching” describes all processes that interfere with QS and therefore help the host against bacterial infections.^{10,87,93,105} In general there are three potential targets for regulating bacterial communication. The production of the signal molecule could be hindered, the signal molecule itself could be modified to alter its function and the cognate receptor protein could be targeted. Some natural compounds (*i.e.* diketopiperazines, furanones) are able to compete with AHLs for binding to the LuxR-like receptor and might therefore prevent bacterial communication.¹³² One of the first AHL mimics, a halogenated furanone, was found in the marine red alga *Delisea pulchra*. The furanone interferes with the QS system of marine bacterial species by displacing the normal ligand from LuxR and promoting its degradation.^{133,134}

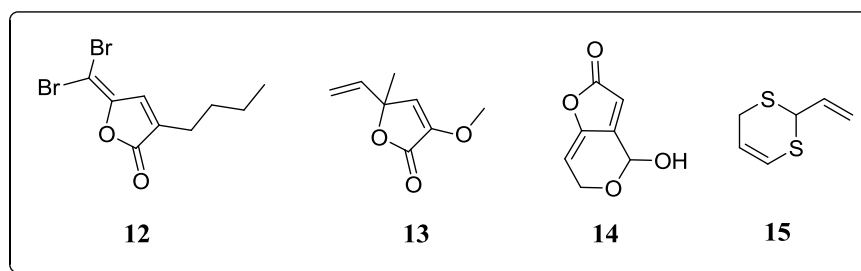


Figure 7: QS inhibitors from natural sources: Furanone **12** from *D. pulchra*, Penicillic acid **13** and Patulin **14** from *Penicillium*, **15** isolated from garlic.¹³²

Diketopiperazines also function as AHLs mimics. It was shown that they act as AHL antagonists in some LuxR based QS systems and as agonists in others.⁷³

To understand how plants react to AHLs one has to have a closer look at the rhizosphere again. In the soil surrounding the roots AHL concentration is affected by hydrolysis of the lactone moiety due to photocatalyzed oxidation or alkaline pH value of the soil as well as adsorption to soil particles and enzymatic degradation by plants and bacteria of a different species.¹³⁵ Under very alkaline pH values the stability of AHLs is reduced to minutes due to lactolysis.¹³⁶

In 2005 Delalande *et al.* have shown in a study with different plants that AHLs are less stable around the roots than in bulk soil and that AHL degradation is temperature-sensitive, plant-specific and AHL-specific. These results suggested that AHLs are degraded by plant roots or root exudates.¹³⁵ Most degrading enzymes that have been identified so far are either AHL-lactonases or AHL-acylases.¹³⁷

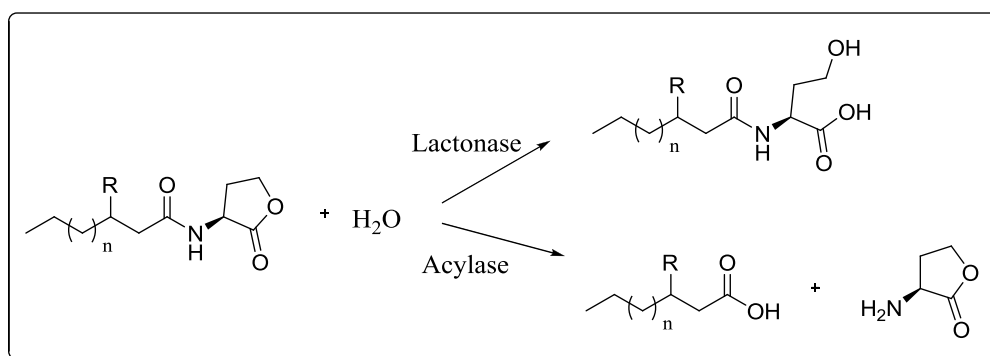


Figure 8: Degradation mechanism of AHL-lactonase and AHL-acylase.

In prokaryotes there have been at least 10 bacterial species identified (*i.e.* *A. tumefaciens*, *Arthrobacter* sp., *P. aeruginosa*) which use QQ enzymes.¹³⁷ Several eukaryotes also possess the ability to degrade autoinducers. Some legumes (*i.e.* clover, lotus, yam beans) were investigated and clearly showed degrading capabilities. The enzymes involved were identified as lactonases.^{135,138}

2 Recent experimental studies

Although the QS system has been intensely studied over the past decades there are still parts of the mechanism which are not fully understood. Identification of plant receptors, the interaction between plants and AHLs and possible alternations of the AHL structure need to be explored more thoroughly in order to interfere with or stop bacterial communication in case of a pathogen. To modulate the QS system the AHL-synthase and AHL-receptor are potential targets. However, only a few studies have been concentrating on the synthase so far, as its crystal structure has just been identified.^{84,139} In 2002, the crystal structure of TraR (AHL-receptor) from the plant pathogen *A. tumefaciens* had been revealed providing scientists with important information on the design of LuxR inhibitors as well as activators.¹⁴⁰ But most important for the understanding of the bacterial communication process is the signal molecule itself and the synthesis of modified ligands that act as agonists or antagonists. The following chapter will focus on the structural variety of AHL analogues, their biological activity and interaction with LuxR-type receptors.

2.1 Interaction of LuxR-type proteins with AHLs

Before one can start designing new AHL mimics that either act as an agonist or antagonist one has to determine which alterations of the ligand structure will still be biologically active. The interaction between natural AHLs and their cognate receptor protein provide important information about possible modifications of the AHL scaffold. In 2002, the crystal structure of TraR (receptor protein of the plant pathogen *Agrobacterium tumefaciens*) with its autoinducer and target DNA was published, giving insight into the general binding mechanisms of LuxR-type receptor proteins and their AHLs.¹⁴⁰ During QS the complex of TraR and *N*-(3-oxo-octanyl)-L-homoserine lactone (also called *Agrobacterium* autoinducer or AAI) binds to the so called tra-boxes to activate gene expression. Being a member of the LuxR family, TraR can also be divided into two functional domains. The C-terminal domain contains the DNA binding motif. The N-terminal domain of LuxR contains residues required for binding *N*-(3-oxo-octanyl)-L-homoserine lactone. Even so the alleged AAI binding site in TraR still has to be determined. The TraR-AAI complex is a dimeric protein with one AAI bound at each monomer.

The crystal structure (see Figure 9) shows that both AHL molecules are completely embedded in each *N*-terminal ligand-binding domain. The DNA is bound to the *C*-terminal domain by a typical helix-turn-helix motif.¹⁴⁰

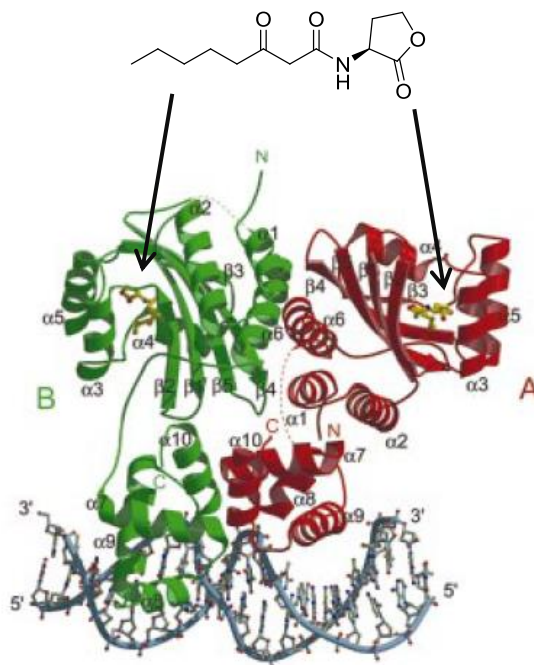


Figure 9: Ribbon diagram of the complex $(\text{TraR/AHL})_2/\text{Trabox}$. The homodimer contains the two subunits A and B with the AHL completely embedded within the receptor.¹⁴⁰

Figure 10 takes a closer look at the structure of the ligand-binding domain. The AHL molecule is completely enclosed between the five-stranded antiparallel β -sheet, the three α helices (α_3 , α_4 and α_5) and lined by a cluster of hydrophobic residues. In addition, the AHL is stabilised by two hydrogen bonds. The first hydrogen bond is formed between the nitrogen of the amide moiety and the oxygen of Asp70. The second one is built between the carbonyl oxygen of the lactone motif and the nitrogen of Trp57. Thus, polar interactions of the two carbonyls with Tyr53 and Thr129 are possible.^{64,140,141} For further information on the crystal structure see Vannini *et al.*¹⁴⁰ In 2007, Bottomley *et al.* have published the crystal structure of LasR from the opportunistic pathogen *Pseudomonas aeruginosa*.⁶⁰

The TraR and LasR crystal structures have since been the basis for computational homology modelling for other LuxR-type proteins as well as the design of new synthetic ligands.

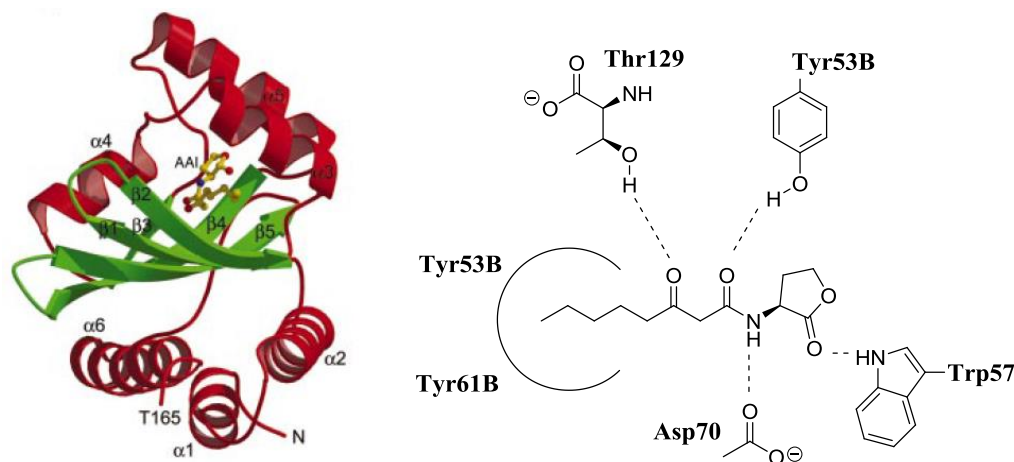


Figure 10: Left: Ribbon diagram of the ligand-binding domain. The ligand (AAI, yellow ball and stick representation) is completely enclosed within the binding domain. Right: Amino acids involved in binding of the native ligand.¹⁴⁰

2.2 Designed AHL mimics

AHL-mediated QS is an ideal target for pharmacological intervention of many important plant diseases but also for taking advantage of beneficial bacterial behaviour. The following chapter will focus on the design of synthetic AHL mimics and their biological activity. Designed AHLs might act as antagonists or agonists. Both compound types bind to the cognate receptor. However, agonists induce the same biological effect as the natural ligand whereas antagonists inhibit the activity of the natural autoinducer. Eberhard *et al.* were the first to synthesise AHL analogues in 1986.¹⁴² The study focused on the agonistic and antagonistic activity of the designed AHLs against 3-oxo-C₈-HSL in *V. fischeri* B-61. This bacterial strain produces more light with the addition of 3-oxo-C₈-HSL. Furthermore, the investigation addressed the question whether the fatty acid chain or the lactone moiety was most important for biological activity. Therefore, the length of the acyl chain was varied as well as the placement of the 3-oxo group.

At one point the γ -lactone was replaced by a γ -thiolactone and a caprolactam. However, AHL analogues containing a thiolactone or lactam moiety either showed no biological activity or inhibited LuxR. The authors concluded that the lactone function was of crucial importance for agonistic activity against LuxR. Furthermore, the authors determined the optimal fatty acid chain length for agonistic activity was six carbons. Longer acyl chains lead to an increased inhibitory activity, with compound **17** being the strongest antagonist Eberhard and co-workers have found. Additionally, the 3-oxo group was shown to be essential for agonistic activity while carbonyls placed at the 2nd or 5th position abolished or decreased agonistic activity. AHL mimics with just one carbonyl at the first position revealed an antagonistic nature against LuxR.^{42,142}

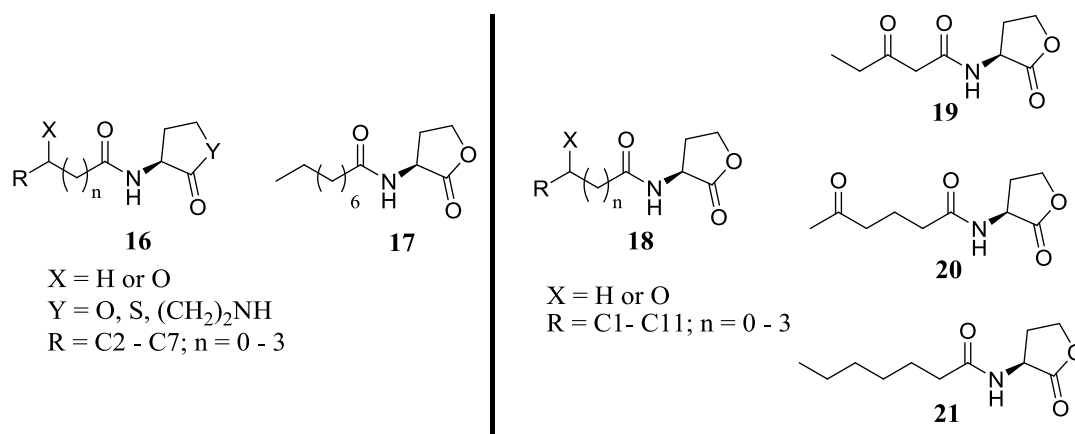


Figure 11: Selected examples of AHL mimics **16** and **17** tested against LuxR by Eberhard and colleagues. Right: structural features of AHL analogues tested against LuxR (**18** - **21**) by Greenberg *et al.*^{142,143}

The next study dealing with AHLs mimics was published a decade later by Greenberg and contributors, who used a certain *E. coli* strain (*E. coli* VJS533 phV2001) which contains LuxR and the *V. fischeri* gene cluster with an inactivated luxI.¹⁴³ This analysis revealed similar results in ligand activity to those reported before. The lactone ring is essential for LuxR binding and only small changes to the functionality (*i.a.* inserting a γ -thiolactone) are tolerable without abolishing biological activity. AHL mimics containing alkene units in the fatty acid chain displayed reduced agonistic activity suggesting that a flexible acyl chain is necessary for binding to LuxR.

One has to keep in mind that these investigations were conducted before the first crystal structures of the receptor protein were reported.¹⁴³

In 2002, Nielsen *et al.* focused on the modification of the lactone ring although previous results have shown that only moderate alternations do not abolish biological activity of the compound.¹⁴⁴ The basis for this research was the discovery of halogenated furanones isolated from the macroalgae *Delisea pulchra* which have a similar structure to AHLs and bear substitutions at the third and fourth position of the ring. These furanones were reported to inhibit several QS systems.⁴² The AHL derivatives by Nielsen were screened for their agonistic or antagonistic nature in *E. coli* JM105 pUC18, a strain which combines the LuxR system of *V. fischeri* (with an inactivated *luxI*) and the reporter gene for GFP (*green fluorescent protein*). Figure 12 depicts their most important AHL derivatives. Compounds **24** and **25** exhibit inhibitory activity at high concentrations. Derivatives with substitutions at the 3-position showed activities similar to the native ligand. *R* stereochemistry at the 3-position also plays an important role for agonistic activity, whereas *L* stereochemistry reduced the agonistic nature of the compound by a 1000-fold. In addition, the introduction of groups such as carbamates at the 3-position abolished all biological activity of the derivative regardless of the stereochemistry.¹⁴⁴

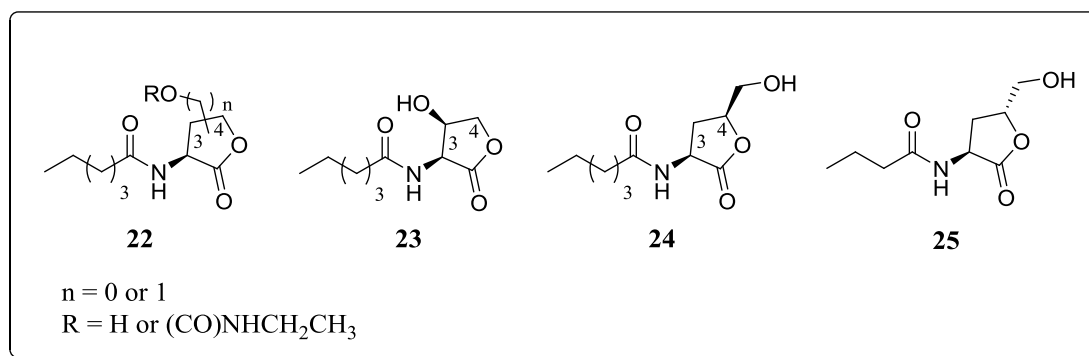


Figure 12: Selected AHL analogues tested against LuxR by Nielsen *et al.*¹⁴⁴

In 2008, Geske and colleagues published a detailed study about several non-natural AHLs in different bacterial species focusing on five LuxR type proteins (LuxR from *V. fischeri*, LasR and RhIR from *P. aeruginosa*, TraR from *A. tumefaciens* and CarR from *E. carotovora*).^{42,145}

Prior to this review only a few non-natural antagonists had been synthesised which were mainly structural mimics of the natural ligand (*e. g.* compound **26** by Zhu¹⁴⁶ and **28** by Reverchon,¹⁴⁷ Figure **13**). Additionally, analyses of mimics that exhibit increased activities compared to the native ligand have hardly been investigated. These compounds are so called “super-activators” as they can initiate bacterial group behaviour at lower cell densities than required in natural environments. However, only three such compounds (Figure **13**) had been identified before Geske’s research.^{145,148,149} Furthermore, the known antagonists and agonists had only been studied in one bacterial species; therefore it is not clear if they target specifically one LuxR-type protein or if they can modulate a wide range of LuxR-type proteins. Previous investigations by Geske *et al.* have resulted in the identification of five potent modulators of LuxR-type proteins in *A. tumefaciens*, *P. aeruginosa* and *V. fischeri*, including antagonists **27** and **29**.¹⁸

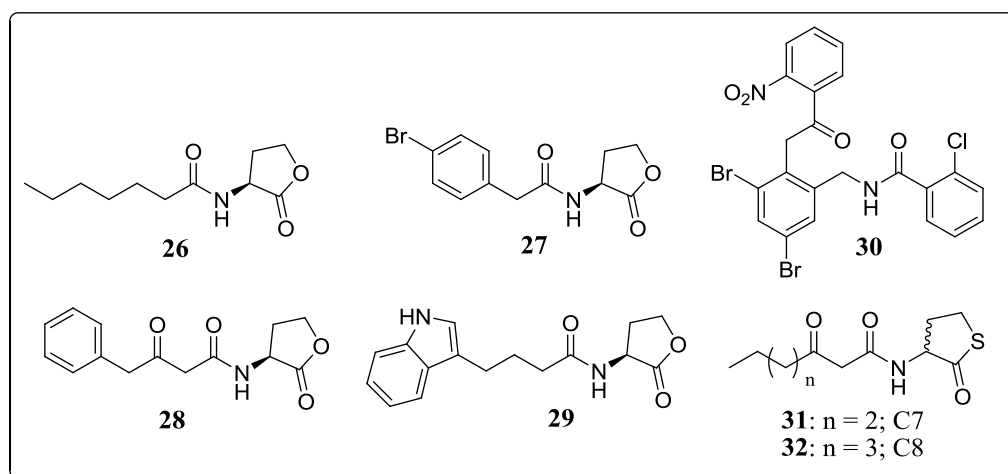


Figure 13: Known synthetic antagonists of LuxR-type protein function (**26 – 29**).¹⁴⁵⁻¹⁴⁷ AHL mimics **31**, **32**¹⁴⁸ and **30**¹⁴⁹ are known super-activators of R protein function.

To address these problems Geske and contributors have designed four combinatorial libraries by solid phase synthesis using the natural AHL ligands together with the structure of previously identified synthetic mimics and the X-ray crystal structure of the TraR protein as guidelines. This systematic study directly compared ~90 AHL analogues in the three above mentioned bacterial species. Due to this strategy a set of ligands was identified that either modulate one, two or all three of the LuxR-type proteins investigated.

Some selected examples are depicted in the Venn diagrams shown in Figure 14. For the first time a broad spectrum of species-selective antagonists of LuxR-type proteins were identified. However, the authors noted that far fewer agonists were discovered compared to antagonists. In addition, these few agonists are by far more selective to one receptor protein. Moreover, the first superagonist of *V. fischeri* **33** was reported.^{24,145} The authors also hypothesized that all ligands target the same site of a given receptor but that not all compounds are binding in the same way as the natural ligand. This binding flexibility would complicate rational structure-based design of mimics in future. The activity of the AHL analogues was also tested at different concentrations. The authors found that most LuxR-type antagonists could also be described as “partial agonists” due to the fact that at high concentrations they were able to activate the transcriptional regulators.^{24,145}

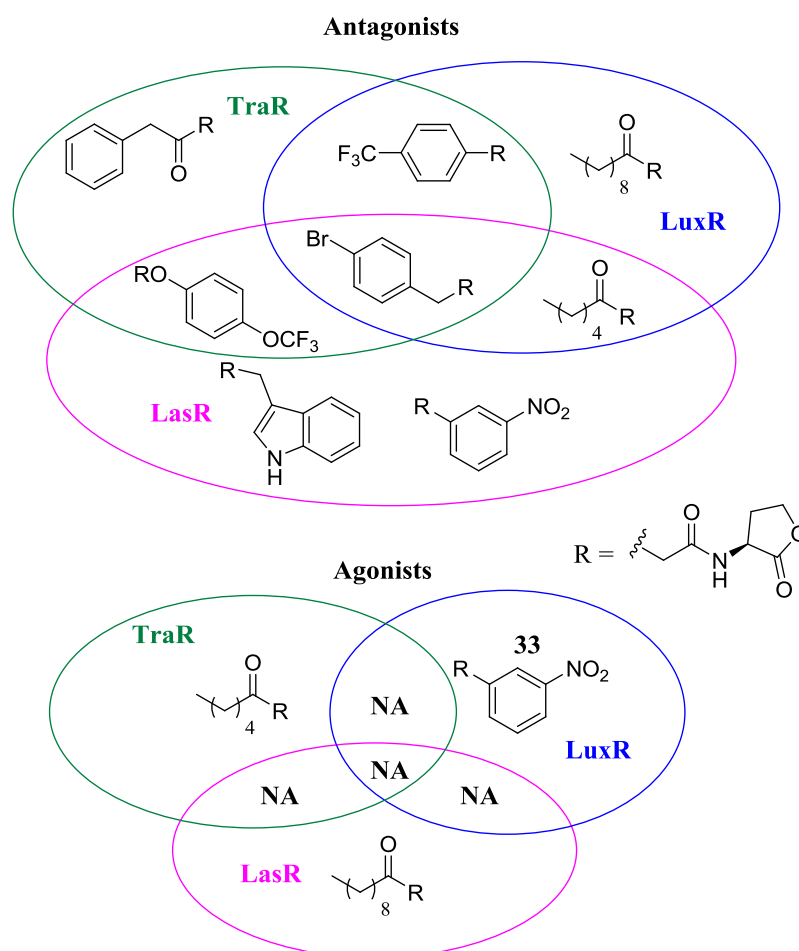


Figure 14: Venn diagrams showing selected LuxR-type protein antagonists and agonists and their selectivity for different LuxR-type proteins from *V. fischeri* (LuxR), *A. tumefaciens* (TraR) and *P. aeruginosa* (LasR). Ligands in the intersection of the circles have shown activity to two or more receptor proteins. NA = no applicable ligands identified.^{24,145}

2.3 Effects of native and non-natural AHLs on plants

Communication in the rhizosphere is based on a complex exchange and perception mechanism of autoinducers from different bacterial species. Although several reports have shown that plants are able to perceive AHLs and respond to them with changes in gene expression and their development, still little is known about the molecular ways of plants reacting to these signals. Hence, the various possible alternations of the acyl chain or lactone moiety of the native as well as non-natural ligands lead to different effects on plants making it hard to decipher the plant-AHL reaction process.

In 2008, von Rad and co-workers investigated the effects of short-chain AHLs on root growth and development in *Arabidopsis thaliana*. The result illustrates that C4- and C6-HSLs promotes root length compared to long chain AHLs (e.g. C8-HSL, C10-HSL), which does not. It was shown that the AHLs (C6-HSL and C10-HSL) are taken up and distributed inside the plant. The intensity of C6-HSLs in the leaves was higher than in the roots confirming the authors' hypothesis that this autoinducer is first transported to the plants' leaves. In contrast, C10-HSL is primarily found in root tissue. This might be due to the increased hydrophobic character of the C10-HSL.¹⁵⁰ In 2014 Sieper *et al.* investigated the uptake and distribution of HSLs in barley, which relies partly on active process within the plant.¹⁵¹ The impact of autoinducers with varying chain lengths (C4 to C14) on *Arabidopsis thaliana*'s root architecture was also thoroughly investigated by the group of Ortíz-Castro. Although long chain AHLs decreased primary root growth, these signal molecules were found to significantly stimulate root hair development. A branched root hair system is necessary for the plants' nutrient uptake.¹⁵² Furthermore, Schuegger *et al.* inoculated tomato plants with the AHL-producing rhizobacterium *S. liquefaciens* MG1 and infected the plants with the leaf pathogen *A. alternata*.¹⁰⁴ Four days after treatment with the pathogen the appearance of necrotic cell death was already reduced by 70% compared to the control group. Plants were also treated with an AHL-negative strain (MG44), which contained a mutated AHL-synthase gene. The comparison of MG1 with MG44 treated plants would show the impact of AHLs in this interaction. Inoculation of the plant with the AHL-negative strain MG44 slowed down cell death by *A. alternata*. Figure 15 shows the effects of root inoculation with rhizobacteria *S. liquefaciens*. The leaves of tomato plants were either non-treated (control), treated with *S. liquefaciens* MG1 (wild type) or *S. liquefaciens* MG44 (AHL-negative mutant).

Three days after inoculation the plants were exposed to the pathogen *A. alternata* (Figure 15, a). The authors even demonstrated the cell-to-cell communication *in situ* between a GFP-marked AHL strain (*P. putida* F117:Tn5-Las) and an AHL-producing bacterial isolate from tomato roots (*P. putida* IsoF). The tomato isolate was tagged to the red fluorescent protein DsRed (Figure 15, c).¹⁰⁴

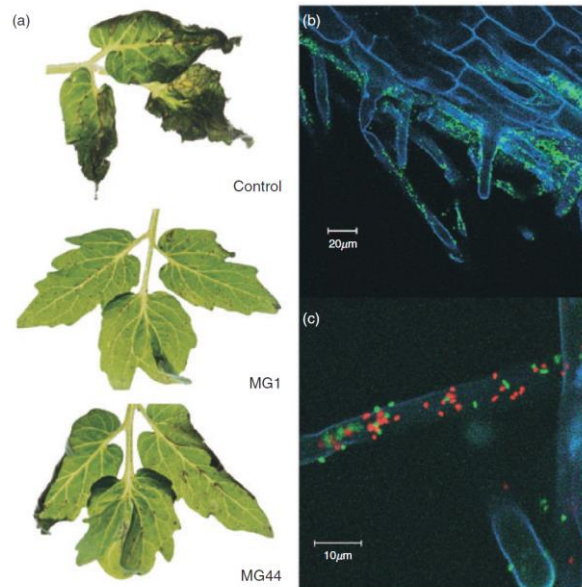


Figure 15: a) Appearance of necrotic cell death four days after treatment with *A. alternata*. b) Colonisation of tomato roots with GFP-tagged *S. liquefaciens* MG1. c) Cell-to-cell communication between GFP-based AHL monitor strain (green dots) and AHL-producing tomato isolate (red cells).¹⁰⁴

Due to the sometimes devastating effects of bacterial pathogens on crop plants, numerous research groups addressed the question whether AHLs are able to induce resistance in plants. Schikora *et al.* have published results indicating that oxo-C14-HSLs and to lesser extend OH-C14-HSL and oxo-C12-HSL have the ability to induce resistance in *Arabidopsis* and barley plants to the pathogen *Pseudomonas syringae* pv *tomato* DC3000. However, autoinducers with a shorter acyl chain (*e.g.* oxo-C12-HSL) mediate a significantly weaker induction of resistance compared to the C14-derivatives. In addition, the application of the signal molecules on roots did not lead to a transport within the plant because no AHLs could be detected in the plant's leaves.^{153,154}

When it comes to non-natural AHLs these autoinducers are usually screened for LuxR-type receptor activity in culture-based assays. These assays normally lack the AHL synthase and contain GFP or β -galactosidase for the LuxR-type receptor. Such idealised conditions simplify the identification of potentially antagonistic and agonistic signal molecules. However, there is still a big difference between an idealised assay and native conditions. To address this problem Palmer and contributors have developed a straightforward route for a better understanding of how non-natural ligands modulate QS in wild-type bacteria on their native eukaryotic hosts.^{155,156}

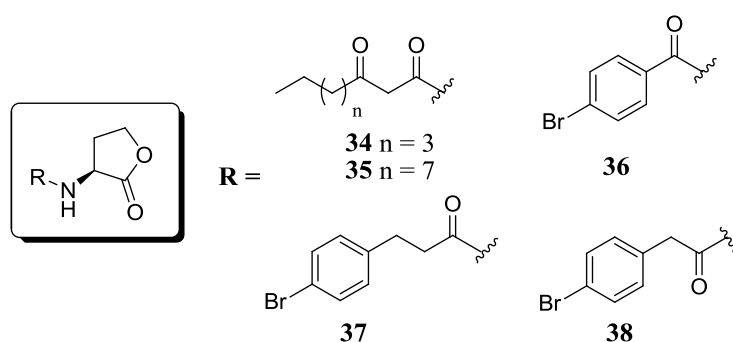


Figure 16: Four AHL antagonists selected for the study. **34** and **35** are native ligands. **36** - **38** are non-natural autoinducers.¹⁵⁵

The researchers investigated the host – pathogen interaction between *P. carotovora* and *Solanum tuberosum* (potato). Two natural AHLs **34** and **35** and three mimics were selected for the modulation of wild-type *P. carotovora* virulence *in vivo* as these compounds were identified as the most potent antagonists. A simple potato tuber infection assay was used and confirmed that the previously identified QS modulator **36** – **38** kept their antagonistic nature when introduced to the potato by syringe. However, the inhibition of virulence in wild-type *P. carotovora* by the AHL-antagonists was highly dependent on the timing of dosing. For maximal inhibition of virulence additional re-introduction of AHL into the potato was required at specific times. The authors suggested that the dosage dependence of the system emphasises the importance of biologically compatible materials that can controllably release QS modulators over a period of time. The researchers have also previously developed a polymer film for the controlled release of autoinducers over four to five days.¹⁵⁷

3 Aims and Objectives

The aim of this PhD thesis was the synthesis of novel, modified *N*-acyl homoserine lactones as chemical probes for the evaluation of plant-bacteria interaction. Despite the importance of QS molecules for plant resistance and development the molecular processes remain widely unexplored. Plant receptors for AHLs have not been isolated so far, although the identification and investigation of these receptors is crucial to fully understand the effects on the plant immune system. Hence, several acyl-chain and lactone-ring modified 3-oxo-C14-AHLs are to be prepared for the elucidation of the plants' perception system and the evaluation thereof. Additionally, the biological activity of the modified autoinducers has to be investigated. First, one has to determine whether bacteria are still able to identify these non-natural AHLs as common autoinducers. Secondly, the effect of the modified signal molecules on plants has to be analysed.

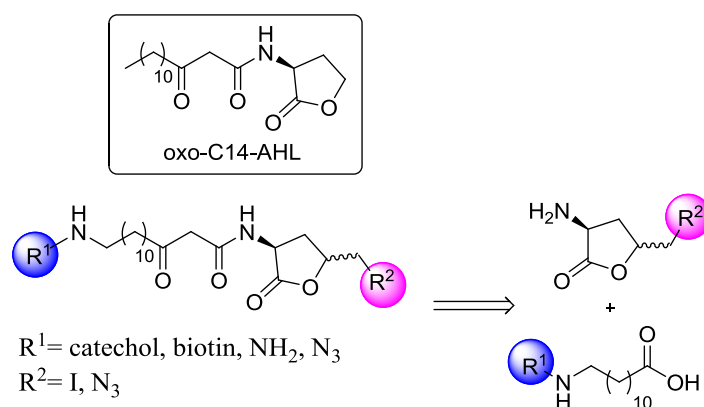


Figure 17: Possible modifications of a 3-oxo-C14 AHL.

For the isolation, identification and characterisation of new QS receptors in plants photoaffinity labelling with AHLs could be a versatile tool. Thus, an AHL derivative containing a photoactive group and a tag that binds to the receptor instead of the natural ligand shall be designed. The photoactive group would be activated by light irradiation and binds irreversibly to the receptor forming a covalent bond. Typical photoactive groups are diazirines or azides. Biotin could be used as an appropriate tag because of its strong binding affinity towards avidin and streptavidin (Figure 18).

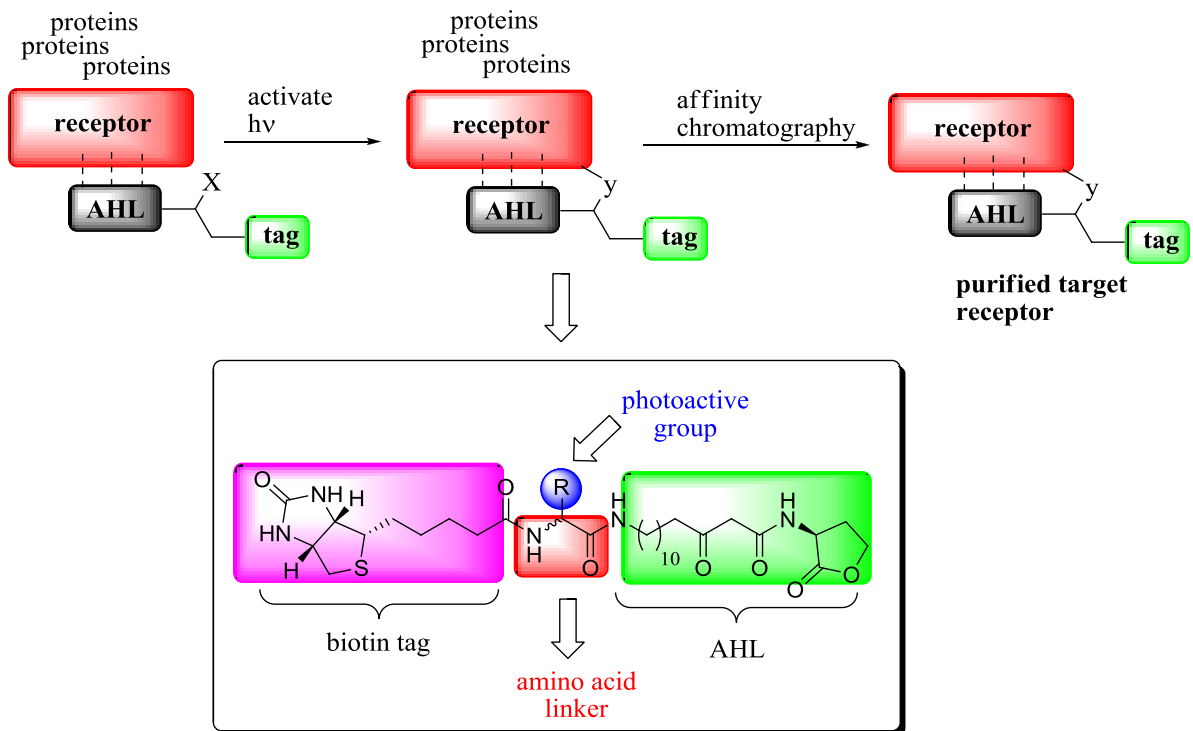


Figure 18: Delineation of a biotin tagged AHL containing a photoactive group for photoaffinity chromatography.

Another approach for the identification of new plant receptors is the conjugation of the AHL scaffold to a metal oxide surface (*e.g.* nanoparticle or bulk material). The immobilised AHLs could be used for affinity chromatography if the autoinducer is used as the stationary phase. The autoinducer would bind to the appropriate receptor which could be separated from other proteins. Another application might be the design of a biological fertiliser. AHL produced by beneficial bacteria could be immobilised on a metal oxide surface having the shape of a fertiliser stick. When inserted into the earth, the AHL might be set free over a certain period of time. For these purposes, the AHL scaffold ought to be conjugated to different anchor groups (*e.g.* catechols, phosphonates), which bind to a TiO_2 nanoparticle.

The coating procedure of the nanoparticle should be evaluated and improved. In addition, the coated nanoparticles ought to be characterised by different analytical methods to determine the overall coverage of the surface with the autoinducer. Afterwards the biological activity should be analysed by using *Arabidopsis thaliana* as a test plant.

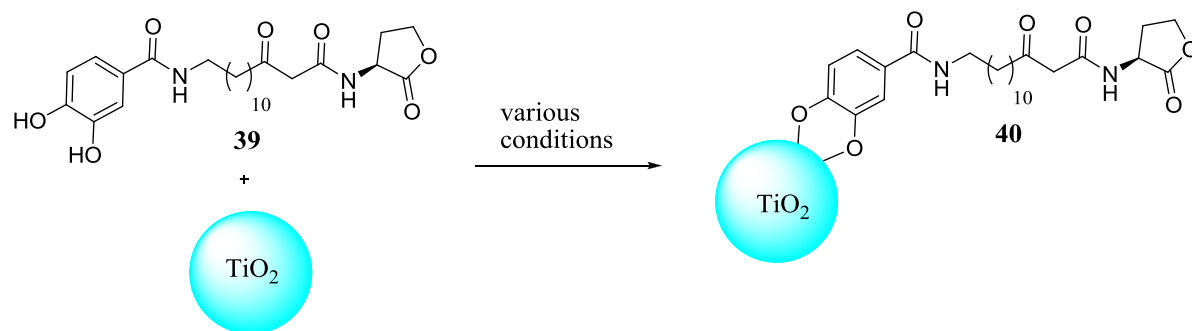


Figure 19: Schematic illustration of a catechol-AHL bound to a TiO₂ nanoparticle.

4 Results and discussion

4.1 Preparation of synthetic *N*-acyl-L-HSLs

One of the most commonly used methods to prepare AHLs in excellent yields is the Meldrum's acid approach (Figure 20). This route is quite effective when R is C₆ or longer and has been used for the synthesis of a large number of synthetic analogues. In the first step Meldrum's acid **42** is coupled to the appropriate fatty acid by standard coupling procedures to form intermediate **43**. Reaction with butyrolactone **46** gives the desired AHL **48**. When R is shorter than C₆ small amounts of side product **47** are produced but can be removed by column chromatography. Intermediate **43** can be also converted to a β -keto ester **45** with the appropriate alcohol.^{31,32}

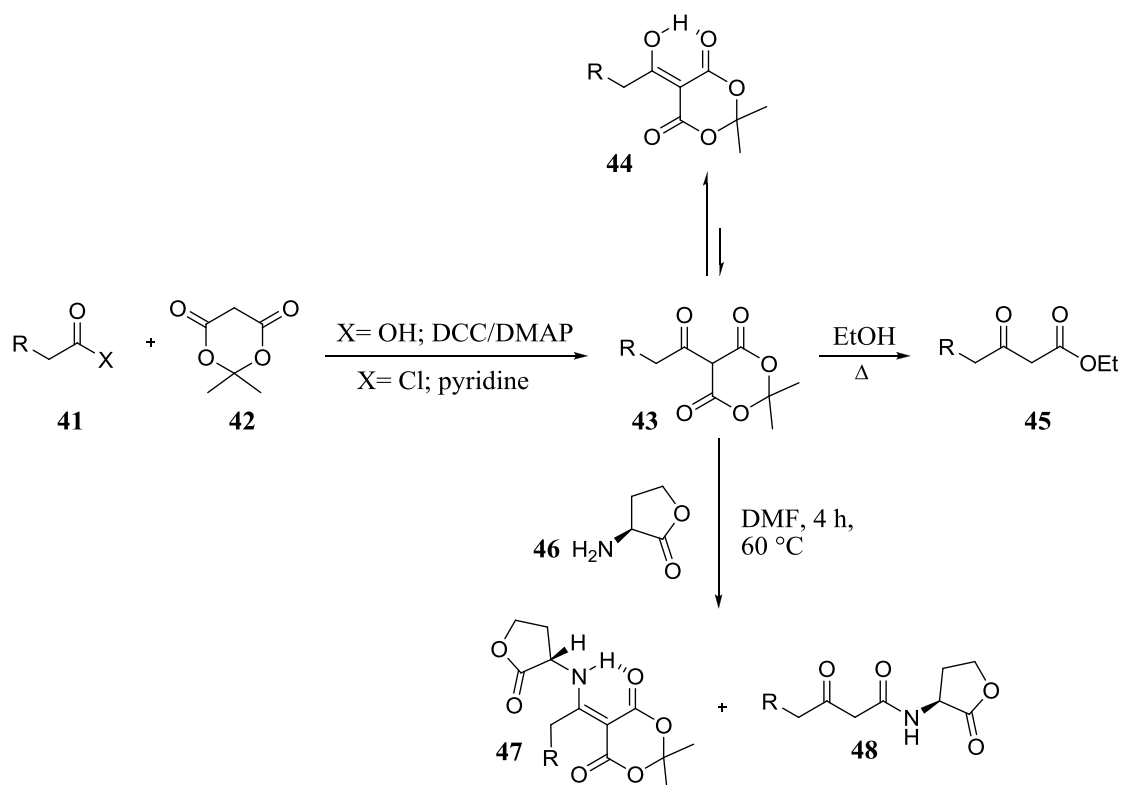


Figure 20: Synthesis of *N*-3-oxo-L-HSL **48**.³²

4.2 Synthesis of acyl-chain modified AHLs

The Meldrum's acid approach was chosen for the synthesis of modified oxo-C14-AHLs and derivatives thereof. In the first step the commercially available fatty acid was Boc-protected in excellent yields. Following a route by Amara *et al.* the Boc-protected acid **49** was converted to the novel oxo-C14-AHL analogue **50** by treatment with Meldrum's acid and (S)-homoserine lactone **46**.³¹ Boc-deprotection of **50** by TFA gave the free amine **51**. From this intermediate different functionalised AHL mimics were prepared. Acylation with acetic anhydride gave the *N*-acetyl derivative **52**. Most notably, the biotin derivative **53** was prepared, which is an interesting molecular probe for a pull-down assay for plant AHL receptors.¹⁵⁸ Only a few biotin-tagged AHLs can be found in literature and derivatives of oxo-C14-AHL are unknown.^{159,160}

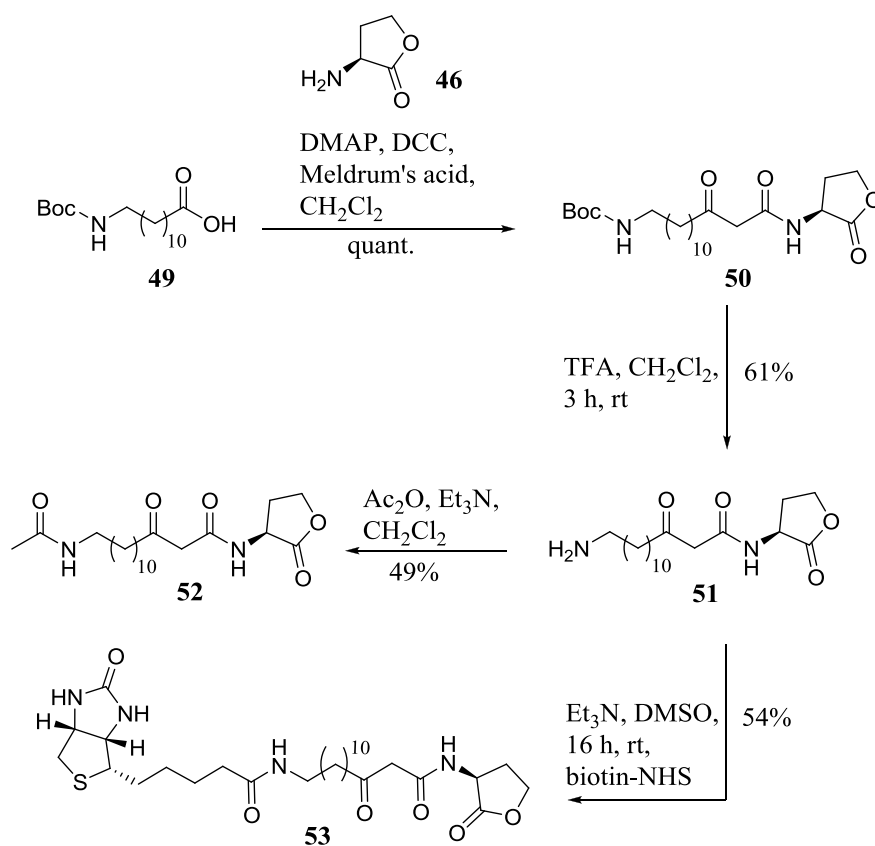


Figure 21: Synthesis of amine **51** and its conversion to the biotin-labelled molecular probe **53**.¹⁵⁸

The NHS-ester approach was used for the conjugation because standard peptide coupling procedures with HOBt/EDC or acid chlorides did not give the desired product and lead to complex product mixtures.¹⁵⁸

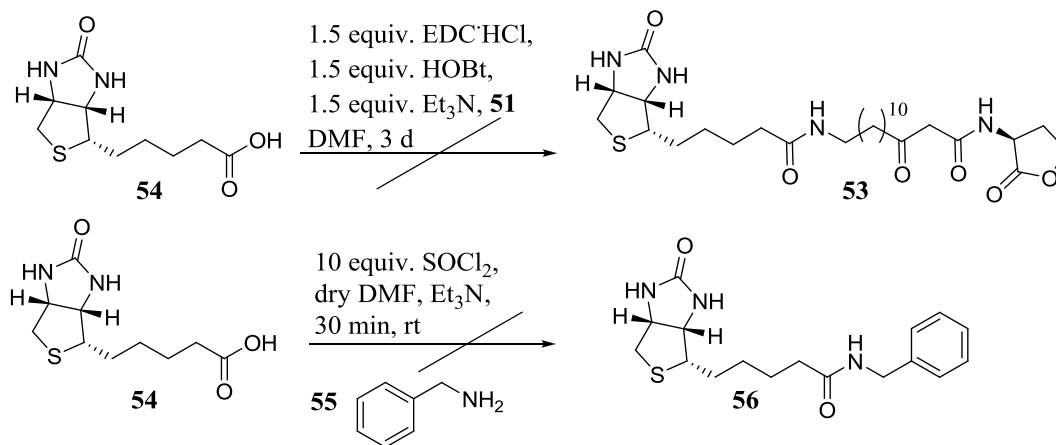


Figure 22: Evaluation of possible coupling conditions for the preparation of biotin-labelled AHL 53. Synthesis of model substance 56 with SOCl₂ failed.

Azide **60** is a versatile intermediate for copper catalysed click-functionalization of oxo-C14-AHL and can be prepared from either azidoacid **58** or Br-AHL derivative **59** with NaN₃ (Figure 23).¹⁵⁸

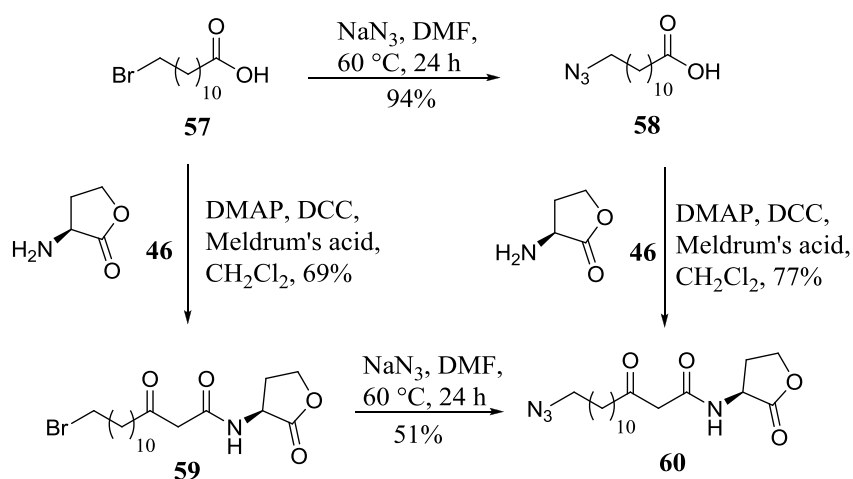


Figure 23: Preparation of azide derivative 60 for click reactions.

Alkyne **63** is another important compound for click reactions (1,3-*Huisgen*-cycloaddition) and can be prepared by the NHS-ester route. The 4-pentynoic active ester **61** was conjugated to the free amine **51** using standard conditions. Another possibility is the direct conjugation of 4-pentynoic acid **62** to the free amine **51** by an EDC/HOBt procedure to give the desired product **63**.

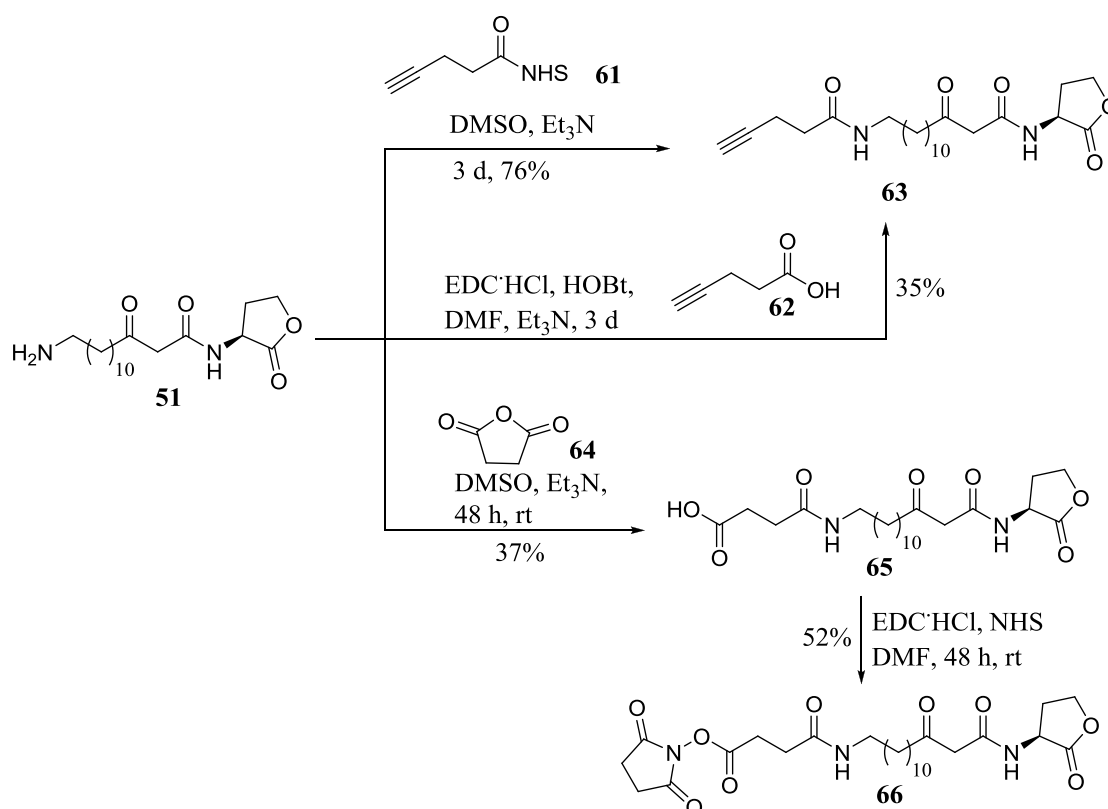


Figure 24: Synthesis of alkyne derivative **63** for click reactions and AHL derivative **65** and **66** for bisphosphonate coupling.

AHL intermediate **51** was also coupled with succinic anhydride **64** in DMSO to give the carboxylic acid **65** in moderate yields. This compound could be used for standard peptide coupling or functionalization on metal surfaces or nanoparticles. In the next step the NHS ester **66** was prepared. This intermediate was later used for coupling reactions with bisphosphonates (see chapter 4.5).

AHL derivative **67** was obtained from azide **60** and 4-pentynoic acid **62** by click reaction using an established protocol with CuSO_4 and sodium ascorbate.

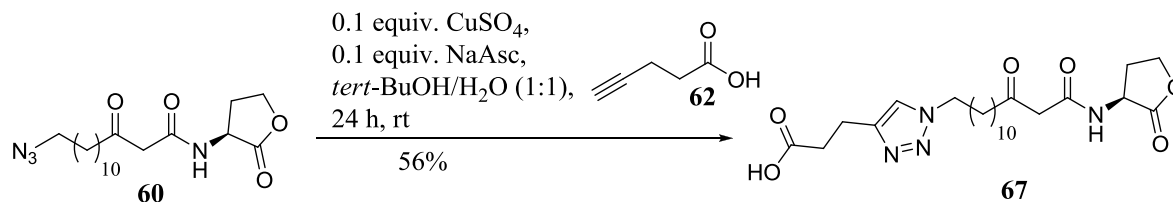


Figure 25: Click reaction with azide **60** and alkyne **62** obtained AHL mimic **67**.

The Meldrum's acid approach was also used to prepare AHL derivative **69** from oleic acid **68** in very good yields (Figure 26). Boc-protected acid **70** was conjugated to (*S*)-homoserine lactone **46** by standard coupling conditions using DMAP and DCC to give the C12-AHL derivative **71** in very good yields. Boc-deprotection with TFA gave the free amine **72**, which is a versatile compound for coupling reactions.

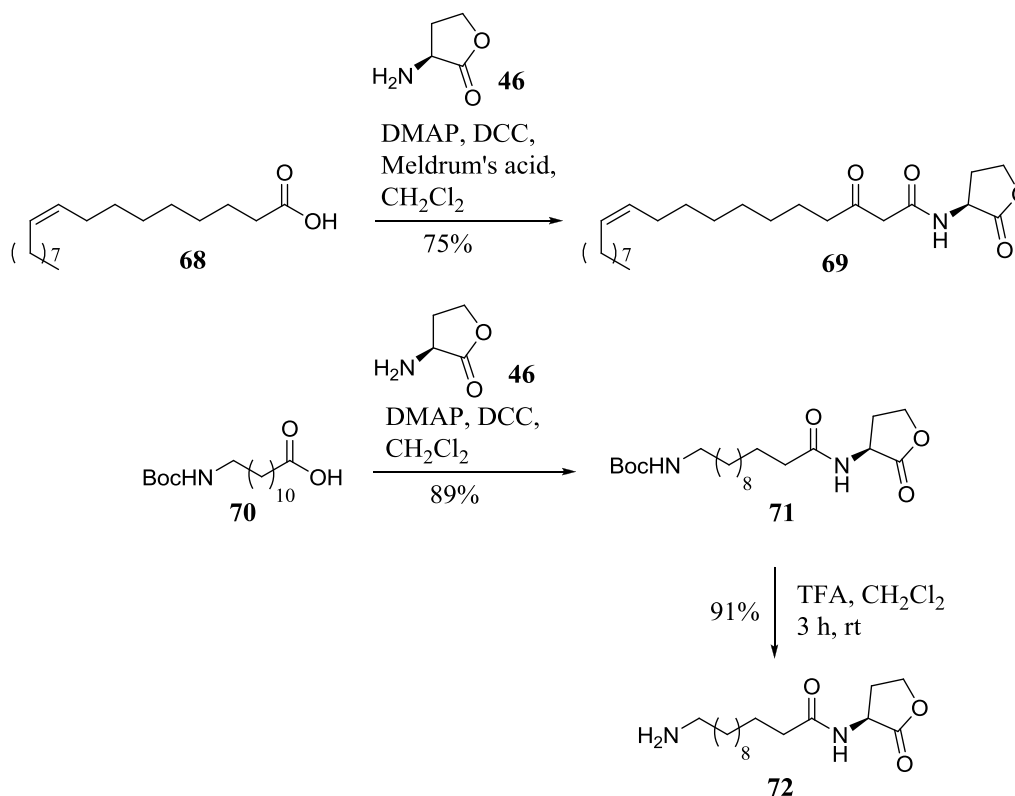


Figure 26: Preparation of an AHL analogue **69** with an unsaturated acyl chain and two C12-AHL-derivatives **71** and **72**.

Figure 27 displays the chosen synthetic route to a modified lactone scaffold. The lactone moiety would be constructed according to the Kazmaier method from *N*-protected allylglycines **75** via Claisen rearrangement of glycine allylesters **74**.¹⁶⁴ Following the Kazmaier route, the synthesis started off with the TFA-protected glycine **73a** to obtain glycine allyl ester **74a**. The following Claisen rearrangement to **75a** proceeded in varying yields up to 74%. In some cases deprotection of the TFA group was observed after work up. In addition, the following iodolactonization to **76a** was accomplished with only 37% yield. In consequence, the protecting group strategy was switched to prepare Cbz-protected glycine allyl ester **74b** and the Boc-protected analogue **74c**. With both derivatives, the rearrangement worked fine and gave the expected allylglycines **75b** and **75c**. Particularly Boc-allyl ester **74c** gave consistently high yields of Boc-allylglycine **75c**. Unfortunately, as already reported by Kazmaier for similar carbamates, the enantioselectivity of these conversions is low.¹⁶⁵ For Boc- and Cbz-allylglycine almost racemic mixtures were obtained. However, both enantiomers of Boc-allylglycine **75c** are easy to separate by HPLC on a chiral phase (see chapter experimental section 8.1.1 for detailed information) and are thus available in pure form if needed.

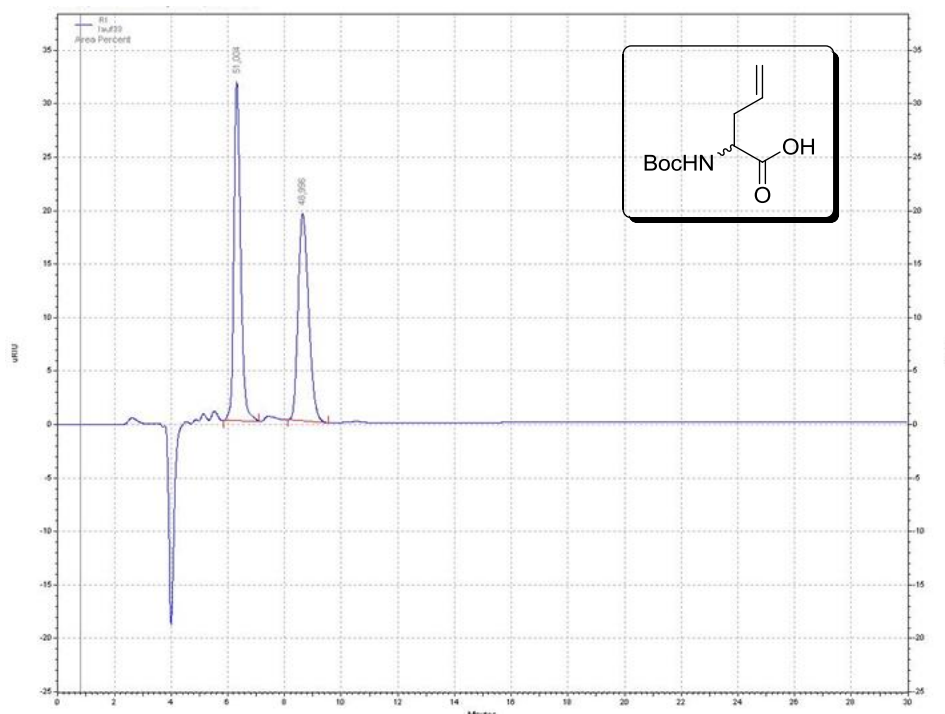
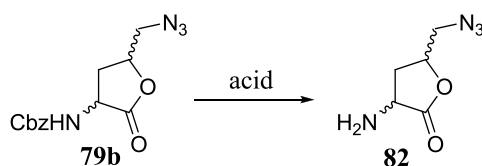


Figure 28: Separation of the racemic mixture **75c** by HPLC with a CHIRALPAK IA column (solvent: *n*-hexane/*i*-PrOH/TFA)¹⁵⁸

For a first evaluation of the 4-substituted AHL analogues the racemic compounds **75b** and **75c** were used. Iodolactonization worked well for the Cbz- and Boc-protected compounds and gave iodolactones **76b** and **76c** in good yields and with good diastereoselectivities for the *cis*-derivatives ($dr_{(cis:trans)} = 10:1$). The deprotection of the Cbz-derivative **79b** to give the free amine **82** proved to be very difficult. Several Lewis acidic reaction conditions were utilised as the lactone moiety would hydrolyse easily under basic conditions (Table 1). However, no product was detectable.



Entry	Conditions	Result
1	EtSH, BF ₃ ·OEt ₂ , 12 h, Ar, THF	No product
2	PhSMe, Et ₂ AlCl, Ar, dry CH ₂ Cl ₂	No product
3	Thioanisole, TMSBr, TFA, 1 h, Ar	No product

Table 1: Deprotection of Cbz under acidic conditions.

In the next step, it was assumed that deprotection under basic condition might lead to the free amine and that the open lactone ring might be restored by adding aqueous HCl (Figure 29). Cbz was deprotected by NaOH to give intermediate **83** which was detected by mass spectrometry. However, addition of aqueous HCl did not lead to the desired product **82**.

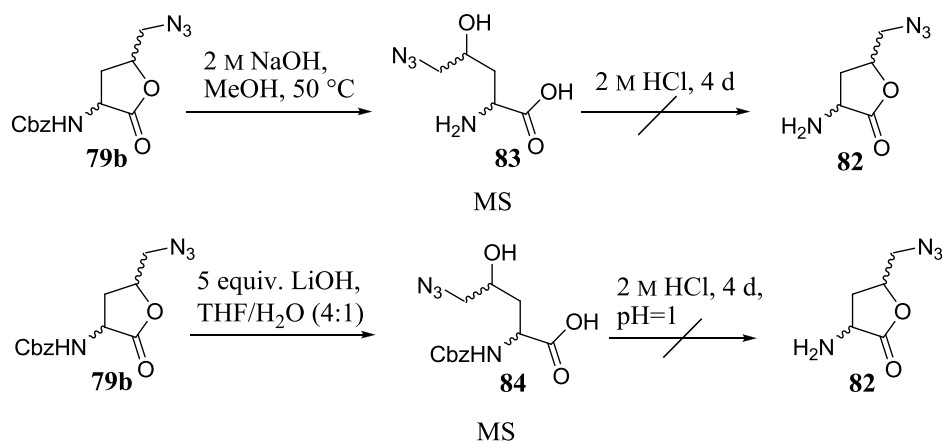
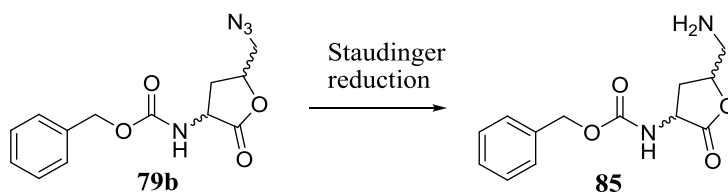


Figure 29: Cbz-deprotection under basic conditions. Intermediates **83** and **84** were detected by mass spectrometry.

Deprotection with LiOH hydrolysed the lactone moiety as expected (intermediate **84**) but did not cleave the Cbz protecting group. Additional LiOH led to a complex mass spectrum and neither product nor intermediate **84** were detectable.

The Boc-derivatives proved to be easier to handle. Deprotection with TFA gave the free amine **77** which was coupled to lauric acid in the presence of Meldrum's acid. The final AHL-analogue **78** was obtained in 43% yield over two steps. Alternatively, an azide moiety was introduced to iodolactone **76** via nucleophilic displacement of iodide with NaN₃ to give the desired products **79b** and **79c**. Deprotection of **79c** to the free amine **80** followed by coupling to lauric acid in the presence of Meldrum's acid gave AHL-analogue **81**. Both derivatives **78** and **81** are versatile AHL mimics because the iodide in **78** may be easily substituted with various nucleophiles and the azide in **81** is an excellent precursor for click functionalization or reduction to amine and subsequent functionalization *via* amide formation.

Although, the Cbz-deprotection proved to be difficult, the Cbz-protected azide **79b** is a versatile model compound for inserting new lactone ring modifications. One possibility was to convert the azide **79b** into a free amine **85** by Staudinger reduction which would be an ideal derivative for coupling reactions. However, standard Staudinger protocols by Svedham¹⁶⁶ and Lebeau *et al.*¹⁶⁷ did not work out.



Entry	Conditions	Result
1	Dry THF, PPh ₃ , 0 °C, 10 h	No product
2	THF/H ₂ O (9:1), PPh ₃ , rt, 12 h	No product
3	THF/H ₂ O (9:1), PPh ₃ , reflux, 12 h	No product

Table 2: Reaction conditions for Staudinger reduction of azide **79b**.

4.4 Synthesis of a bifunctional AHL mimic

One of the major aims to fully understand the QS system is the identification of new receptors in plants. Photoaffinity labelling with small molecules could be therefore a useful tool for the isolation, identification and characterisation of new QS receptors. Figure **31** depicts the basic principle of photoaffinity labelling. An AHL mimic containing a photoactive group (X) and a tag binds to the receptor instead of the natural ligand.

The photoactive group (X) is activated by light irradiation and binds irreversibly to the biological receptor at the site of interaction forming a covalent bond (Y). An appropriate tag *e.g.* biotin will then allow isolation and identification by affinity chromatography.^{168,169}

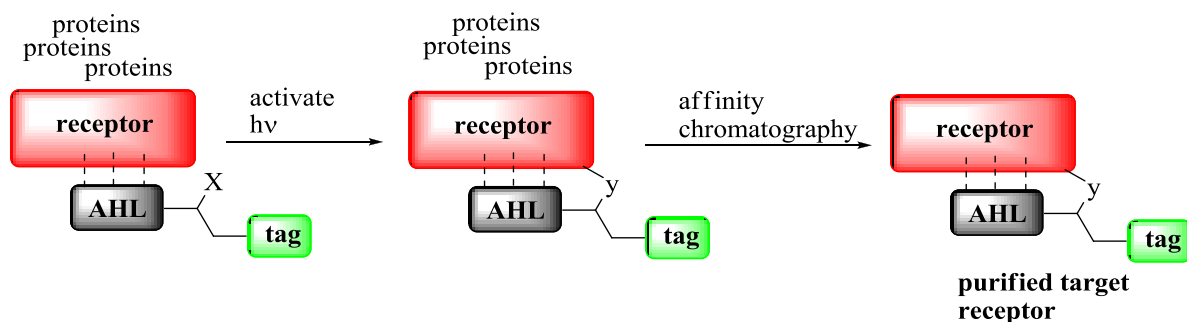


Figure 30: Labelling of unknown receptors with bifunctional AHL mimics. The AHL derivative contains a photoactive group X and a tag for affinity chromatography. Through light irradiation the photoactive group X binds covalently to the receptor (indicated by Y). Due to the appropriate tag, the receptor-AHL-tag-complex can be purified by affinity chromatography.¹⁷⁰

Biotin is the compound of choice for being a “tag” because it binds specifically to the proteins avidin and streptavidin, which can each embed four biotin molecules. The biotin-avidin and biotin-streptavidin bond is one of the strongest non-covalent bonds in nature. Immobilised avidin or streptavidin can be used to retrieve and purify biotinylated AHL-receptor-complexes. The complexes could be purified by affinity chromatography using an avidin or streptavidin coated solid phase or by magnetic beads that are immobilised with the biotin binding proteins.¹⁷¹

Several photoactive groups that are commonly used in literature for photoactive labelling are displayed in Figure 31. Especially aryl azides are frequently utilised because of their chemical stability in the dark and easy way of usage during synthesis.

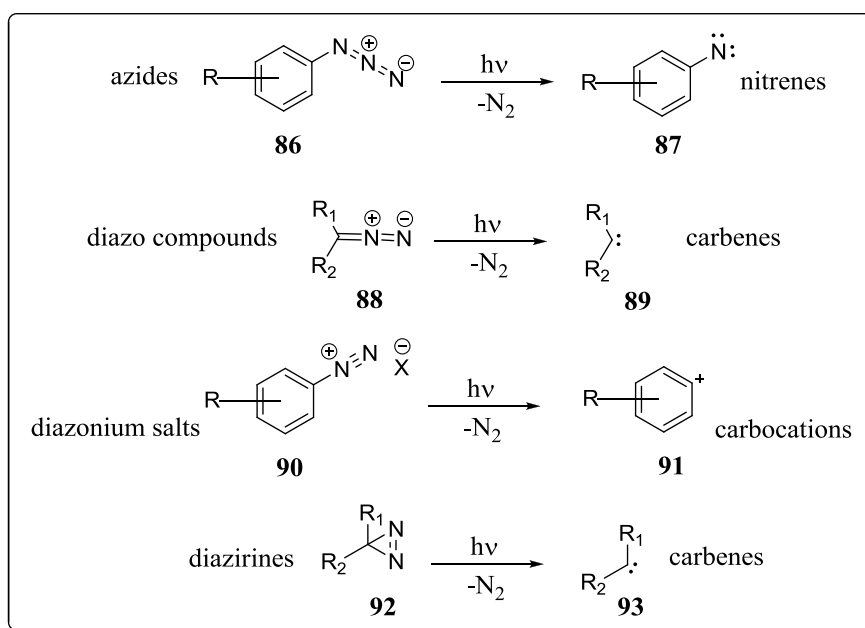


Figure 31: Typical photoaffinity probes.¹⁷¹

In 2009, Dubinsky and co-workers published the first AHL derivative containing a diazirine for photoaffinity labelling. Since lactone ring modifications might sometimes lead to a reduced biological activity the researcher focused on small alternations of the acyl chain, choosing the smallest possible photoactive group. The diazirine is activated by light irradiation to generate a highly active carbene. Figure 32 depicts the retro-synthetic approach to a bifunctional AHL mimic for affinity chromatography based on the most important aspects found by Dubinsky and co-workers.¹⁷⁰

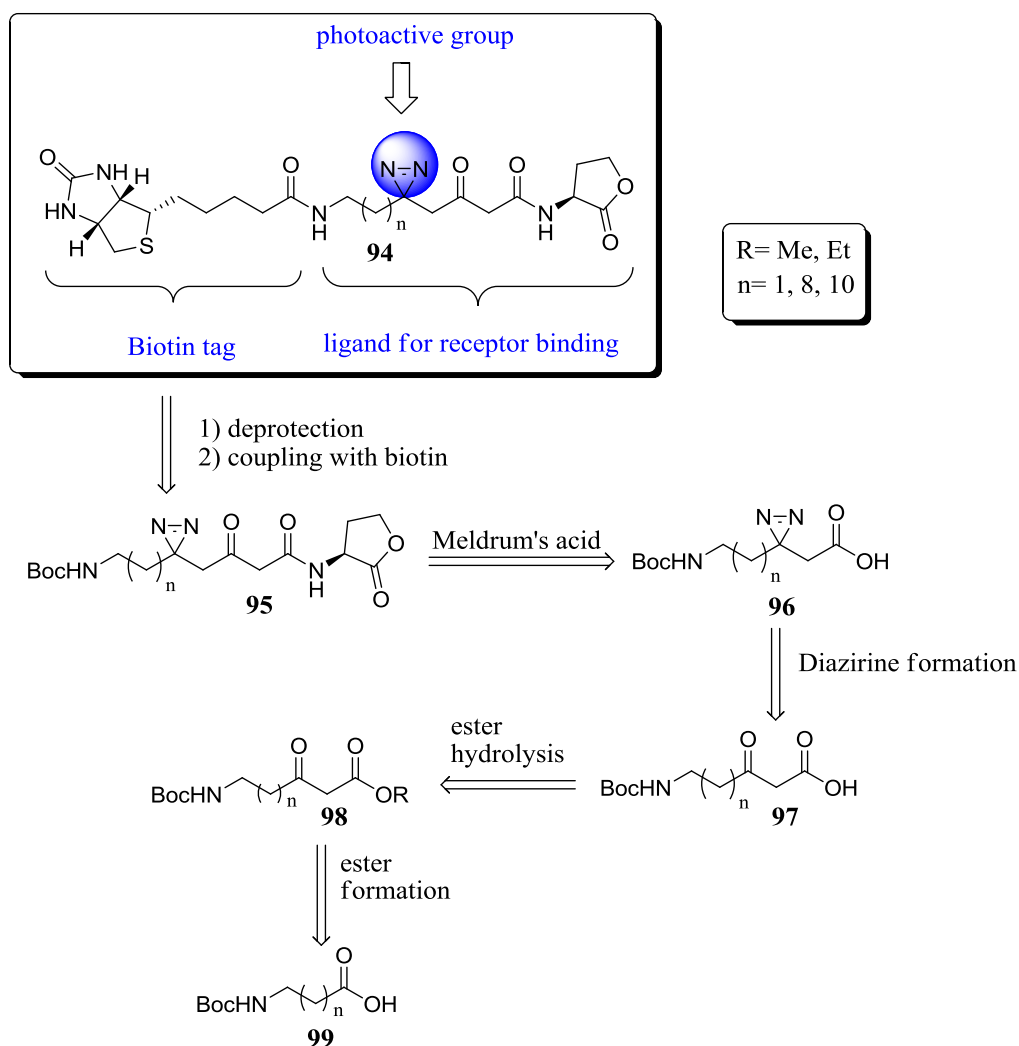


Figure 32: Retro-synthesis scheme for the preparation of bifunctional AHL **94** containing a biotin tag and a diazirine moiety as a photoactive group.

The synthesis of biotinylated AHL derivative **94** starts with the Boc-protected fatty acid **99** which is converted to an ethyl- or methyl ester **98**. Hydrolysis of the ester should give the free carboxylic acid **97**. The diazirine is then introduced at the 3-oxo position using standard conditions described by Dubinsky *et al.*¹⁷⁰ Coupling with Meldrum's acid and (S)-homoserine lactone gives the characteristic AHL scaffold **95**. Deprotection with TFA and introduction of biotin leads to the bifunctional AHL derivative **94** for affinity chromatography (Figure 32).

The commercially available 12-aminododecanoic acid was Boc-protected using the already mentioned protocol to get Boc-protected fatty acid **49**. The carboxylic acid was converted to the ester **100** and **101** via the Meldrum's acid approach and the appropriate alcohol (Figure 33). Synthesis with EtOH obtained the ethyl ester **101** in excellent yields after 3 h. Formation of the methyl ester **100** needed 24 h to give the desired product in good yields.

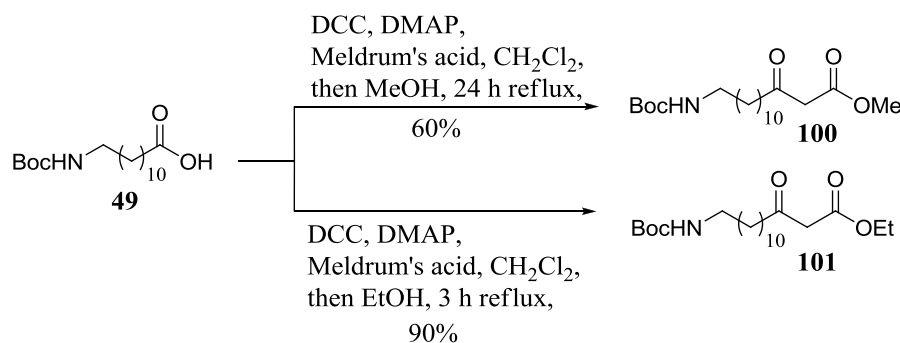


Figure 33: Synthesis of methyl ester **100** and ethyl ester **101**.

In addition, several esters with varying acyl chain lengths were prepared. Nucleophilic substitution of 10-bromodecanoic acid **102** gave 10-aminodecanoic acid **103b** in quantitative yield. Both free amines (**103a** and **103b**) were Boc-protected in equally good yields. Preparation of the esters was accomplished by using the Meldrum's acid approach and the appropriate alcohol. In the next step, the esters were tried to be hydrolysed to give the corresponding carboxylic acids. β -Ketoesters contain a very acidic proton that could be easily abstracted in the presence of a base and might lead to intramolecular ring closing. However, saponification of β -ketoesters with NaOH protocols can be found in literature.^{32,172} Dekhane and co-workers used this method to gain the free carboxylic acid which was coupled to (*S*)-homoserine lactone in the next step to obtain the AHL scaffold.¹⁷² Though, it is also stated in literature that the free carboxylic acid is not stable at room temperature.^{173,174} Nevertheless, saponification with LiOH and NaOH was tested with different esters.

Each saponification was carried out with LiOH and observed by mass spectrometry after a time period of 24 h and additional 24 h if necessary (see Table 3). Hydrolysis of the esters **105a** and **105b** did not lead to desired product.

Both reactions were carried out until the ester signal vanished. However, formation of the product could not be observed by mass spectrometry. Saponification of the methyl ester **105c** and four equiv. LiOH did not hydrolyse the ester. After addition of another five equiv. base and stirring for 24 h the product could be observed using mass spectrometry. As a consequence, 2 M aqueous HCl was added until a pH value of seven was reached. The solvent was then evaporated *in vacuo*. The crude residue was analysed but no product could be detected.

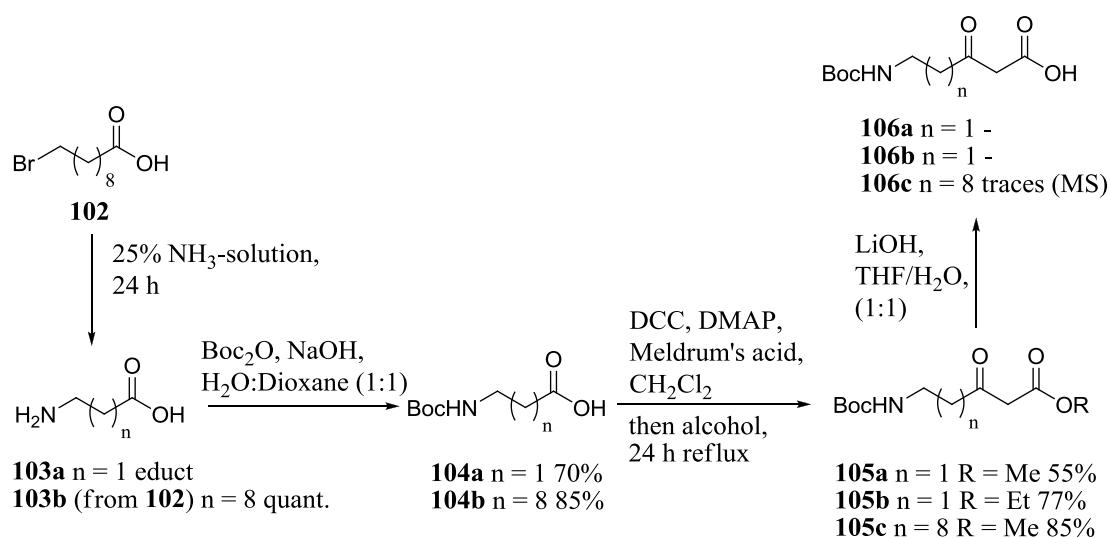


Figure 34: Synthesis of different diazirine precursors. The esters were prepared using the appropriate alcohol (MeOH, EtOH), respectively.

Compound	equiv. LiOH	time	result
105a	3	24 h	-
105b	25	48 h	-
105c	4	24 h	educt
105c	9	48 h	product only MS

Table 3: Saponification with LiOH. The product could only be detected by mass spectrometry.

These observations confirm the problems of β -ketoester hydrolysis described in literature. Though, Dekhane *et al.* published the preparation of AHLs using this method.¹⁷² In summary, these reaction conditions are not sufficient for the synthesis of a bifunctional AHL. Next to this route, another approach was designed using an azide moiety as photoactive group. The new route is depicted in Figure 35.

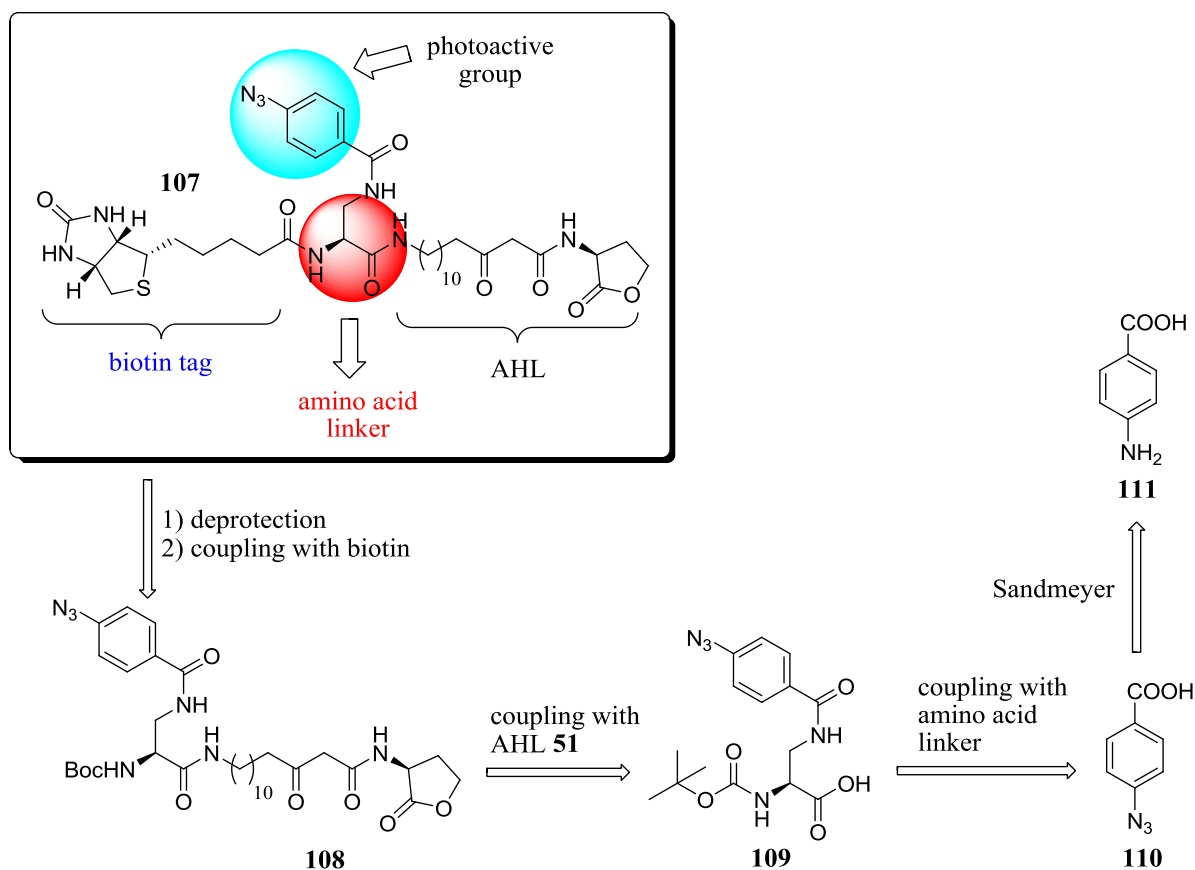


Figure 35: New approach to a bifunctional AHL.

In the first step, the commercially available amine **111** is converted to an azide by a Sandmeyer protocol to obtain the photoactive group **110**. Activation of the carboxylic acid **110** by NHS would allow coupling to an amino acid linker (*e.g.* Boc-Dap-OH **113**) and give intermediate **109**. AHL **51** could then be introduced either directly by EDC/HOBt coupling or through an NHS activated amino acid linker. Deprotection and additional coupling would lead to the bifunctional AHL **107**.

Figure 36 depicts the preparation of photoactive AHL **107** from starting compound **111**. The synthesis started with the preparation of azide **110** by a Sandmeyer protocol using NaNO_2 , NaN_3 and conc. HCl .¹⁷⁵ The photoactive azide **110** was obtained in quantitative yield. Preparation of the active ester **112** was accomplished in excellent yield. In the next step, commercially available Boc-Dap-OH **113** was coupled with **112** to give the photoactive amino acid linker **109** in very good yield of 85%. The synthesis of Boc-protected AHL derivative **108** can be achieved by utilising two different ways. First, a NHS strategy can be used to form the active ester **114** with DCC as a coupling agent. In addition, AHL mimic **51** is coupled to **114** to obtain **108** with 63% over two steps. The second way describes the direct coupling reaction of carboxylic acid **109** to AHL mimic **108**.

EDC/HOBt were used as coupling agents. After stirring for three days Boc-protected photoactive AHL **108** was gained in very good yield. Finally, **108** was deprotected using the established TFA approach to give the product as a TFA salt. In the second step, the product was treated with 0.1 M aqueous HCl to give **115** in 68% yield.

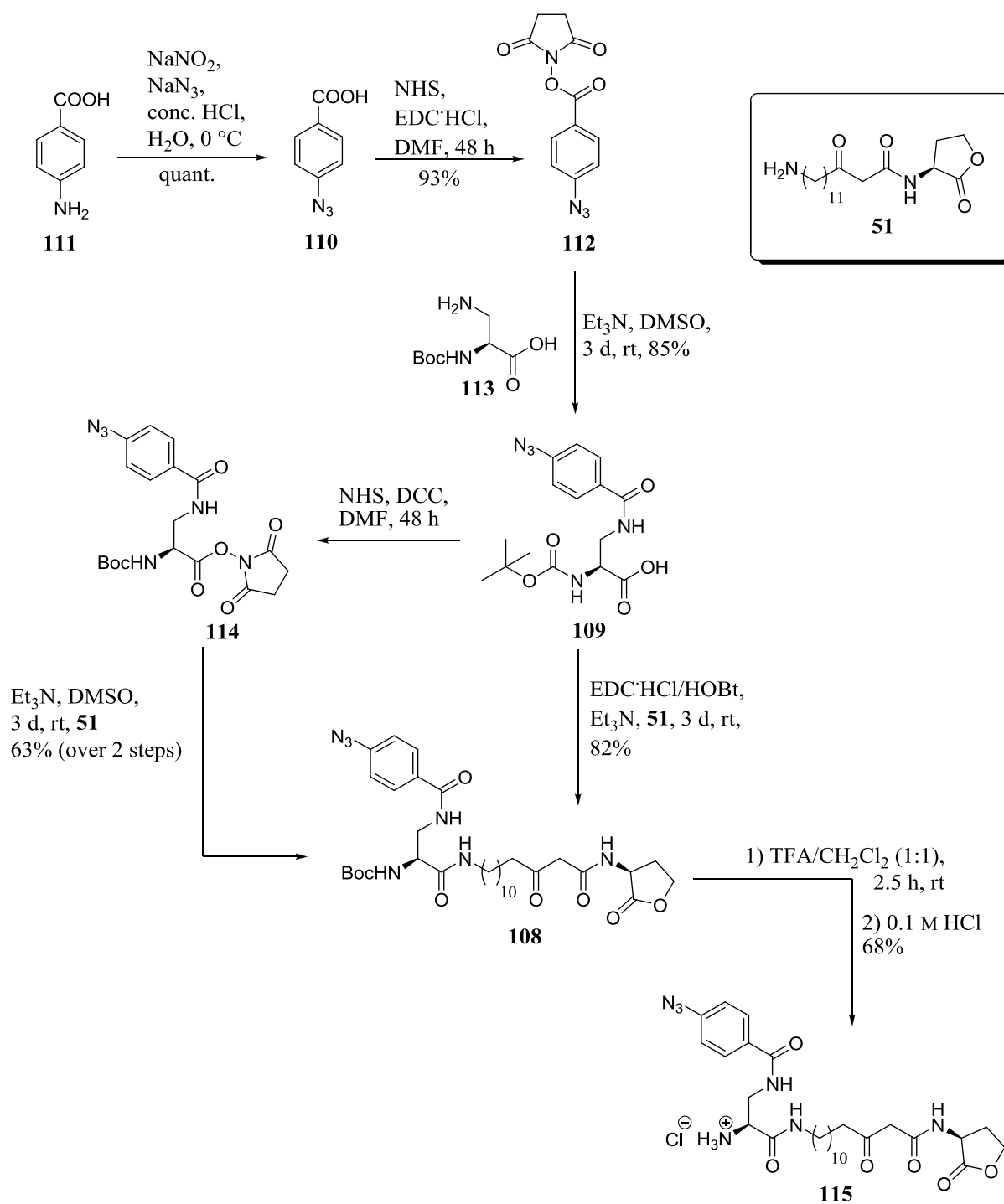
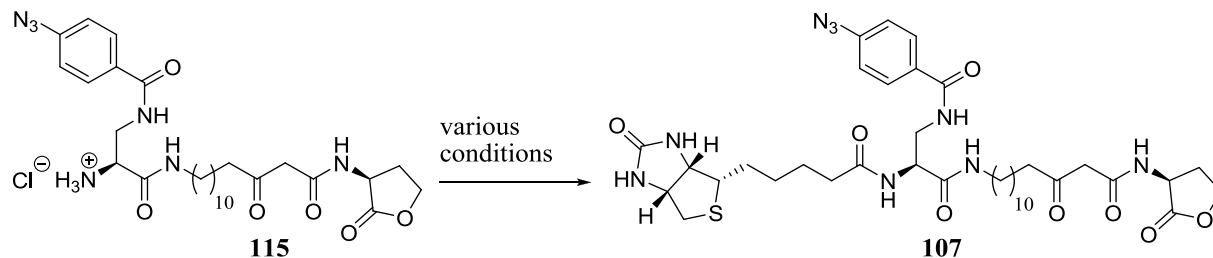


Figure 36: Synthesis of photoactive AHL **115**. Preparation of azide **110** is literature known.¹⁷⁵

For the preparation of the photoactive AHL **107** different coupling procedures were tested (see Table 4).



Entry	Conditions	result
1	Biotin-NHS ester, Et ₃ N (1.3 equiv.), DMSO, 3 d, rt	traces of product (MS)
2	Biotin-NHS ester, Et ₃ N (1.3 equiv.), DMSO, 5 d, rt	traces of product (MS)
3	Biotin, HOBt (1.4 equiv), EDC·HCl (1.4 equiv.), Et ₃ N (1.4 equiv.), DMF, 3 d	no product
4	Biotin-NHS, abs Et ₃ N (1.5 equiv.), abs DMSO, 3 d, rt	no product
5	Biotin-NHS, abs Et ₃ N (1.5 equiv.), abs DMF, 3 d, rt	no product
6	Biotin, HOBt (1.4 equiv), DCC (1.4 equiv.), Et ₃ N (1.4 equiv.), DMF, 4 d, rt	no product

Table 4: Reaction conditions for the preparation of biotinylated photoactive AHL **107**.

Different reaction conditions were tested to prepare biotinylated photoactive AHL **107**. The standard NHS ester approach (Table 4, entry 1 and 2) lead to traces of the product which were analysed by mass spectrometry. Column chromatography of the crude product did not lead to a purified fraction. Moreover, traces of the product could be found in each fraction by mass spectrometry. In addition, the coupling agents HOBt/EDC lead to complex mixtures which could not be analysed (entry 3). Other approaches were tested (entry 4-6) but did not lead to the desired product. Each reaction was observed by mass spectrometry but the product could not be detected.

The problem of these reactions could be steric hindrances, as the bulky photoactive moiety might shield the free amine of compound **115**. Biotin itself is also a bulky substance.

Figure 37 depicts another strategy to synthesis the desired product **107**. Deprotection of the photoactive linker **109** would give the free amine **116** which would be coupled to biotin. In the last step the AHL moiety would be inserted to give product **107**.

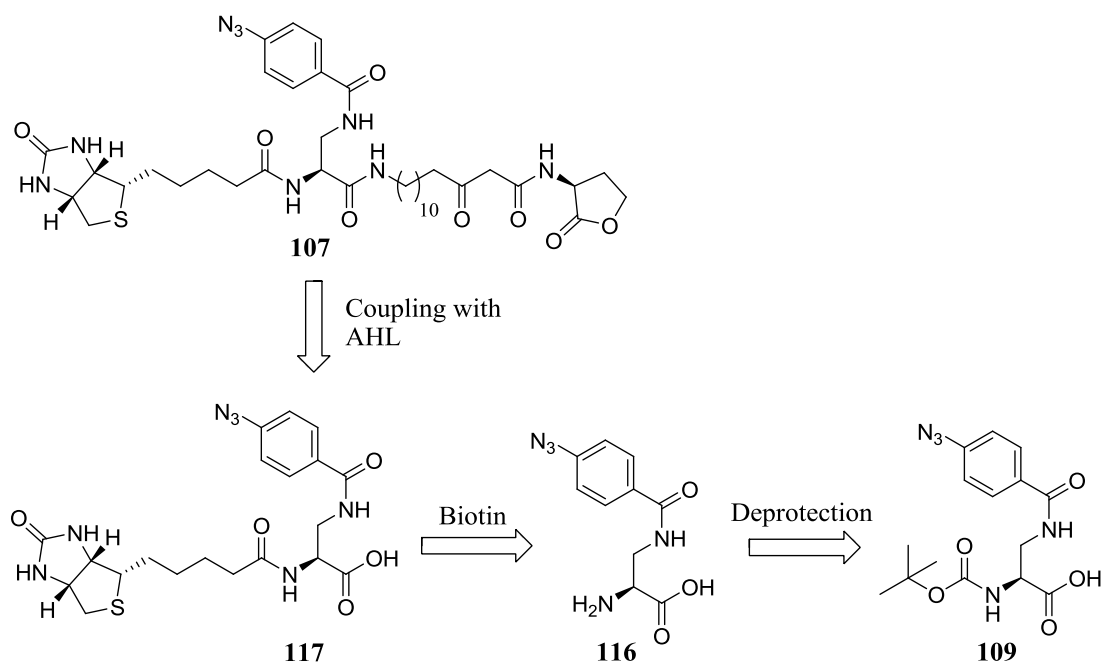


Figure 37: New approach to biotinylated photoactive AHL **107**.

Deprotection of the photoactive linker **109** was performed in very good yields (Figure 38).

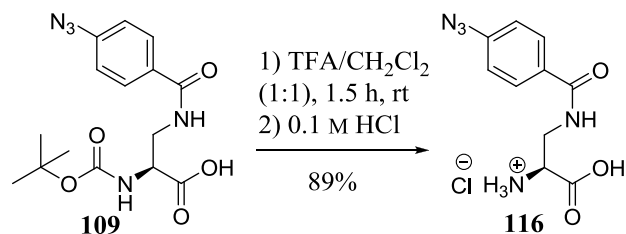
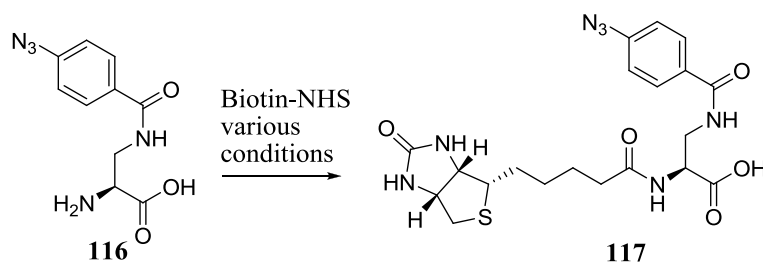


Figure 38: Deprotection of photoactive linker **109**.

In the next step, the biotin moiety was inserted using two different methods (see Table 5). Although some characteristic signals could be observed in the NMR spectrum, the desired product could not be seen in a mass spectrum. The coupling reaction of biotin to the photoactive linker **116** needs to be optimized. Other coupling agents like HOAt/DIC could be tested because they are used for coupling reactions of Boc-Dap-OH derivatives.



Entry	Conditions	Results
1	Et ₃ N (2 equiv), DMSO, 48 h	traces of crude product
2	Et ₃ N (3 equiv), dry DMF, 48 h	traces of crude product

Table 5: Preparation of biotinylated photoactive linker **117**.

4.5 Synthesis of AHLs for surface applications

Another approach for the affinity purification of bacterial and putative plant AHL-receptors is the preparation of AHLs immobilised on metal oxide surfaces (nanoparticles or bulk material). Catechol groups, phosphates or phosphonates are common surface anchors and have been widely used in literature for different applications.¹⁷⁶ Catechol derivatives bind strongly to various inorganic and organic surfaces *e.g.* noble metals, metal oxides, ceramics and polymers.^{177,178} For details on catechol immobilisation on surfaces see chapter 4.7. A library of AHLs containing these groups ought to be synthesised for further investigation.

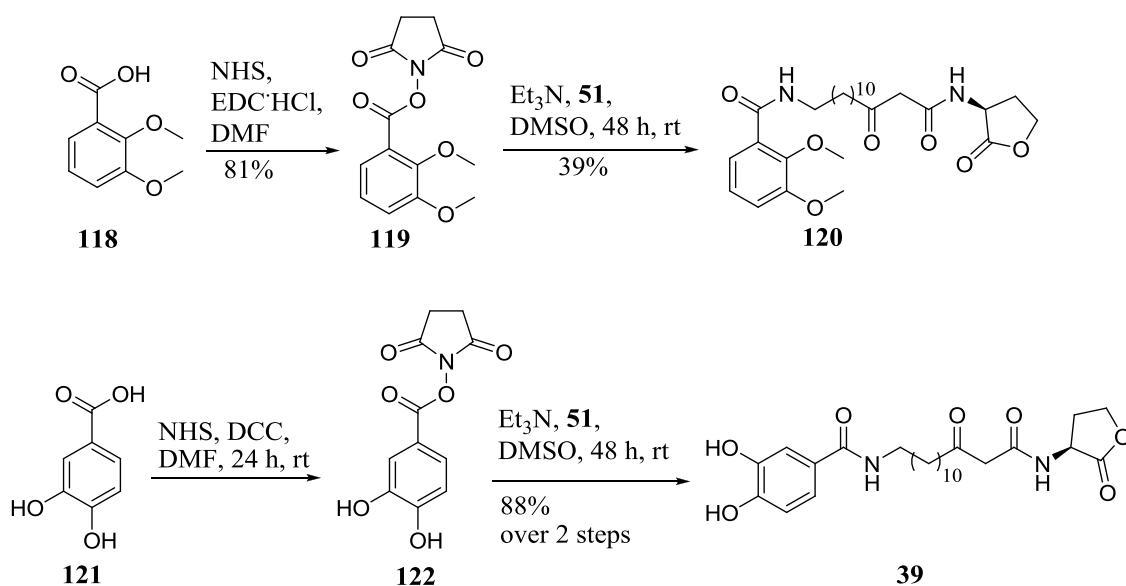


Figure 39: Preparation of several catechol-AHL.

The synthesis of several catechol containing AHLs is depicted in Figure 39. The carboxylic acids 3,4-dihydroxy benzoic acid **121** and 2,3-dimethoxy benzoic acid **118** are commercially available and were converted to the corresponding NHS ester **122** and **119**. In the next step the active esters **122** and **119** were conjugated to the 3-oxo-C14-AHL derivative **51**.

Additionally, catechol **125** was obtained by the 1,3-*Huisgen*-cylcoaddition (Figure 40). First, dopamine **123** was coupled to the NHS ester of 4-pentenoic acid **61** to give the intermediate **124** in good yields. The product **125** was synthesised in moderate yields using azide **60** and the established click reaction condition.

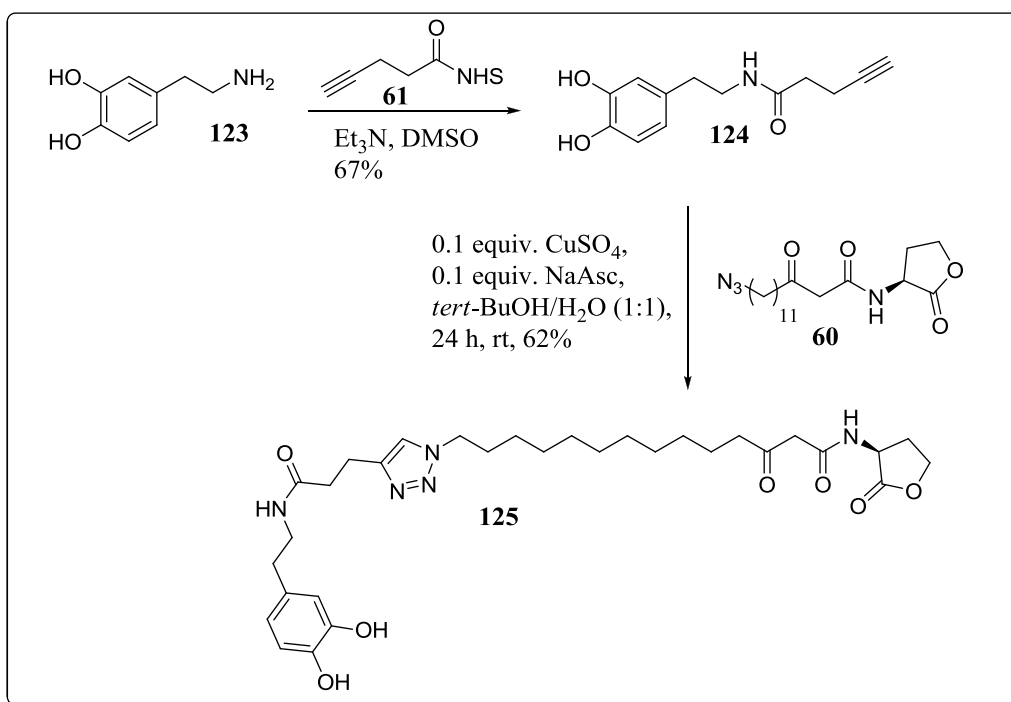


Figure 40: Preparation of compound **125** by click reaction.

Figure **42** shows two different approaches to synthesise catechol linker **128** from the starting material dopamine **123**. Dopamine is a neurotransmitter and is prepared from L-Tyrosine **126** by a metabolism reaction. The dopamine derivatives shown in Figure **41** could all be used as potential anchor groups.

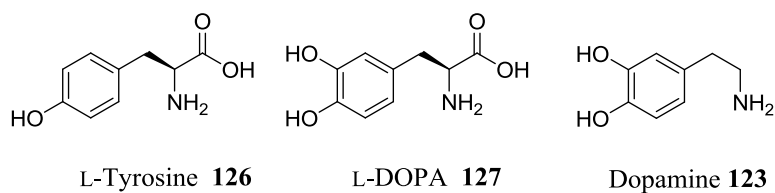


Figure 41: L-Tyrosine, L-DOPA and dopamine as potential anchor groups.

In the next step, the linker **128** would be converted into an active ester **130** for further coupling reactions. Because the preparation of catechol **124** using dopamine without protected hydroxyl groups worked very well, dopamine was used directly for the reaction with succinic anhydride. Pyridine was added and the reaction was stirred for three days. However, the product could not be detected by NMR or mass spectrometry.

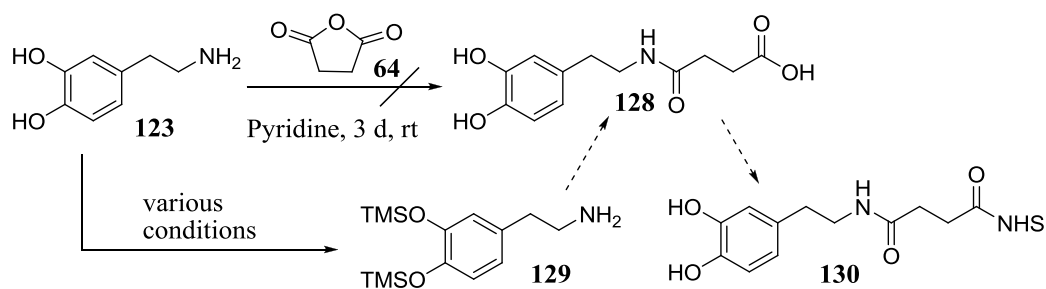


Figure 42: Two approaches to catechol linker **128** and active ester **130**.

At this point, one has to keep in mind that dopamine is easily oxidised under alkaline conditions and in the presence of oxygen. The catechol moiety forms a quinone **131** which starts a polymerisation reaction.¹⁷⁹ Polymeric dopamine **135** can form thin layers on different surfaces including glass, metals or ceramics.¹⁸⁰⁻¹⁸²

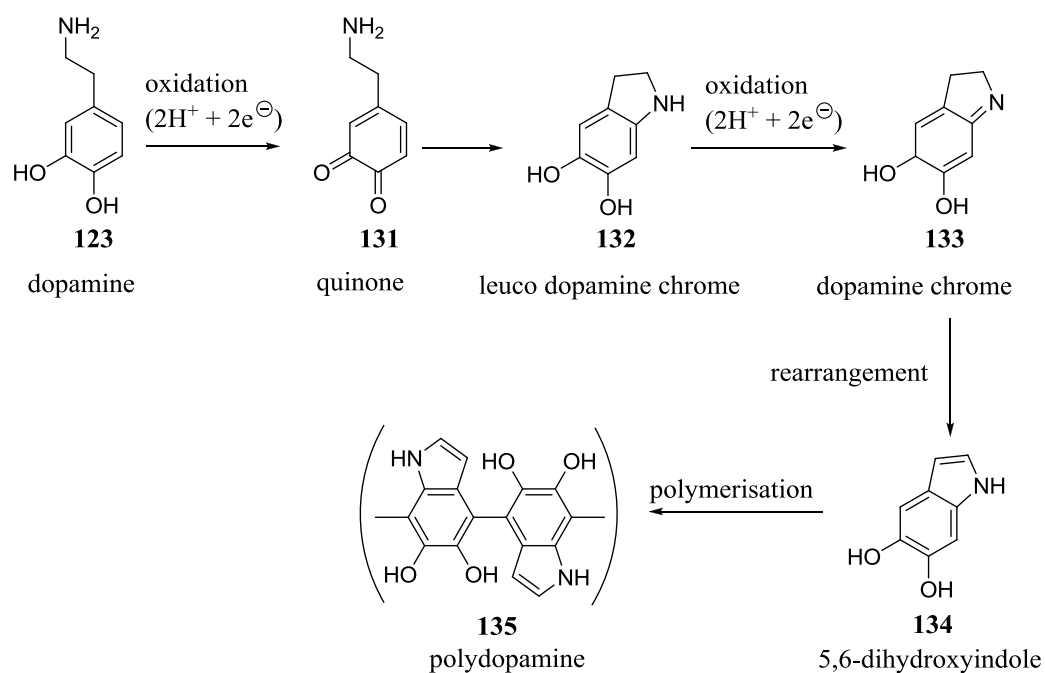


Figure 43: Formation of polydopamine by oxidation.

Protection of the amine function or hydroxyl groups should prevent oxidation to the quinone. The first catechol-AHL-derivatives have recently been introduced by Gademann. For the preparation of the autoinducers Gademann and contributors used TMS-protected dopamine.¹⁸³ Although, Gademann's TMS protocol was used only the educt could be re-isolated (Table 6, entry 1). The reaction conditions were modified changing the solvent from THF/DMSO to DMF and increasing the equivalents of TMSCl and base (entry 2 and 3). The reactions were controlled by TLC but only the educt could be detected after 24 h (entry 2). Therefore, additional five equivalents of TMSCl and imidazole were added and the reaction was stirred for another 24 h (entry 2) but the desired product could not be obtained.

entry	conditions	result
1	TMSCl (2.3 equiv), Imidazole (2.7 equiv) THF/DMSO, rt/22 h	educt
2	TMSCl (5 equiv.) Imidazole (5 equiv.), DMF, rt/24 h (TLC) after 24 h: (+ 5 equiv. TMSCl and imidazole, rt, 24 h)	educt
3	TMSCl (10 equiv.), Et ₃ N (10 equiv.) DMF, rt/3 d (TLC)	educt

Table 6: entry 1: TMS protection using Gademann's protocol; entry 2 and 3: reaction was controlled by TLC but only the educt could be protected.

Common anchor groups are phosphonic acids and esters for surface immobilisation. Over the last decades several research groups have demonstrated that phosphonic acids react with a wide range of metal salts and oxides building 1D or 3D metal organic frameworks (MOFs) which are called "metal phosphonates".¹⁸⁴ The phosphonic acid moiety was often found to be superior to other inorganic substrates because of the high stability of the metal-O-P bond. The only exceptions are glass and silica surfaces for which silane groups are the functional groups of choice.^{184,185}

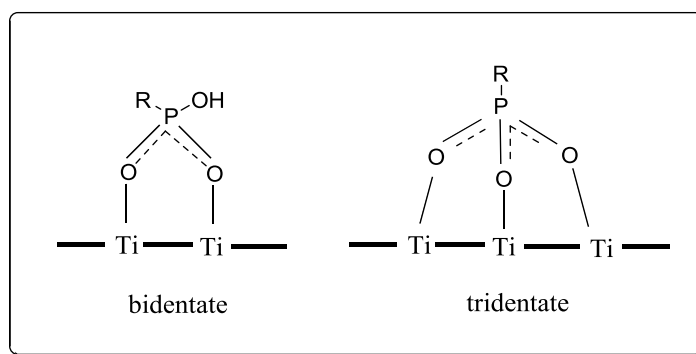


Figure 44: Main bonding modes of diethylphosphonate compounds on a TiO_2 surface.¹⁸⁶

Geminal bisphosphonates show an even higher binding stability towards inorganic surfaces compared to their monophosphonic analogues. These compounds are structurally related to inorganic pyrophosphate **136** but have a methylene group (P-C-P) replacing the oxygen bridge between the phosphorus atoms (P-O-P) increasing their stability towards chemical hydrolysis and making them completely resistant against enzymatic hydrolysis.^{184,185} Bisphosphonates are particularly interesting pharmacological compounds because they exhibit a strong binding affinity for bones and are used for treatment of bone disorders *i.a.* Paget's disease, osteoporosis or tumor induced osteolysis. Recent investigations have shown that bisphosphonates also inhibit growth of cancer cells and promote their apoptosis. Though, these molecules are widely used in medicine, they possess a low biological availability (less than 1% of the oral dose) because of their poor lipophilicity and the presence of negative charges at physiological pH value.¹⁸⁷

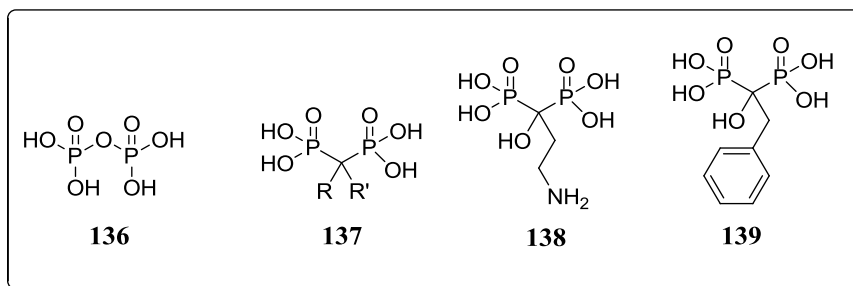


Figure 45: Pyrophosphate **136**; general structure of *gem*-bisphosphonates **137**; bisphosphonates clinically in use: pamidronate **138** and risedronate **139**.^{185,187}

As mentioned before the P-C-P bridge of bisphosphonates was found to be relatively stable against chemical hydrolysis. However, in 2008 Turhanen and contributors published results showing the degradation of a novel etidronate derivative **140** under mild basic conditions (Figure 46).¹⁸⁸

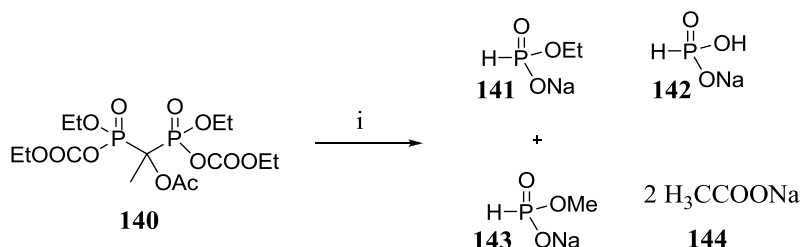


Figure 46: Degradation of bisphosphonate **140** to acetate **144** and phosphites **141** - **143**; i) 4 equiv. NaOH (40% NaOH in H₂O), MeOH, 30 min, rt.¹⁸⁸

The synthesis of AHL-derivative **148** started from commercially available diethyl phosphonoacetic acid **145** which was converted to the NHS ester **146** in excellent yields. The desired product **148** was obtained by NHS ester coupling of amine **51**. **148** can also be prepared by coupling diethylphosphonoacetic acid directly to the free amine **51** with EDC/HOBt as coupling reagents.

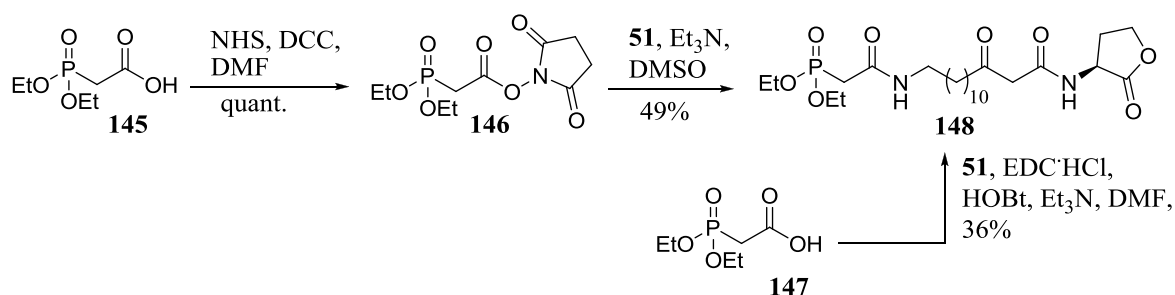


Figure 47: Synthesis of the first phosphonate AHL **148**.

The 1,3-*Huisgen*-cycloaddition had already been used several times for the preparation of AHL derivatives and is again a versatile tool for the synthesis of phosphonate AHLs (Figure 48). The precursor azide **150** was prepared from 3-bromo-1-propen-phosphonoacid-diethylester **149** in excellent yields. At first, the established click reaction conditions (CuSO₄, NaAsc, *tert*-BuOH/H₂O) were used for the synthesis of **151** but only traces of the product could be detected by mass spectrometry. For the second attempt TBTA was added to accelerate the reaction and stabilise the Cu(I) oxidation state in aqueous medium. The TBTA acts as a tetradentate ligand and blocks the coordination sites at the metal centre before oxidants can attack forming a copper (II) ion.¹⁸⁹ The product was obtained in good yields.

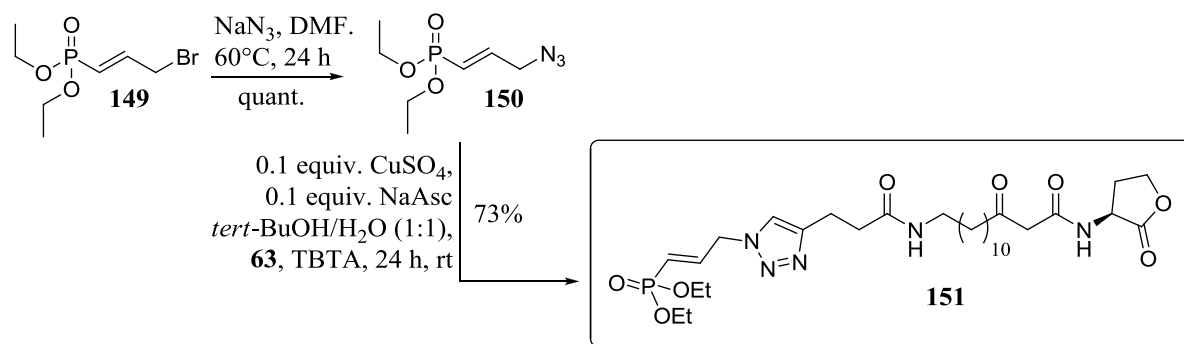


Figure 48: Preparation of AHL derivative **151** by click reaction.

The aza-Michael addition is a commonly used method for the introduction of two phosphonate groups to a free amine.¹⁹⁰ Figure 49 depicts the test reaction between benzylamine **55** and two equivalents of diethylvinylphosphonate **152**. After stirring for 24 h the product **153** was obtained in excellent yields.¹⁹⁰

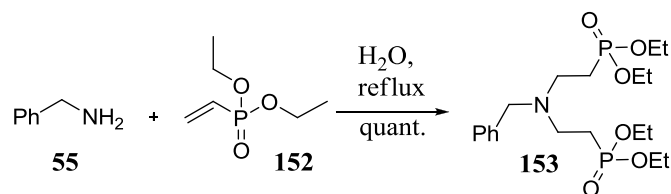
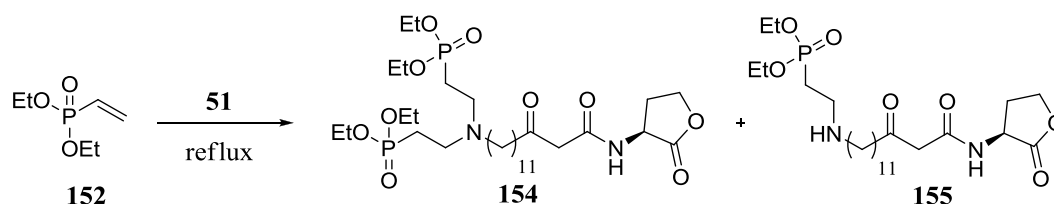


Figure 49: Preparation of literature known compound **153** as a test reaction.¹⁹⁰

Slightly modified conditions (Table 7, entry 1) were used to conjugate two phosphonate groups to AHL derivative **51** by an aza-Michael addition. After 24 h two more equivalents of diethyl vinylphosphonate **152** were added because at this point only the starting materials could be detected by mass spectrometry. However, after additional 24 h of stirring the product **154** could still not be observed. One reason might be the high amount of base added to the reaction. So for the second approach the equivalents were reduced to one making sure the pH did not exceed a value of 8 (entry 2). In addition, more EtOH was added increasing the solubility of AHL **51**. After three days of stirring traces of diethyl vinylphosphonate **152** as well as compound **154** and **155** could be detected by mass spectrometry.



entry	152 (equiv. in total)	solvent	base (equiv. Et ₃ N)	time (in total)	154	155
1	4	H ₂ O/EtOH (9:1)	1.5	48 h	-	-
2	4	EtOH/H ₂ O (9:1)	1	3 d	traces (MS)	traces (MS)
3	4	EtOH	1	5 d	-	89%
4	4	BuOH	1	3 d	-	-
5	4	<i>tert</i> -BuOH	1	3 d	-	-

Table 7: Evaluation of the aza-Michael addition for the preparation of phosphonate-AHL derivatives.

For the third approach only EtOH (entry 3) was used as a solvent and the reaction was controlled by mass spectrometry. After three days the double and mono substituted products **154** and **155** as well as the starting material **152** could be detected. Two equivalents of diethyl vinylphosphonate **152** were added and the reaction was stirred under reflux for two more days. A new mass spectrum revealed that the mono substituted product **155** had formed but no double substituted product **154** could be detected anymore. The raw product was purified by column chromatography giving 89% of the desired product **155**. Changing the solvent to BuOH and *tert*-BuOH did not lead to neither products (entry 4 and 5).

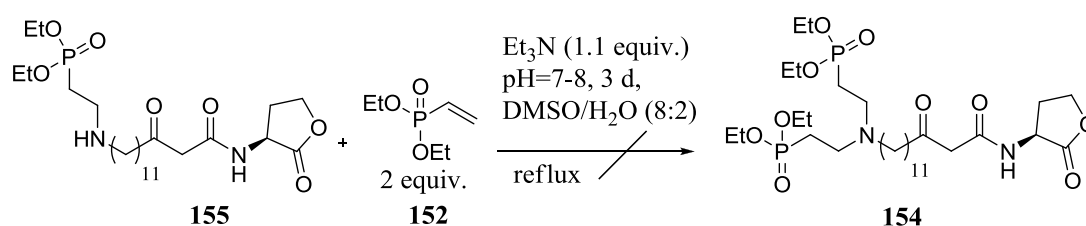
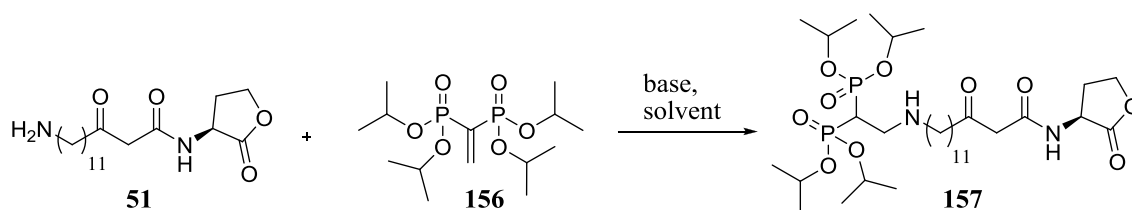


Figure 50: aza-Michael addition with DMSO/H₂O.

In literature aza-Michael additions which lead to the double substituted product are sometimes carried out using water as a solvent.¹⁹⁰ Therefore, DMSO/H₂O were used as solvents but after stirring for three days no product **154** could be detected.

The aza-Michael reaction was also applied to the synthesis of a bisphosphonate AHL derivative **157**. Standard conditions with H₂O as a solvent were used for the first approach (Table 8, entry 1) but only traces of the product could be detected. Houghton and colleagues conjugated different phosphonates to free amines using DMAP as a catalyst and dry CH₂Cl₂ as a solvent.¹⁹¹ Following this route, traces of bisphosphonate AHL derivative **157** could be detected (entry 2).



entry	solvent	base	temp	time	result
1	H ₂ O	Et ₃ N (1.2 equiv.)	reflux	48 h	traces (MS)
2	dry CH ₂ Cl ₂	cat. DMAP	rt	3 d	traces (MS)

Table 8: Synthesis of bisphosphonate AHL derivative **157**.

Pamidronate **138** is one of the most prominent examples from the bisphosphonate family.^{192,193} Because of its free hydroxyl groups it is quite difficult to handle during synthesis. In a test reaction NHS-ester **66** ought to be coupled to the free amine of pamidronate **138** under basic conditions. However, there was no product to be isolated. The main reason for this result might be that higher alkaline conditions are needed as the pamidronate **138** is a very strong phosphonic acid. In literature coupling reactions with pamidronate are carried out using high amounts of NaOH to deprotonate the free hydroxyl groups. Admittedly, these conditions cannot be applied because the lactone moiety would hydrolyse. Therefore, it would be more practical to work with protected bisphosphonates and try to deprotect the hydroxyl groups after coupling to the AHL.

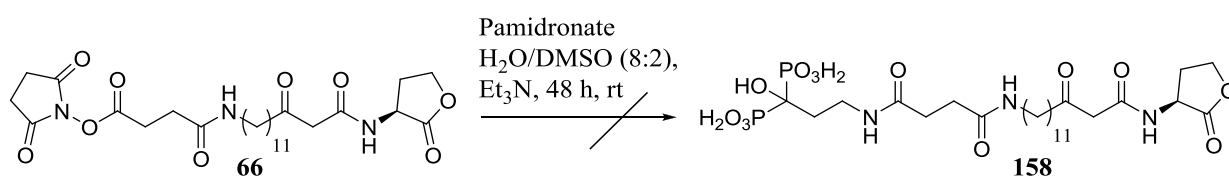
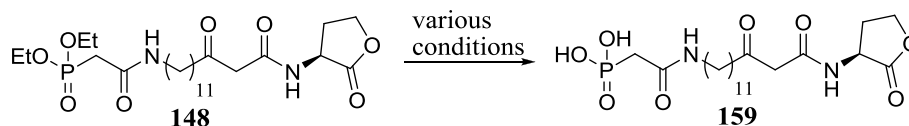


Figure 51: Failed synthesis of pamidronate-AHL **158** (Pamidronate had been prepared before by E. Franzmann).

For the immobilisation on metal oxide surfaces the phosphonate-AHL derivatives have to be deprotected to give the free acids. Various conditions were carried out but none of them led to the desired product **159** (Table 9).



entry	conditions	temp	result
1	conc. HCl	reflux	no product
2	conc. HCl, formic acid	reflux	no product
3	conc. HCl, acetic acid	reflux	no product
4	TMSBr, dry CH ₂ Cl ₂ , Ar	rt	no product
5	TMSBr, dry CH ₂ Cl ₂ , allyltrimethylsilane, Ar	rt	no product

Table 9: Deprotection of the esters.

Although, AHL are generally stable in the presence of strong acids the use of conc. HCl under reflux lead to complex mixtures that could not be analysed. Formic acid and acetic acid were added to increase the solubility of the educt AHL **148**. The common method in literature to hydrolyse the esters is the use of TMSBr.^{194,195} However, TMSBr might also be too strong for the AHL scaffold because neither the product nor the educts could be isolated. The evaluation of the deprotection reaction has to be carried out in future to establish a new set of autoinducers which might be immobilised on metal oxide surfaces.

All three strains were treated with five native AHL molecules (C6-HSL, oxo-C₍₈₋₁₄₎-HSL). AHLs were dissolved in acetone (except **53** which was dissolved in DMSO) and applied to lawns of reporter bacteria in different concentrations. GFP signals were recorded 2 h after application.¹⁵⁸ Analysis of the obtained results revealed that reporter bacteria slightly differ in their AHL perception. While *P. putida* recognizes oxo-C10-AHL to oxo-C14-AHL, *E. coli* perceives oxo-C8-AHL but also all other tested native AHLs. *E. coli* and *P. putida* also recognise oxo-C14-AHL. In the next step it was investigated, whether the three bacterial strains recognise the modified oxo-C14-AHL derivatives. *P. putida* recognizes **49** in a similar concentration range as oxo-C14-AHL as well as **51** and **52** at high concentration. *E. coli* on the other hand, recognizes **51** and **53** comparably to oxo-C14-AHL. *E. coli* also recognized **52** and **78**, though only at high concentration. *S. liquefaciens* recognises **51** and **52** only at high concentrations.¹⁵⁸

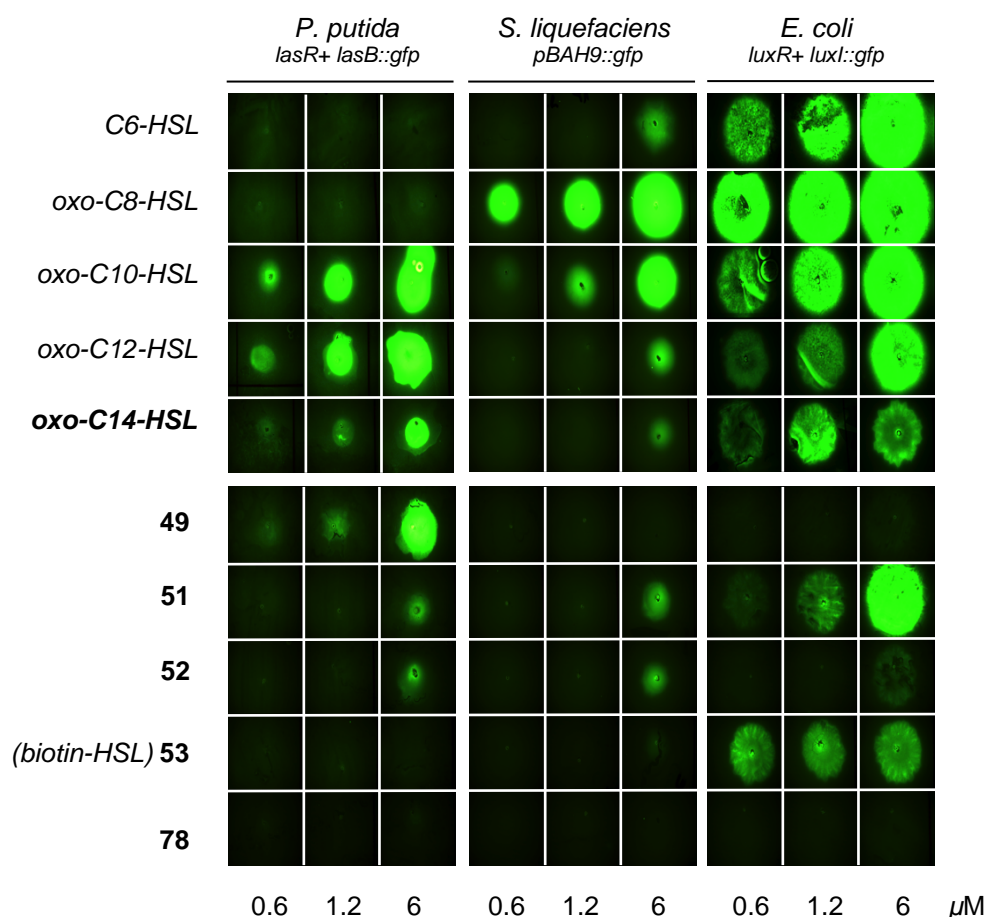


Figure 53: Detection of non-natural AHLs with biosensor bacteria. GFP signals were observed with fluorescence binocular using GFP filter Em: 505 – 550 nm.¹⁵⁸

In order to verify the potential of biotinylated AHL **53**, an exploratory pull-down experiment with a member of the LuxR AHL-receptor family (Sinme_0536) from *Sinorhizobium meliloti* was performed. *S. meliloti* is a soil borne bacterium known to produce and perceive oxo-C14-AHL.¹⁹⁹ Sinme_0536 was cloned and purified as 6xHis-tagged recombinant protein. Using streptavidin-coated beads, it was attempted to precipitate LuxR protein in the presence of solely biotin (negative control, lane 1) or in the presence of **53** (lane 4). As an additional control a pull-down setup without 6xHis-Sinme_0536 was used (lane 2). Proteins pulled down in the presence of **53** were probed for the occurrence of 6xHis-Sinme_0536 with a specific anti-His antibody. In the presence of **53** (lane 4) but not free biotin (lane 1) 6xHis-Sinme_0536 was found in the precipitate (α His, lane 4). In addition, this protein was precipitated from a sample mixed with the total *Arabidopsis* protein extract (lane 3), showing that the specific interaction of the ligand **5** and target receptor (LuxR) allows a pull-down even in the presence of a complex protein matrix.¹⁵⁸

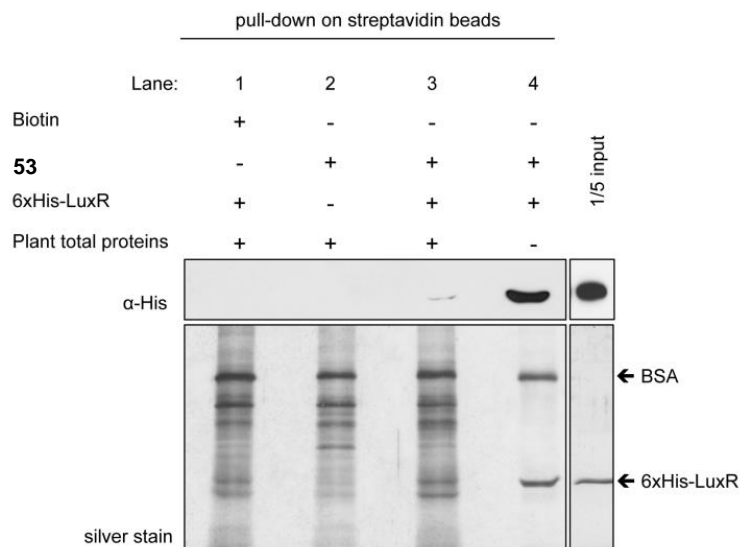


Figure 54: Pull-down of the His-tagged oxo-C14-AHL receptor 6xHis-LuxR from *S. meliloti*. The biotinylated AHL-derivative **53** was immobilized on streptavidin beads, which were pretreated with BSA to minimize unspecific protein binding. Protein bands were visualized with silver stain and 6xHis-LuxR was detected by a His-specific antibody (α -His). BSA: bovine serum albumin.¹⁵⁸

Plants are sessile and have therefore developed a broad range of defence reactions to pathogens. Recent reports suggest that AHLs produced by soil bacteria can actively affect plant health and development.^{104,153,154,200}

An early plant response to pathogen attack is transcriptional activation of defense related genes. Among them are pathogen-inducible WRKY transcription factors which form a superfamily of proteins with up to 100 representatives in *A. thaliana* and have to date only been found in plants. The WRKY family is among the 10 largest families of transcription factors in higher plants. The most important structural element of WRKY transcription factors is their DNA binding domain, also called the WRKY domain. It is defined by the amino acid sequence *WRKYGQK* at its *N*-terminus and a zinc-finger motif. Its cognate binding site is called “W box”.²⁰¹⁻²⁰³ The WRKY transcription factors are activated (phosphorylated) by Mitogen-Activated Protein Kinases (MAPK) which are key elements in early defense signaling.

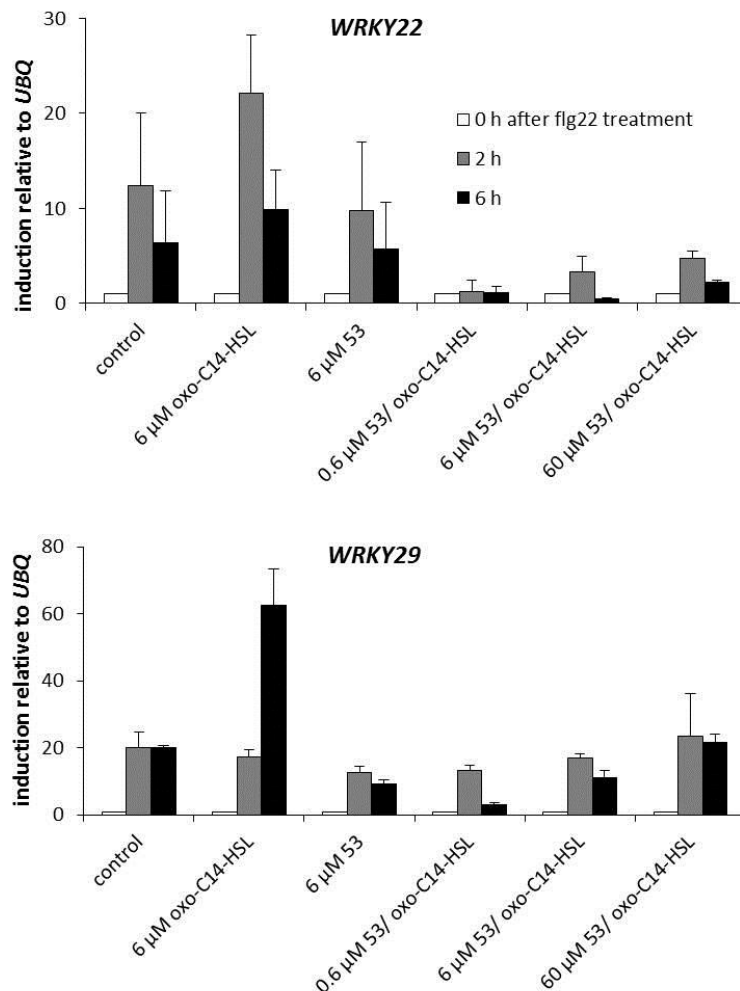


Figure 55: The biotinylated AHL derivative **53** acts as an antagonist for plant AHL-induced resistance responses, measured by the transcriptional activation of plant transcription factors WRKY22 and WRKY29 in the presence of the natural autoinducer oxo-C14-AHL and the modified analogue **53**. Error bars represent SD.¹⁵⁸

Consistent with this, MPK6 is activated (phosphorylated) by MKK4/MK5 due to a combined treatment of *A. thaliana* with oxo-C14-AHL and the bacterial signal molecule flg22 (flagellin 22). In the next step MPK6 phosphorylates *WRKY22* and *WRKY29* which leads to a positive feedback loop by *WRKY22* and *WRKY29* activating the transcription of themselves. This positive feedback loop is the observed transcriptional upregulation of both *WRKY22* and *WRKY29*.²⁰⁴⁻²⁰⁷ The longer activation of MAPK6 is the molecular base for AHL-induced resistance.¹⁵⁴ Bacterial flagellin triggers defence responses in various plants. “flg 22” is a 22-amino acid peptide from a conserved flagellin domain. It is able to activate the fast transcriptional induction of at least 1.100 *A. thaliana* genes.²⁰⁸ In order to compare the activity of native oxo-C14-AHL and its derivatives, the impact of **53** on the relative expression levels of *WRKY22* and *WRKY29* (Figure **55**) was examined.¹⁵⁸ Two-week-old *Arabidopsis* seedlings were pretreated with 6 μ M oxo-C14-AHL (positive control), AHL derivatives or combinations of both and subsequently treated with 100 nM flg22. Total RNA was extracted and transcript levels of *WRKYs* normalized to the expression of *UBQ4* (*At5g25760*). Pretreatment with the AHL followed by treatment with 100 nM flg22 resulted in upregulation of *WRKY22* and *WRKY29* (Figure **55**). In contrast, pretreatment with modified AHL derivative **53** had no impact on *WRKYs* expression pattern. Notably, however, when **53** was added in addition to oxo-C14-AHL the observed AHL effect was abolished. It can be suspected that **53** is an antagonist to oxo-C14-AHL in plants. Given the fact, that **53** induced GFP expression in bacterial reporter strains (agonistic action) this antagonistic effect in plants is remarkable. It is likely that **53** binds to the cognate AHL receptor(s) preventing oxo-C14-AHL binding and initiation of defence priming in the plant. Whether **53** is a direct antagonist will have to be investigated in future.¹⁵⁸

The following non-natural AHLs (Figure **56**) have also been investigated according to their biological activities.

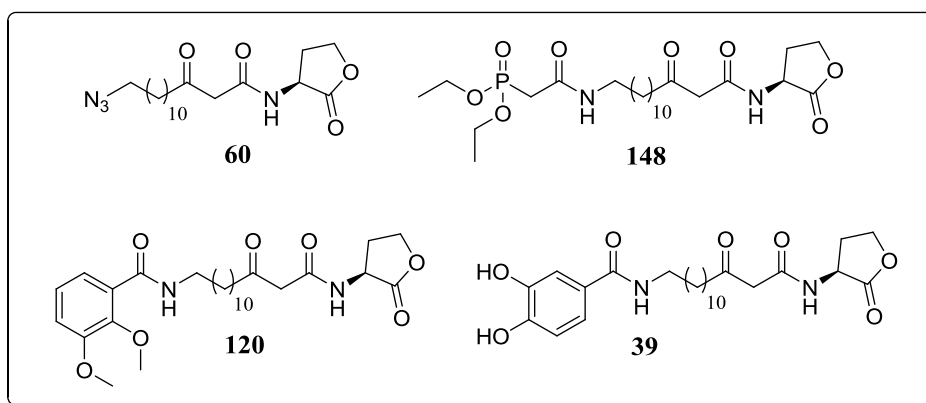


Figure 56: Several modified AHLs that were tested for their biological activities.

Consequently, it was tested whether the novel AHLs **60** – **39** are still recognised by bacteria. In accordance with the above-mentioned test *E. coli* (MT102 GFP pJBA89) carrying the *Green Fluorescent Protein* was used for the visualisation (Figure 57). AHLs **60** and **39** are recognised by the bacterium, while 120 and 148 only show a weak fluorescence at high concentrations. The bacterium does not recognise the protected catechol AHL derivative **120** while **39** containing the free hydroxyl groups is recognised even at low concentrations.

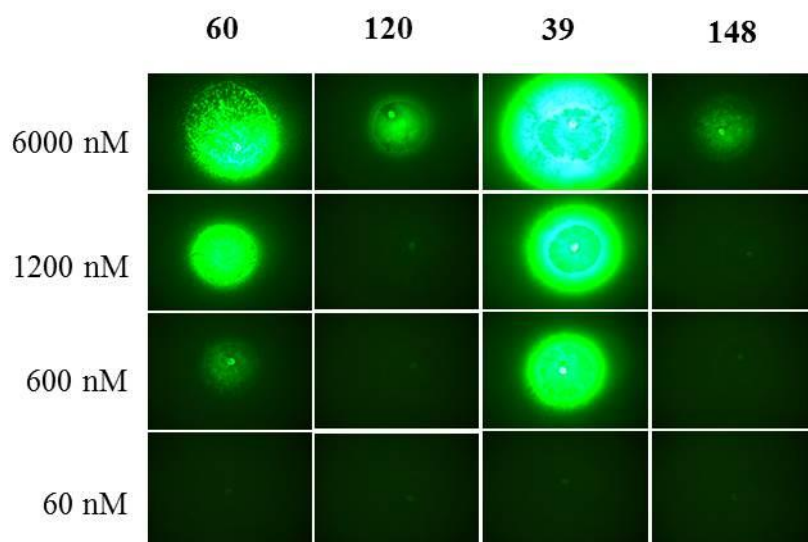


Figure 57: Detection of non-natural AHLs with a biosensor *E. coli* strain. GFP signals were observed with fluorescence binocular using GFP filter Em: 505 – 550 nm

In accordance with the above mentioned *WRKY* test another one was performed investigating possible induced resistance reactions due to the modified AHLs **60** – **148** (Figure 58): Two-week-old *Arabidopsis* seedlings were pretreated with 6 μ M oxo-C14-AHL (positive control), AHL derivatives and were subsequently treated with 100 nM flg22. Total RNA was extracted and transcript levels of *WRKY*s normalised to the expression of *UBQ4* (*At5g25760*). There is no significant impact seen of the modified AHLs compared to the native ligand (control) in the *WRKY22* expression pattern. However, an upregulation can be observed for all AHL-derivatives if compared to the control group. Compound **60** shows a high upregulation even 6 h after flg 22 treatment compared to the other derivatives and the control group.

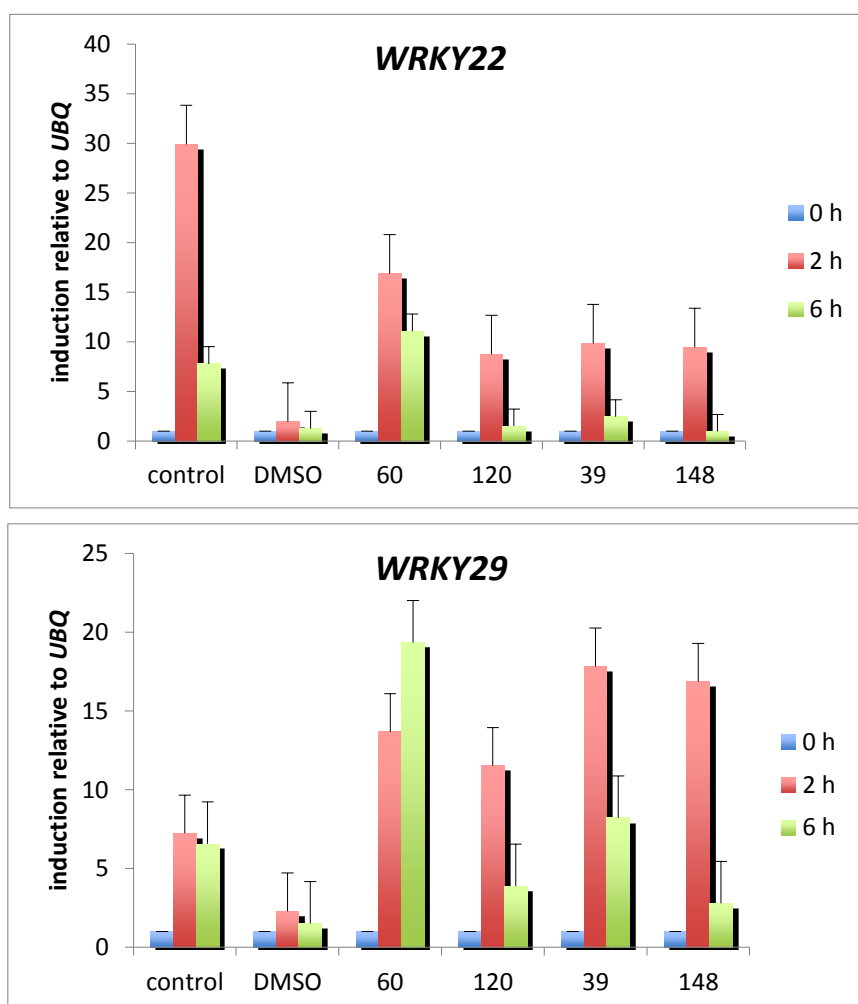


Figure 58: Impact of modified AHLs **60** – **148** on the relative expression levels of *WRKY22* and *WRKY29*.

4.7 Immobilisation of catechol-AHL derivatives on TiO₂ nanoparticles

4.7.1 The catechol-TiO₂ System

Catechols have been key components as surface anchors since the first so called mussel adhesion protein (MAP) was found and investigated.^{182,209,210} Many marine organisms *e.g.* mussels have developed excellent strategies to stick on different surfaces in their environment like stones and wood. The mussel adhesion protein enables permanent adhesion to these surfaces and was first discovered by Brown.²¹¹ However, the molecular structure or functional group that is responsible for the strong binding affinity had not been identified. Waite and contributors were the first to decipher the constitution of the “adhesion protein” and discovered a high amount of L-DOPA (3,4-dihydroxyphenyl-L-alanine) in the protein structure.^{212,213}

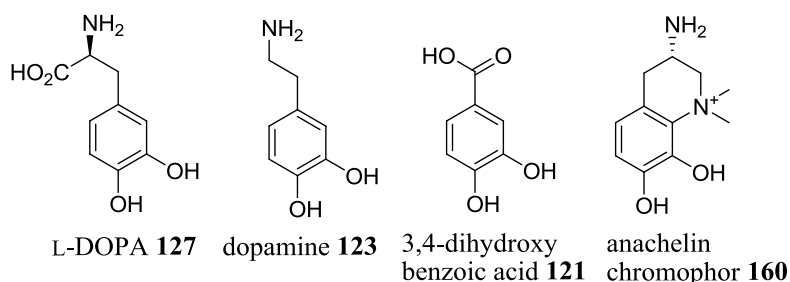


Figure 59: Selected catechol anchors.¹⁷⁶

Although catechols have often been used as anchor groups, the exact binding mechanism between the catechol and the TiO₂ surface remained vague for a long time. Deprotonation of the catechol is necessary for immobilisation on TiO₂ as stated by Grätzel and co-workers.²¹⁴

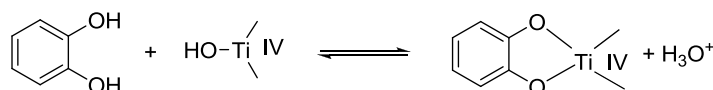
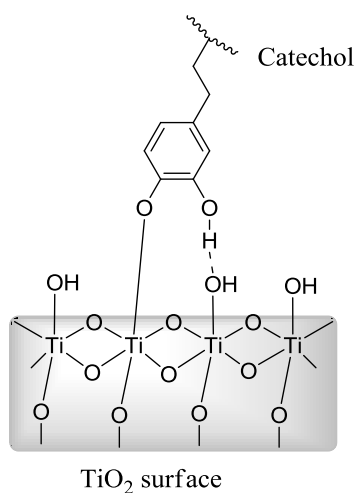


Figure 60: Deprotonation of the catechol moieties for TiO₂ surface binding.

Detailed investigation of the immobilisation of dopamine derivatives on TiO_2 surfaces finally lead to the decipherment of the adsorption mechanism. Catechols form a monodentate or a bidentate bond to Ti atoms on surfaces. In the case of a monodentate bond a hydrogen bond is formed between one hydroxyl group of the catechol whereas the second hydroxyl group forms a covalent bond to the Ti-atom. Bidentate binding of a catechol is characterised by two binding modes, chelation and formation of a “bridge” to the Ti-atoms.^{215,216}

molecular adsorption, monodentate binding



bidentate binding to surface

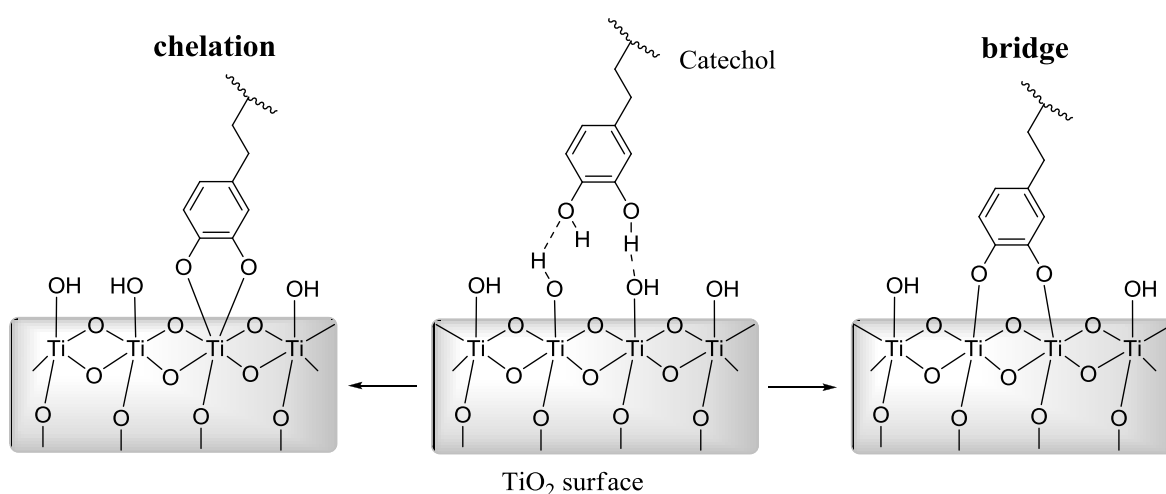


Figure 61: Monodentate and bidentate binding modes for catechols on TiO_2 surfaces.

Derivatives of dopamine favor the chelate bond while other catechol compounds prefer the formation of a bidentate bridge after deprotonation. The bonding mode also depends on the modification of the TiO₂ surface (rutile or anatase).^{215,216}

Recently, TiO₂ nanoparticles were modified with the dye Alizarin Red S and have been used as probes to gain insight into nanoparticle uptake and distribution within the plants.²¹⁷ Gademann and colleagues were the first to immobilise AHL derivatives on TiO₂ beads using catechols as anchor molecules. These functionalised TiO₂ beads could be used for a controlled release of autoinducers modulating QQ and therefore prevent bacterial biofilms.¹⁸³ However, the immobilisation and controlled release of AHLs from a metal oxide could also be useful for the promotion of QS. Fertilizer sticks coated with plant beneficial autoinducers could be prepared. In addition, nanoparticles bound to AHLs could be utilised for the identification and purification of plant receptors by affinity or size exclusion chromatography. Herein, the immobilisation of catechol AHL derivative **39** on TiO₂ nanoparticles (P25) is described as well as the characterisation by different analytical techniques. TiO₂ exists in three modifications: rutile, anatase and brookite. TiO₂ nanoparticles can mainly be found in the anatase modification, while the constitution of bulk TiO₂ is rutile.^{218,219}

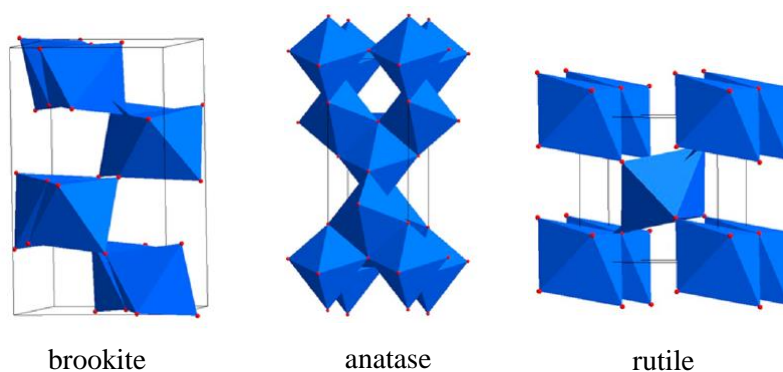
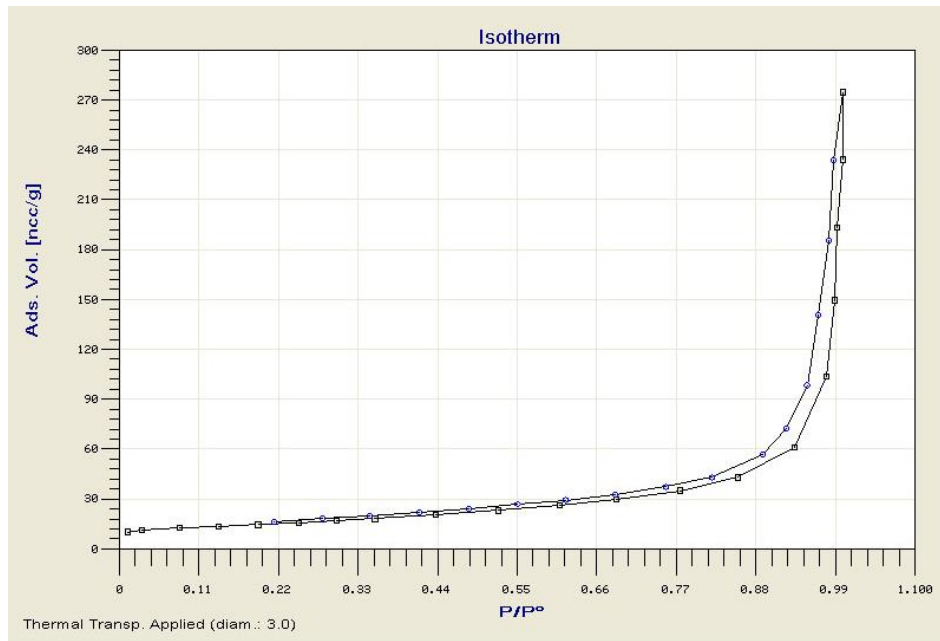


Figure 62: Unit cell structure of TiO₂ anatase, rutile and brookite.²²⁰

4.7.2 Immobilisation of AHL derivative 39 on TiO₂ (P25) nanoparticles

BET

Before starting off with the immobilisation of a catechol containing AHL on TiO₂ nanoparticles the specific surface area of the purchased nanoparticles had to be determined. This value is necessary to calculate how many molecules are needed to fully cover the surface of a certain amount of nanoparticles. Sometimes agglomeration of the particles is possible. The adhesion of atoms, ions or molecules from a gas, liquid or dissolved solid on a surface is called adsorption and can be divided into chemisorption and physisorption. This process creates a film of the adsorbate on the surface. Chemisorption describes the chemical reaction between a surface and the adsorbate. New chemical bonds (often covalent bonds) are formed while physisorption (also physical adsorption) involves the interaction between the adsorbate and the surface by Van-der-Waals forces.²²¹ Desorption of the adsorbate (either chemically or physically adsorbed) always needs a certain activation energy. A dynamic equilibrium is formed between the free gas molecules and the adsorbed particles which can be described by the so called adsorption isotherms as a function of pressure or concentration at a constant temperature. The simplest example for adsorption of gases on surfaces is expressed by the Langmuir Isotherm: Here, each adsorption site is equivalent to the other and only has the capacity for one adsorption molecule. In addition, only one monolayer is formed. However, each new layer of adsorbate is actually a new surface on which molecules or particles can be adsorbed.²²¹ The Brunauer-Emmett-Teller (BET) isotherm takes this problem into account. It is the technique of choice to determine the specific surface area of an adsorbant.²²² TiO₂ (P25) nanoparticles were analysed and the specific surface area 51.2708 m²/g was obtained. Figure 39 shows the isotherm and the results of the analysis.



Surface area calculation

Calculation method:	B.E.T.
Range for Calculation (P/P°)	.05 - .3
Monolayer Volume (ncc/g):	11.78381
Specific Surface Area (m ² /g):	51.2708
Correlation Factor:	.999919
C Value of BET Equation:	1023.085
Pore Specific Volume (cm ³ /g):	.2555
Pore Specific Volume at P/P°:	.99

Figure 63: BET isotherm of TiO₂ (P25) nanoparticles and the determined specific surface area: 51.2708 m²/g.

For the immobilisation of AHL **39** on TiO₂ different procedures should be tested to evaluate if the catechol does bind to the surface at all before testing the biological activities.

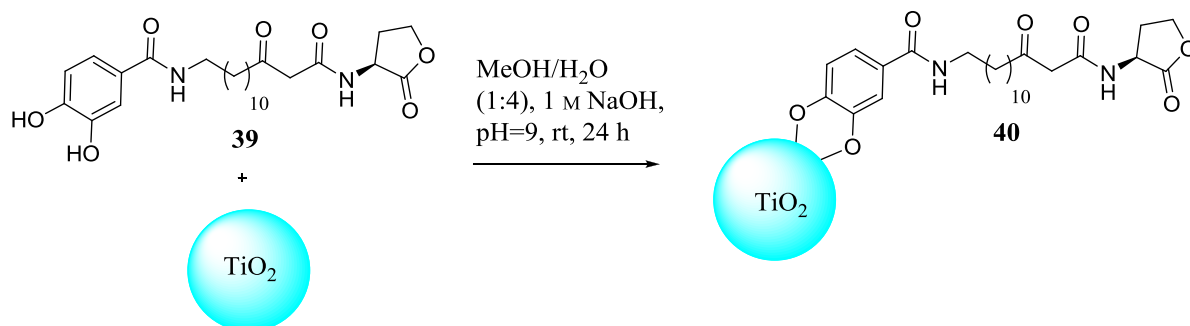


Figure 64: Schematic immobilisation of AHL **39** to a TiO₂ nanoparticle.

Calculation

The following calculation describes how to determine the appropriate amount of AHL **39** needed for a total coverage of the nanoparticles' surface.

Example: AHL immobilisation on 50 mg TiO₂ (P25) nanoparticles

Specific surface area A: 51.2708 m²/g

$$A = m^2/g \quad (1)$$

Assumption: For a full coverage of the particles' surface an area of 24 Å² per molecule (about four molecules per nm²) is assumed. This assumption is commonly used in literature.¹⁸⁶ In addition, a 5-fold excess of AHL **39** is used to guarantee a full coverage of the surface (for the calculation see experimental section **8.8**). Therefore, for a total coverage of 50 mg TiO₂ P25 nanoparticles 41 mg AHL derivative **39** are needed, taking a huge excess into account.

Coating Procedures

Method A

AHL derivative **39** was solved in MeOH/H₂O (1:9) and the nanoparticles were added to the mixture. The pH value was adjusted to 8 with 1 M aqueous NaOH. After 24 h of ultrasonic treatment the nanoparticles were separated from the solution by centrifugation. Thereafter, the particles were washed twice with H₂O and separated from the solvent by centrifugation each time. In the end the TiO₂-nanoparticles were dried by lyophilisation.

Method B

The particles were treated as described in method 1, but the pH value was adjusted to 9. After ultrasonic treatment the particles were washed four times with H₂O.

Method C

The particles were treated with MOPS buffer solution (0.1 M MOPS/0.6 M NaCl/0.6 M K₂SO₄) AHL derivative **39** and 1 mL MeOH. The mixture was stirred for 1 h at 50 °C following Gademann's protocol for the immobilisation of AHLs on TiO₂ beads.¹⁸³ However, by adding MeOH a white solid participated, which was not separable from the nanoparticles after centrifugation. Usually, MOPS buffer is used for coating the nanoparticle's surface with PEG (polyethylene glycol) and should not be necessary for the immobilisation of AHLs. Therefore methods A and B were used for routine functionalization of nanoparticles.

4.7.3 Analytics

Thermo Gravimetric Analysis (TGA)

TGA is a versatile tool to determine the characteristic changes of materials that exhibit *e.g.* mass loss/gain due to decomposition, the loss of volatiles or oxidation. The TGA instrument weights the probe continuously as it is heated up to the desired temperature. If the material is thermally stable no mass loss will occur which should be the case with pure TiO₂ P25 nanoparticles. However, when the particles are functionalised with catechol-AHLs a mass loss should be observed. TGA can therefore be used to evaluate the catechol loading on nanoparticles and optimize immobilization procedures.

The expected mass loss when the surface of the TiO₂ nanoparticles is fully coated with catechol-AHL is 13.9% (calculation see experimental section **8.8**).

The functionalised nanoparticles were prepared according to method A (pH = 8) and AHL-derivative **39**. The particles were heated to 700 °C. Figure **65** depicts a weight loss of 9% recorded as a function of time (blue curve). In comparison, pure TiO₂ particles, which were treated with MeO/H₂O according to method A but without addition of AHL-derivative **39** exhibited a loss of 1%.

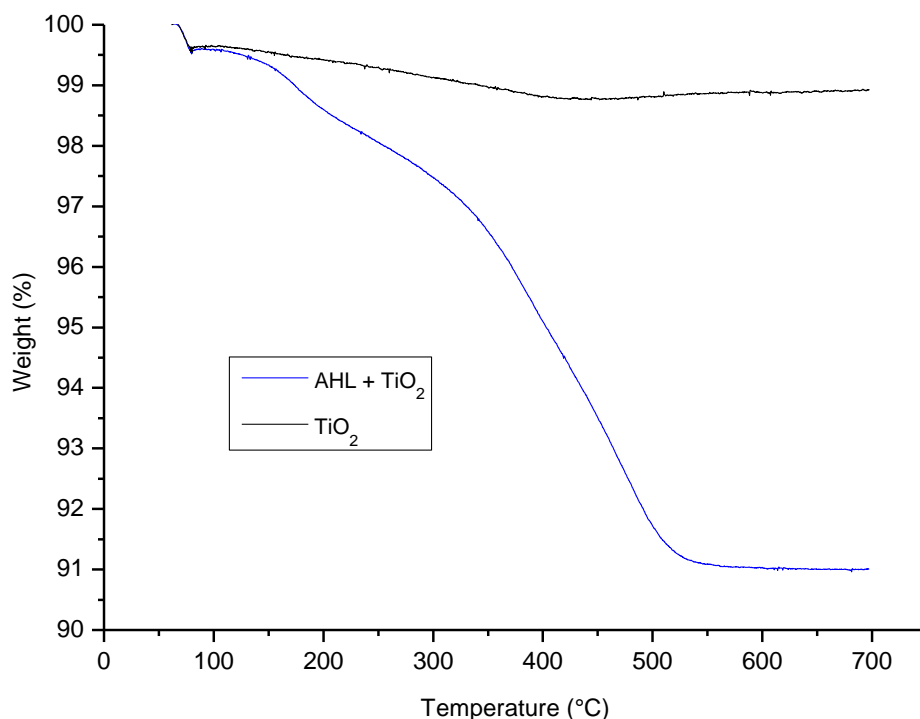


Figure 65: TGA of catechol coated TiO₂ prepared by method A. Heating up to 700 °C results in a weight loss of 9% (blue curve). In comparison, the particles treated with the solution but without adding the AHL-derivative exhibit a loss of 1% (black curve).

The next set of nanoparticles was prepared as described in method B again with the addition of AHL-derivative **39**. The pH value was adjusted to 9 by adding 1 M aqueous NaOH to the solution. In a control experiment, pure TiO₂ particles were treated with MeOH/H₂O but no ligand was added. The latter uncoated particles exhibited a mass loss of 2.5% (Figure **66**). The mass loss of the coated nanoparticles in turn was 13.5% (Figure **66**, blue curve). The spectrum shows two significant thermal degradations. The first mass loss (4%) occurs between 150 °C - 200 °C and is caused by degradation fragments and/or solvent residues (water). The second mass loss (9.5%) is caused by the catechol-AHL-derivative indicating an almost complete coverage of the surface.

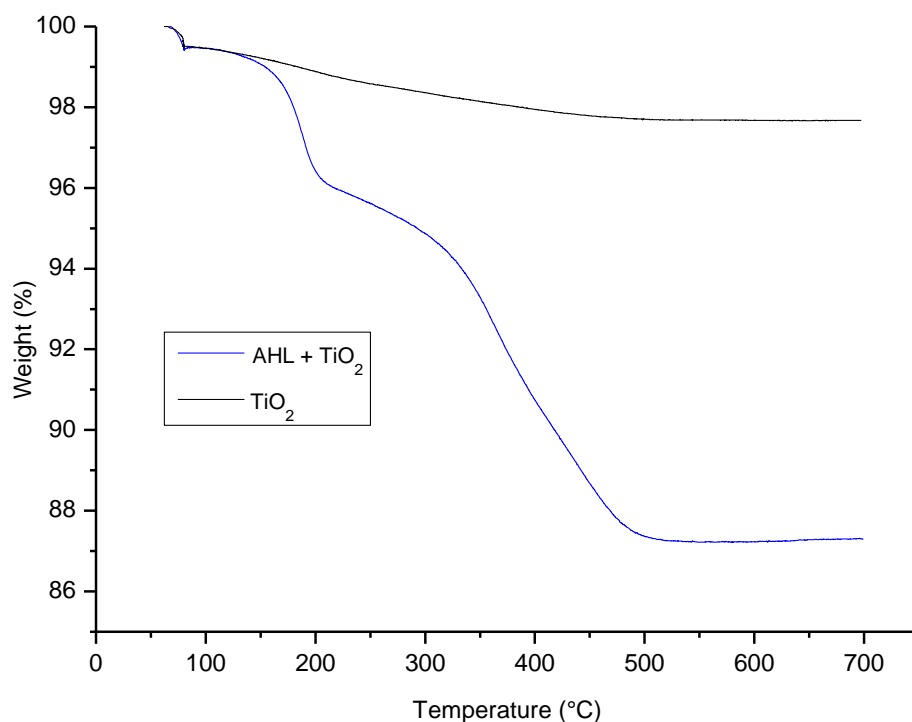


Figure 66: TGA of TiO₂ nanoparticles which were treated with the solution but without adding AHL-derivative **39** (black curve). Heating up to 700 °C results in a mass loss of 2.5%. The coated nanoparticles treated according to method B exhibit a mass loss of 13% (blue curve).

Infrared Spectrometry

Fourier Transformed Infrared Spectrometry (FTIR) was used. Coated nanoparticles were synthesised according to method B. Figure **67** shows the IR spectra for pure AHL-derivative **39** (black), uncoated TiO₂ particles which were just treated with the solution but without adding **39** (red) and coated particles which have been treated with **39** (blue). To investigate the coated nanoparticles a differential spectrum was recorded. Because TiO₂ does also absorb in the area of the ligand's signals it can happen that characteristic AHL signals are being concealed by TiO₂ signals. For this purpose a blank TiO₂ spectrum was measured and subtracted from the spectrum of the coated nanoparticles. That means the pure nanoparticles were treated as the background.

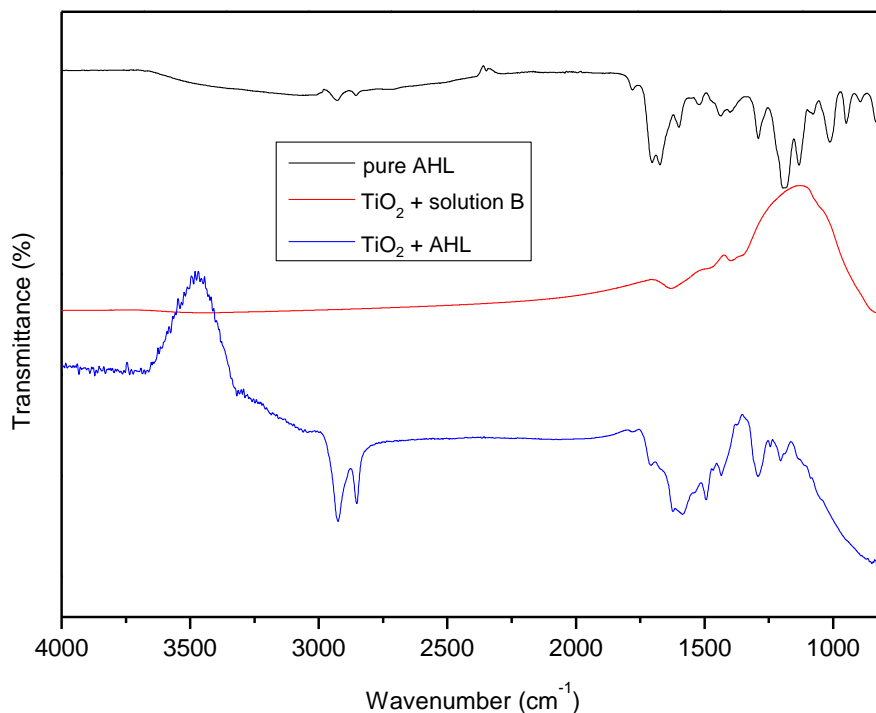


Figure 67: Characteristic FTIR spectrum of the pure AHL **39** (black), TiO₂ nanoparticles treated according to method B but without the ligand (red) and the functionalized TiO₂ nanoparticles (blue).

Transmission electron microscopy (TEM)

Transmission electron microscopy was used to create a direct image of the pure and coated TiO₂ nanoparticles. For this purpose an electron beam is scattered on the probe creating an image due to the interaction between the electrons and the probe. TEM is a versatile technique to determine the size and shape of nanoparticles or for a general analysis of surfaces. Figure **68** shows different TEM images of pure TiO₂ nanoparticles (A – C) and AHL coated TiO₂ nanoparticles (D – F). Agglomeration of the pure particles can be observed (A, B) as well as different spherical shapes of the single particles (C). TEM images of the AHL functionalised TiO₂ nanoparticles also show agglomeration of the particles (D, F). Particularly interesting is image (E) because a huge grey area surrounded by nanoparticles can be observed.

This is probably organic material which did not bind to the particles but is embedded between them. After the immobilisation process every probe had been washed at least four times to get rid of the AHL ligand. Of course traces of organic material can still be found.

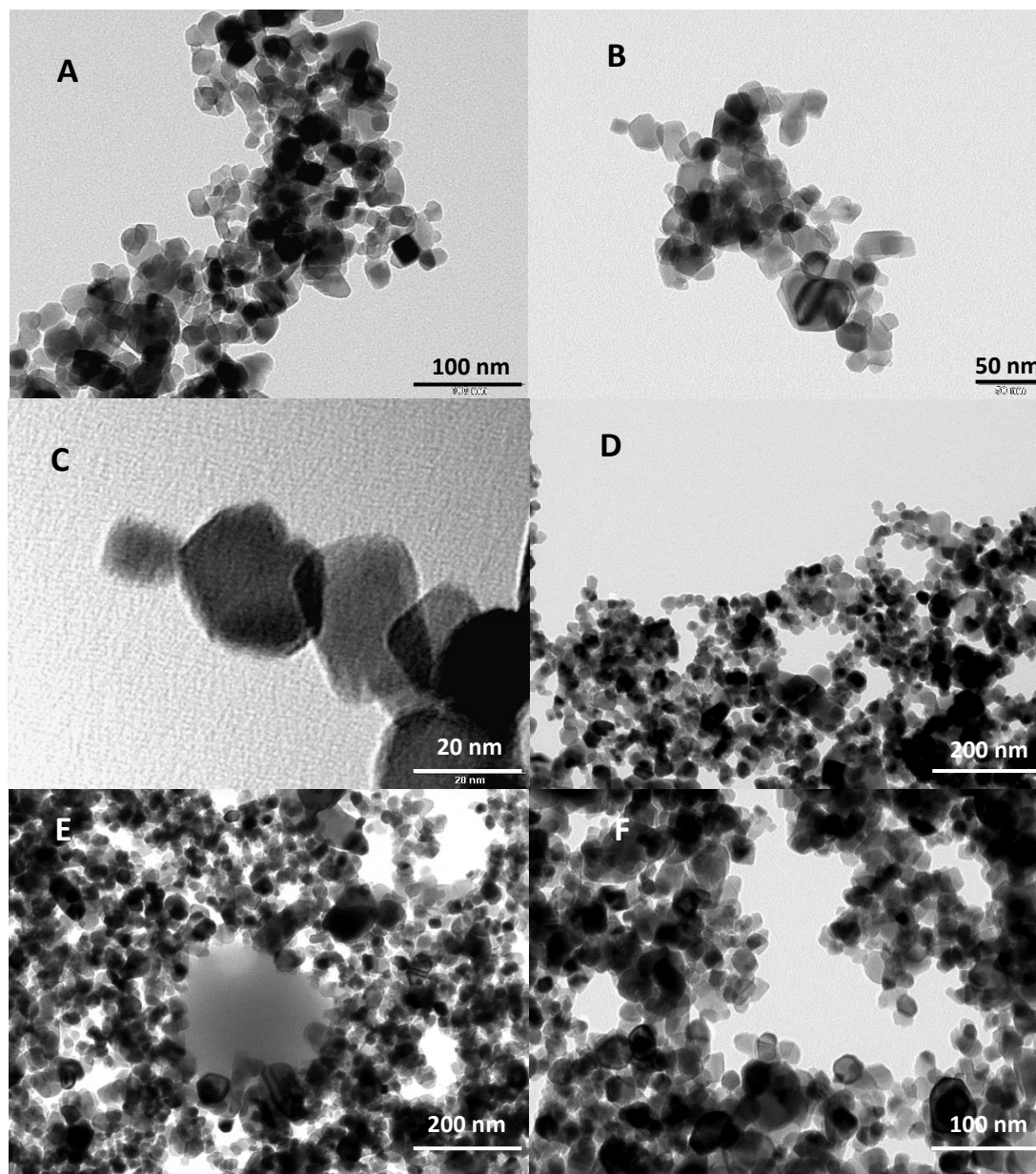


Figure 68: TEM images of pure (A – C) and AHL functionalised (D – F) TiO₂ nanoparticles.

UV/Vis

The spectrum of pure TiO₂ (red curve) correlates with literature known UV-Vis experiments on TiO₂ nanoparticles.²²³ The catechol-AHL shows absorption maxima at 180 nm and 200 nm. The spectrum of the coated nanoparticles looks like a combination of the pure TiO₂ and catechol-AHL spectrum. The absorption maxima at 180 nm and 380 nm can be seen correlating with the catechol moiety. The shifting of the second absorption maximum is due to the binding of catechol on the nanoparticles' surface. The shifting of catechol maxima after functionalization on TiO₂ surfaces has been also observed in literature.^{224,225} The characteristic TiO₂ plateau between 200 and 340 nm can also be seen. However, with increasing wavenumber the absorbance does not decrease as it does in the TiO₂ spectrum. This might be due to the bounded catechol-AHL.

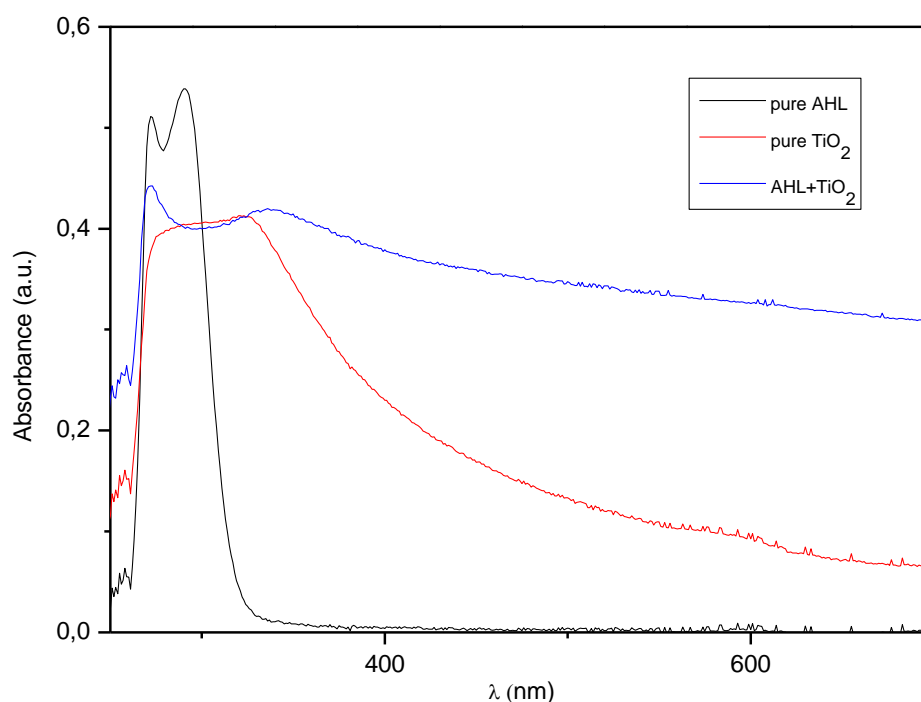


Figure 69: UV-Vis spectrum of the catechol-AHL (black curve), the pure TiO₂ nanoparticle (red curve) and the catechol-AHL immobilised on TiO₂ (blue curve).

For a complete analytical evaluation of the coated nanoparticles a XRD spectrum was recorded (see Appendix 13).

Different photoactive groups (e.g. diazirine, azide) were tested and the azide moiety proved to be easy to handle. Biotin was chosen as a tag because of the interesting biological activity of biotinylated AHL **107**. The coupling of biotin to **115** still needs to be improved but the remaining synthetic route was successfully established and is easy to handle.

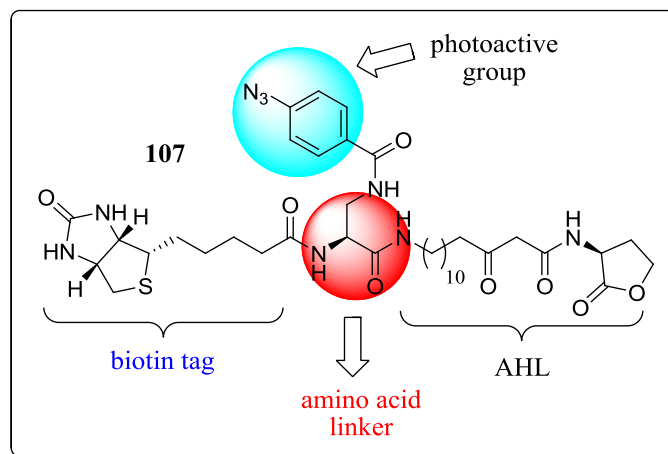


Figure 71: Biotinylated AHL containing a photoactive group.

For the immobilisation of signal molecules on TiO₂ nanoparticles (P25) several AHLs containing catechols or (bis)-phosphonates as anchor groups were synthesised. Catechol derivative **39** was a particularly attractive molecule because it is easily to prepare and can be immobilised on TiO₂ nanoparticles. Hence, the immobilisation procedures were evaluated and improved. The functionalised nanoparticles were investigated by TGA to determine the coverage of the surface. Additionally, the AHL containing particles were analysed by BET, IR and TEM and could now be used for affinity chromatography of putative AHL-interacting proteins in plants.

To sum up, several lactone-ring and acyl chain modified AHLs have been successfully synthesised and their biological activities were investigated. Additionally, AHLs containing different anchor groups were successfully immobilised on TiO₂ nanoparticles.

6 Zusammenfassung

Das Ziel dieser Arbeit war die Synthese verschiedener, modifizierter *N*-acyl-homoserin Lactone zur Erforschung der Interaktion zwischen Pflanzen und Bakterien. Pflanzliche Rezeptoren für AHLs sollten identifiziert und die Auswirkungen der Signalmoleküle auf das pflanzliche Immunsystem analysiert werden. Dafür wurden mehrere nicht natürliche 3-oxo-AHLs hergestellt. Die Modifizierungen der Signalmoleküle erfolgten entweder am Lactonring oder an der Kohlenstoffkette. Letztere sind interessante Verbindungen zur Untersuchung der Pflanzen-Bakterien Interaktion. Die biologische Aktivität dieser Substanzen wurde in Kooperation mit der Arbeitsgruppe von *Dr. Adam Schikora* analysiert. Als besonders interessant stellte sich dabei das Biotin enthaltende AHL **53** heraus, da es von verschiedenen bakteriellen Spezies als Signalmolekül erkannt wird und für Pull-down Experimente eingesetzt werden kann. Dies wurde erfolgreich am Pull-down des oxo-C14-AHL Rezeptors LuxR von *S. meliloti* demonstriert.

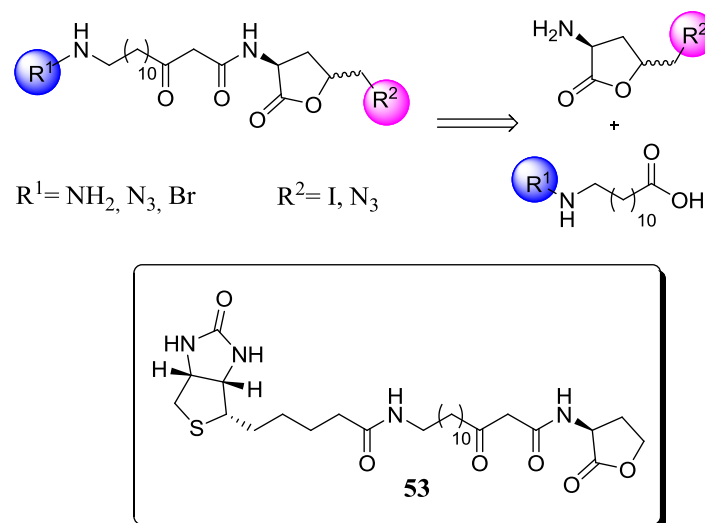


Abb. 1: Ausgesuchte Beispiele nicht natürlicher AHLs.

Des Weiteren wurde ein Signalmolekül mit einer fotoaktiven Gruppe und einem „tag“ synthetisiert. Diese Verbindung kann für Photoaffinity Labelling eingesetzt werden, da die fotoaktive Gruppe bei Lichteinstrahlung irreversibel an den Rezeptor bindet. Ein geeigneter „tag“ ermöglicht dann die Isolierung und Identifizierung des Rezeptors durch Affinitätschromatographie.

Verschiedene fotoaktive Gruppen wurden getestet (z.B. Diazirine, Azide), wobei die Azide letztendlich am einfachsten zu handhaben waren. Aufgrund der interessanten biologischen Aktivitäten biotinhaltiger AHLs wurde auch dieses Mal Biotin als „tag“ gewählt. Die Kupplung von Biotin an das Molekül muss zwar noch verbessert werden, allerdings wurde mit dieser Route eine geeignete und einfache Möglichkeit geschaffen derartige Signalmoleküle darzustellen.

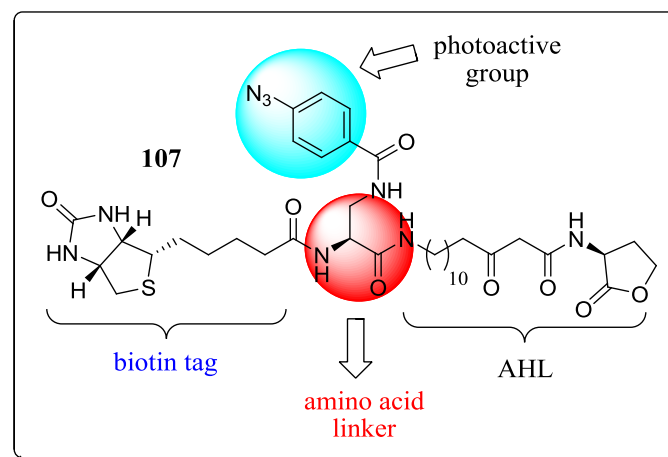


Abb. 2: Signalmolekül mit Biotin und fotoaktiver Gruppe.

Für die Immobilisierung der Signalmoleküle auf TiO₂ Nanopartikel (P25) wurden verschiedene AHLs mit Catechol- oder (Bis)-phosphonat Ankergruppen synthetisiert. Das Catecholderivat **39** wurde auf TiO₂ Nanopartikel aufgebracht und die Immobilisierungsprozedur verbessert. Die funktionalisierten Nanopartikel wurden anschließend mittels TGA untersucht, um den Anteil der Oberflächenbeschichtung mit AHLs zu bestimmen. Des Weiteren wurde die Partikel mit BET, IR und TEM analysiert und könnten nun für Affinitätschromatographie zur Erforschung AHL-interagierender Proteine in Pflanzen genutzt werden.

Es wurde eine Vielzahl am Lactonring und an der Kohlenstoffkette modifizierter AHLs erfolgreich dargestellt und ihre biologische Aktivität überprüft. Des Weiteren wurden die Signalmoleküle mit verschiedenen Ankergruppen konjugiert und auf TiO₂ Nanopartikel immobilisiert.

7 Outlook

The synthesis of a photoactive AHL containing biotin as a tag was investigated during this PhD. The route presented in this thesis was easy to handle except for the last step, the coupling of biotin to the AHL scaffold. Due to this problem the route needs to be optimised. Main reasons for the difficulties are steric hindrances. The bulky photoactive group might shield the free amine of compound **115** making it hard for the carboxylic acid of the biotin to attack. To avoid this problem different linkers could be used which contain a longer acyl chain **162**. In addition, various photoactive groups could be utilised and compared to the azide moiety. When the conditions of the coupling reaction are optimised, compound **115** is a key intermediate for the conjugation to other interesting functional groups like catechols or phosphonates.

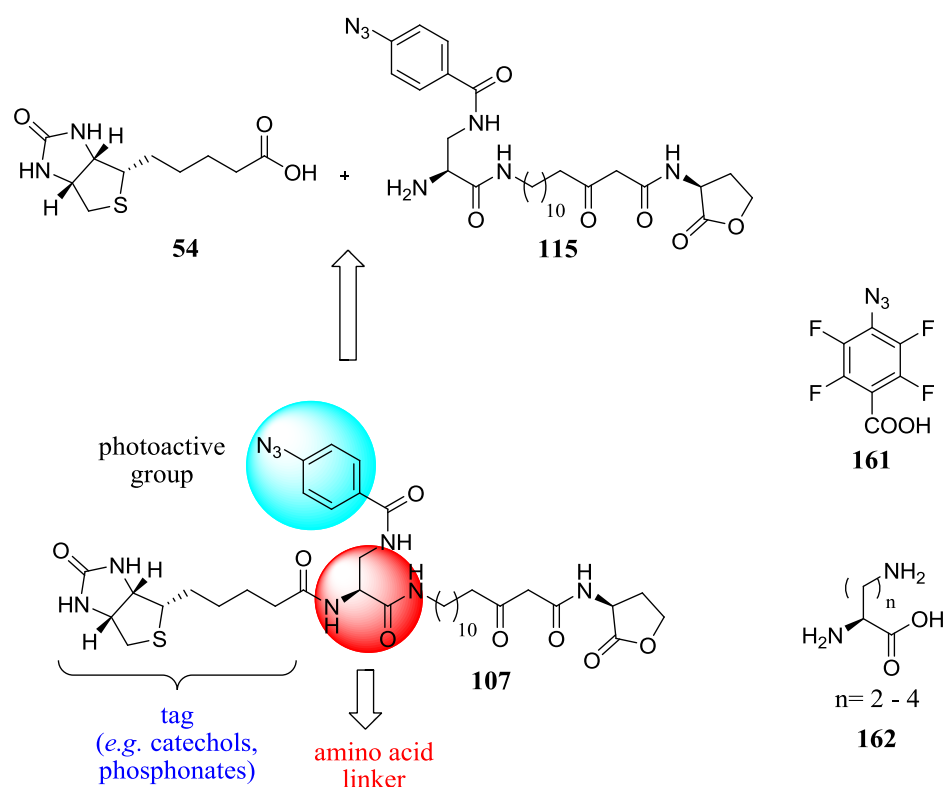


Figure 72: Synthesis of photoactive AHL **107**. Amino acid **162** could also be used as a linker while perfluorophenyl azide **161** could be used as a photoactive group.

Several phosphonate containing AHLs have been synthesised during this PhD thesis, but the deprotection of the esters proved to be difficult. The deprotection route needs to be optimised in order to immobilise these AHLs on TiO_2 nanoparticles and to compare their binding stability to other anchor groups *e.g.* catechols. Additionally, AHLs conjugated to bis-phosphonates could be prepared, deprotected and compared to mono-substituted AHLs. An interesting bisphosphonate is Pamidronate because of its biological activity. For this purpose an appropriate deprotection route is necessary because the free acids of pamidronate **138** and other bisphosphonates are not easy to handle during synthesis. Strong basic conditions are needed which would hydrolyse the lactone moiety of the AHL.

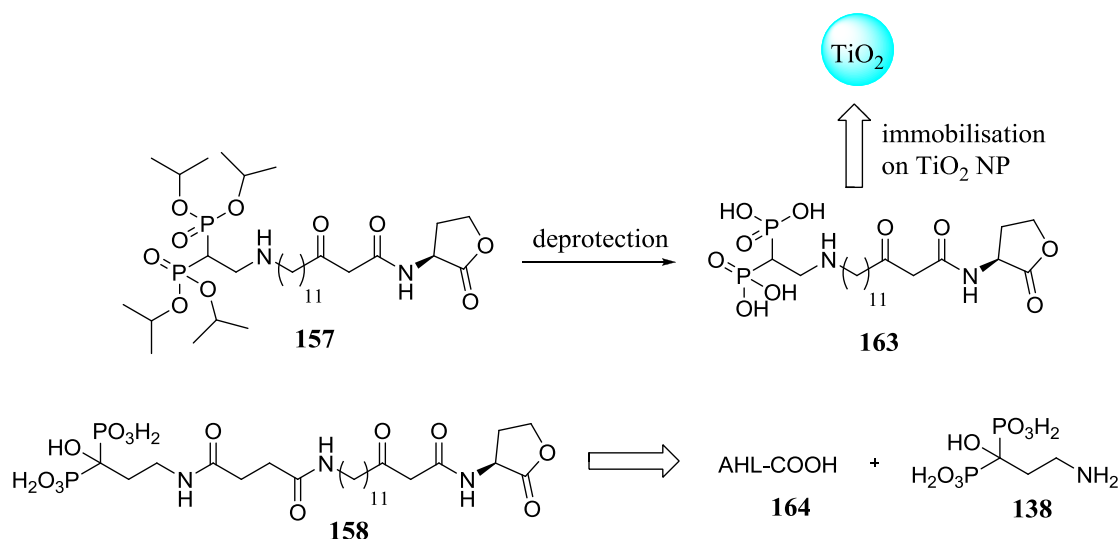


Figure 73: Deprotection of bisphosphonate **157** and synthesis of a pamidronate-AHL **138**.

The so created library of catechol-AHLs or (bis)-phosphonate-AHLs has to be evaluated concerning their biological activities. First, one has to investigate if these compounds are still recognised as autoinducers by different bacteria. Afterwards, they could be used for affinity chromatography.

8 Experimental

8.1 Material and Methods

All chemicals used in this work were purchased from the companies Merck, Sigma Aldrich, Acros Organics or Fluka. Solvents were dried by distillation from sodium under nitrogen atmosphere prior to application. If necessary, reactions were performed under nitrogen 5.0 (Airliquide) or argon 5.0 atmosphere (Airliquide).

TLC was performed on silica gel aluminum sheets purchased from Macherey-Nagel or Merck (silica gel 60 F₂₅₄, particle size distribution 60 - 200 μm). Reagents used for developing plates include cerium stain (5 g molybdato-phosphoric acid, 2.5 g cerium sulfate tetrahydrate, 25 mL sulfuric acid and 225 mL water), potassium permanganate (0.5% in 1 N NaOH w/v) and detection by UV light was used when applicable. Flash column chromatography was performed on silica gel (60 – 200 μm) purchased from Macherey-Nagel or Merck.

8.1.1 Analytics

NMR spectra were recorded at ambient temperature on either a Bruker Biospin GmbH Avance II (200 MHz) “Microbay”, Avance II (400 MHz) WB, Avance III (600 MHz) or DRX 500 (500 MHz) instrument. ¹H chemical shifts are referenced to residual non-deuterated solvent (CDCl₃, $\delta_{\text{H}} = 7.26$ ppm; DMSO-*d*₆, $\delta_{\text{H}} = 2.50$ ppm; CD₃OD, $\delta_{\text{H}} = 3.31$ ppm). The data is presented as follows: chemical shift (in ppm on the δ scale), integration, multiplicity (s = singlet, d = doublet, t = triplet, q = quartet, m = multiplet, br = broad), assignment and the coupling constant (*J*, in Hertz). The ¹³C NMR spectra were recorded at 200 MHz or 100 MHz using the same instruments. ¹³C chemical shifts are referenced to the solvent signal (CDCl₃, $\delta_{\text{C}} = 77.16$ ppm; DMSO-*d*₆, $\delta_{\text{C}} = 128.06$ ppm; CD₃OD, $\delta_{\text{H}} = 49.00$ ppm). ¹H – ¹H COSY, HSQC, HMBC, HMQC spectra were measured for a complete characterisation of the probes. ³¹P spectra were recorded at 160 MHz on the same instruments. The numeration required for the analysis of the NMR spectra in this work does not follow the IUPAC guidelines and therefore does not coincide with the nomenclature of the molecules.

ESI mass spectra were recorded on a TOF instrument operated in positive mode (Bruker MicrOTOF Q). Samples were dissolved in MeOH or H₂O/MeCN-mixtures and directly injected *via* syringe.

Elemental analysis was performed using an elemental Vario EL III and Eurovector Euro EA analyser. **Melting points** were determined on a Büchi M-560 apparatus and are uncorrected. **Specific rotation** was recorded on an A. Krüss Optronic GmbH P8000-T. **IR** spectra were recorded on a Shimadzu FT-IR IR Affinity-1 instrument. The wavelengths of the maximum absorbance (ν_{\max}) are quoted in cm⁻¹. IR spectra were also recorded on a Jasco FT-IR 4100 with an ATR unit.

XRD was performed on a Panalytical X'Pert Pro (radiation: Cu; wavelength: 1.54 Å; voltage: 45 kV; Current: 40 mA). A PIXcel detector was used (mode: scanning; active length: 3.347 °; number of active channels: 255). Gonio Scanning was utilised (10 °-80 ° scan range; step size: 0.0131 °, scan mode: continuous; scan speed: 0.045277 °/s). The Panalytical contains a Ni filter (thickness: 0.020 mm). Radiated length: 12 mm.

TEM was performed on a Joel JEM-1011 with a LaB6 cathode. The probes were measured at 100 kV on a Cu-grid. The Cu-grid (G2400C, 400 Square Mesh, 3.05 mm) for the probe was functionalised with a thin carbon layer before measurement.

TGA was measured on a Perkin Elmer Pyris Series 1 with the software Pyris Series 1. The functionalised nanoparticles were directly used for the analysis without any prior probe preparation. **BET** was performed on a Thermo Scientific Surfer unit. The nanoparticles were heated up to 40 °C for 2 h prior to the BET analysis. **UV-Vis** was measured on a Thermo Scientific BioMate 3S.

HPLC

Analytical HPLC analysis was recorded on a VWR HITACHI ELITE LaChrom L-2130 HPLC (RI Detector: L2490). The following chiral column was used: CHIRALPAK IA (DAICEL Chemical Industries; Particle size: 5 μ m; Dimensions: 4.6 mm ϕ x 150 mm).

Sample Boc-protected Claisen product **75c**: 4.7 mg/1mL

Run time: 30 min

Solvent: *n*-hexane: *i*-PrOH: TFA (80:20:0.1)

Flow rate: 0.5 mL/min

Peak 1: Retention time=6.50 min; Area%=51.004

Peak 2: Retention time= 7.0 min; Area%= 48.996

8.2 General procedures

General procedure 1: Coupling with Meldrum's acid

1 equiv. of the appropriate fatty acid was dissolved in CH_2Cl_2 and 1 equiv. DMAP, 1 equiv. DCC and 1 equiv. of Meldrum's acid were added to the mixture. The solution was stirred overnight at room temperature and then filtered to remove the *N,N*-dicyclohexyl urea formed in the reaction. The filtrate was concentrated *in vacuo* and the resulting residue was dissolved in DMF. 1 equiv (*S*)- α -amino- γ -butyrolactone hydrobromide was added and the mixture was stirred at room temperature for 1 h and additional 4 h at 60 °C. The solvent was distilled off *in vacuo* and the residue was dissolved in EtOAc. The organic phase was washed three times with saturated sodium bicarbonate solution, 1 M sodium hydrogen sulfate solution and brine. Afterwards, the organic phase was dried over Na_2SO_4 , filtered and then the solvent was distilled off. The crude product was purified by flash chromatography if necessary.

General Procedure 2: Boc deprotection

The Boc protected amine was dissolved in TFA/CH₂Cl₂ (1:1; 5 mL per 0.1 mmol educt) and stirred at room temperature for 3 h. The solvent was distilled off *in vacuo*. The crude product was purified by flash chromatography if necessary.

General Procedure 3: Preparation of glycine allyl esters

1 equiv. *N*-protected glycine was dissolved in CH₂Cl₂ and cooled to 0 °C. 1 equiv. of allylic alcohol was added and the solution was cooled to -15 °C. A solution of 1 equiv. DCC and 0.1 equiv. DMAP in CH₂Cl₂ was added and the reaction was stirred at room temperature for 12 h. The precipitated *N,N*-dicyclohexyl urea was filtered off and washed with CH₂Cl₂. The organic layer was washed with 1 M aqueous HCl and saturated aqueous NaHCO₃⁻ solution. The organic phase was dried over Na₂SO₄, filtered and the solvent was evaporated *in vacuo*.

General Procedure 4: Claisen rearrangement

LHMDS solution was prepared by adding 1 equiv. 1.6 M *n*-BuLi in hexane at room temperature under argon atmosphere to 1.2 equiv. hexamethyldisilazane in abs THF. The solution was stirred for 20 min. In a second flask 0.2 equiv. of the *N*-protected glycine ester, 0.2 equiv. Al(*O*Pr-*i*)₃ and 0.5 equiv. quinidine were dissolved in abs THF under argon atmosphere and cooled to -78 °C. The LHMDS-solution was added slowly and the reaction was stirred at room temperature for 12 h. The mixture was treated with 1 M aqueous KHSO₄ and the organic layer was dried over Na₂SO₄. After filtration the solvent was distilled off *in vacuo* and the crude product was purified by flash chromatography if necessary.

General Procedure 5: Iodolactonization

The Claisen product was dissolved in THF at 0 °C and 1 equiv. I₂ was added. The reaction was stirred for 12 h at room temperature and then diluted with EtOAc. Afterwards the mixture was quenched with saturated aqueous Na₂S₂O₄⁻ solution. The organic layer was washed with brine, dried over Na₂SO₄ and filtered. The solvent was evaporated *in vacuo* and the crude product was purified by flash chromatography.

General Procedure 6: Preparation of azido lactones

To a solution of the iodide in DMF NaN_3 was added and the mixture was stirred at 40 °C for 24 h. The solvent was distilled off *in vacuo* and the residue was dissolved in EtOAc. The organic layer was washed with water and brine. The organic phase was then dried over Na_2SO_4 , filtered and the solvent was evaporated *in vacuo*. The crude product was purified by flash chromatography.

General procedure 7: NHS-ester coupling

1 equiv. carboxylic acid, 1 equiv. NHS-Ester and 1.3 equiv. Et_3N were dissolved in DMSO. After stirring at room temperature for 24 h the solvent was distilled off *in vacuo* and the crude product was purified by flash chromatography if necessary.

General procedure 8: Click reaction

1 equiv. alkyne, 1 equiv. azide, 0.1 equiv. CuSO_4 and 0.1 equiv. sodium ascorbate were dissolved in freshly degassed *tert*-BuOH/ H_2O (1:1) under argon atmosphere and stirred for 24 h at room temperature. The solvent was distilled off *in vacuo* and the residue was dissolved in EtOAc. The organic phase was washed three times with 0.1 M aqueous EDTA- solution, dried over Na_2SO_4 and the solvent was evaporated *in vacuo*. The crude product was purified by flash chromatography.

The following compounds were synthesised according to literature procedures:

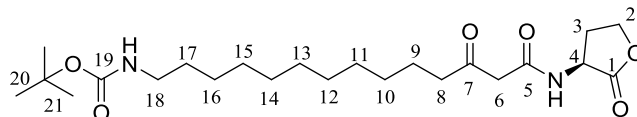
Boc-protected acid **49**,¹⁶⁵ biotin-NHS ester,¹⁵⁹ TFA-glycine allylester **74a**,¹⁶⁴ TFA-allylglycine **75a**,¹⁶⁴ TFA-iodolactone **76a**,¹⁶⁴ Boc-protected iodolactone **76c**,²²⁶ Boc-protected lactone **79c**,²²⁶ Cbz-glycine allylester **74b**,^{227,228} phosphonate test reaction **153**,¹⁹⁰ 10-aminodecanoic acid **103b**,³¹ 4-pentynoic NHS ester **61**²²⁹

Literature known compounds that were synthesised differently from commonly used procedures: Boc-protected methyl ester **105a**,²³⁰ Boc-protected ethyl ester **105b**.²³¹ The compounds Boc-protected 10-amino decanoic acid **104b**²³² and Boc-protected β -alanine **104a**²³³ are literature known but were synthesised according to general procedure 1.

The nomenclature is not in accordance with UPAC guidelines.

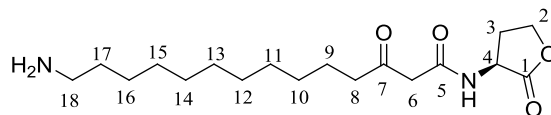
8.3 Acyl chain modified AHL-derivatives

AHL-derivative 50



According to general procedure 1, the title compound **50** (278 mg, quant.) was obtained from carboxylic acid **49** (200 mg, 0.63 mmol), DMAP (77.5 mg, 0.63 mmol), DCC (131 mg, 0.63 mmol), Meldrum's acid (91.4 mg, 0.63 mmol) and (*S*)- α -amino- γ -butyrolactone hydrobromide (116 mg, 0.63 mmol) as a colourless solid. $^1\text{H NMR}$ (CDCl_3 , 400 MHz) δ (ppm) = 4.62 – 4.44 (m, 2H, 4-H, 2-H), 4.30 – 4.23 (m, 1H, 2-H), 3.46 (s, 2H, 6-H), 3.11 – 3.05 (m, 2H, 18-H), 2.79 – 2.70 (m, 1H, 8-H), 2.51 (t, 1H, 8-H, $J = 9.4$ Hz), 2.29 – 2.12 (m, 1H, 3-H), 1.94 – 1.90 (m, 1H, 3-H), 1.73 – 1.64 (m, 2H, 9-H), 1.64 – 1.53 (m, 2H, 17-H), 1.43 (s, 9H, 21-H), 1.20 – 1.18 (m, 14H, 16-H, 15-H, 14-H, 13-H, 12-H, 11-H, 10-H); $^{13}\text{C NMR}$ (CDCl_3 , 100 MHz) δ (ppm) = 206.5 (C7), 174.8 (C1), 166.4 (C5), 156.1 (C19), 78.9 (C20), 65.8 (C2), 48.9 (C4), 48.1 (C6), 43.9 (C8), 40.6 (C18), 33.8 (C3), 30.0, 29.8, 29.4, 29.2, 28.9, 28.4, 26.8, 25.6, 24.9, 23.3 (C21, C17, C16, C15, C14, C13, C12, C11, C10, C9); **HRMS** (ESI) m/z calcd for $\text{C}_{23}\text{H}_{40}\text{N}_2\text{NaO}_6$ [$\text{M}+\text{Na}$] $^+$ 463.2779, found 463.2784; $[\alpha]_{\text{D}}^{20} = -3.0^\circ$ ($c = 0.7$, CHCl_3); **Mp.**: 88.1 $^\circ\text{C}$; **IR** (KBr, cm^{-1}): 3349, 2920, 2852, 1778, 1718, 1646, 1632; **CHN** calcd. for $\text{C}_{23}\text{H}_{40}\text{N}_2\text{O}_6$: C, 64.73%; H, 10.54%; N, 4.44%. Found: C, 64.36%; H, 10.53%; N, 4.10%.

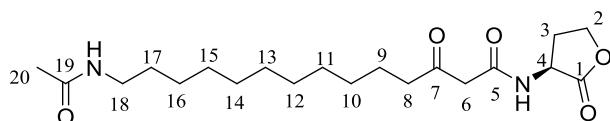
AHL-derivative 51



According to general procedure 2, the title compound **51** (51 mg, 61%) was obtained as a colourless solid from AHL **50** (108 mg, 0.25 mmol). $^1\text{H NMR}$ (CD_3OD , 400 MHz, COCH_2CO signal is hidden under solvent peak) δ (ppm) = 4.61 (dd, 1H, 4-H, $J = 9.1$ Hz, 9.1 Hz), 4.44 (ddd, 1H, 2-H, $J = 9.8$ Hz, 9.3 Hz, 1.8 Hz), 4.33 – 4.27 (m, 1H, 2-H), 2.91 (t, 2H, 18-H, $J = 8.0$ Hz), 2.58 (t, 2H, 8-H, $J = 5.3$ Hz), 2.35 – 2.24 (m, 1H, 3-H), 1.68 – 1.52 (m, 5H, 17-H, 9-H, 3-H), 1.42 – 1.28 (m, 14H, 16-H, 15-H, 14-H, 13-H, 12-H, 11-H, 10-H);

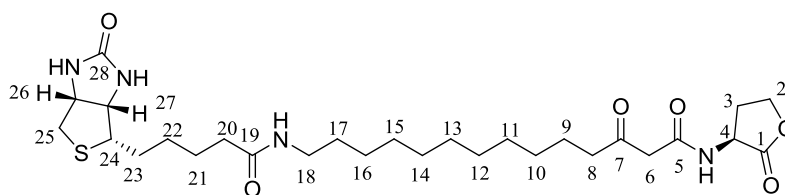
^{13}C NMR (DMSO- d_6 , 100 MHz) δ (ppm) = 204.6 (C7), 174.8 (C1), 166.4 (C5), 65.3 (C2), 50.0 (C4), 48.1 (C6), 42.6 (C8), 41.9 (C18), 34.0, 33.3, 28.8, 28.7, 28.4, 28.3, 28.1, 26.9, 25.7, 22.8 (C17, C16, C15, C14, C13, C12, C11, C10, C9, C3); **HRMS** (ESI) m/z calcd for $\text{C}_{18}\text{H}_{33}\text{N}_2\text{O}_4$ $[\text{M}+\text{H}]^+$ 341.2435, found 341.2440; $[\alpha]_{\text{D}}^{20} = -8.0^\circ$ ($c = 0.2$, MeOH); **Mp.**: 64.5 $^\circ\text{C}$; **IR** (KBr, cm^{-1}): 2928, 2848, 1776, 1681, 1208, 1127; **CHN** calcd. for $\text{C}_{18}\text{H}_{32}\text{N}_2\text{O}_4$: C, 62.70%; H, 9.15%; N, 6.36%. Found: C, 62.51%; H, 9.46%; N, 6.57%.

AHL-derivative 52

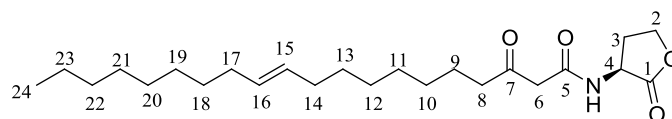


Method 1: AHL-derivative **51** (272 mg, 0.80 mmol) was dissolved in CH_2Cl_2 (40 mL) and cooled to 0 $^\circ\text{C}$. Acetic anhydride (0.75 mL, 8.00 mmol) and pyridine (0.64 mL, 8.00 mmol) were added and the solution was stirred 3 h at room temperature. The solvent was evaporated *in vacuo* and the crude residue was purified by flash chromatography (EtOAc/MeOH, 9:1, $R_f = 0.3$, cerium stain) to give the title compound **52** (32 mg; 10%) as a brown solid.

Method 2: AHL-derivative **51** (95 mg, 0.28 mmol), acetic anhydride (0.13 mL, 1.39 mmol, 5 equiv.) and Et_3N (0.39 mL, 2.79 mmol, 10 equiv.) were dissolved in CH_2Cl_2 (30 mL) and stirred for 12 h at room temperature. The solvent was evaporated *in vacuo* and the crude residue was purified by flash chromatography (EtOAc/MeOH, 9:1, $R_f = 0.3$, cerium stain) to give the title compound **52** (52 mg; 49%) as a brown solid. ^1H NMR (CD_3OD , 400 MHz) δ (ppm) = 4.64 – 4.58 (dd, 1H, 4-H, $J = 8.9$ Hz, 8.9 Hz), 4.47 – 4.41 (ddd, 1H, 2-H, $J = 9.8$ Hz, 8.9 Hz, 2.4 Hz), 4.33 – 4.27 (m, 1H, 2-H), 3.28 (s, 2H, 6-H), 3.13 (t, 2H, 18-H, $J = 8.2$ Hz), 2.57 (t, 3H, 8-H, $J = 8.2$ Hz), 2.35 – 2.25 (m, 1H, 3-H), 1.91 (s, 3H, 20-H), 1.60 – 1.44 (m, 5H, 17-H, 9-H, 3-H), 1.29 – 1.26 (m, 14H, 16-H, 15-H, 14-H, 13-H, 12-H, 11-H, 10-H); ^{13}C NMR (CD_3OD , 100 MHz) δ (ppm) = 206.5 (C7), 177.0 (C19), 173.4 (C1), 169.1 (C5), 67.1 (C2), 64.7 (C4), 50.2 (C6), 43.9 (C8), 40.7 (C18), 30.6, 30.5, 30.4, 30.3, 30.2, 30.0, 29.6, 28.1, 28.0, 24.4 (C17, C16, C15, C14, C13, C12, C11, C10, C9, C3), 22.5 (C20); **HRMS** (ESI) m/z calcd for $\text{C}_{20}\text{H}_{34}\text{N}_2\text{NaO}_5$ $[\text{M}+\text{Na}]^+$ 405.2360, found 405.2382; $[\alpha]_{\text{D}}^{20} = -5.0^\circ$ ($c = 0.4$, DMSO); **Mp.**: 94.3 $^\circ\text{C}$; **IR** (KBr, cm^{-1}): 2926, 2837, 1641.

Biotin-labelled-AHL 53

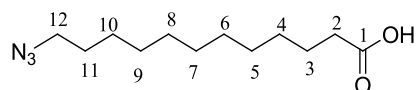
Biotin-NHS ester (109 mg, 0.32 mmol) was dissolved in DMSO (40 mL). **51** (103 mg, 0.30 mmol) and Et₃N (0.057 mL, 0.42 mmol, 1.3 equiv.) were added to the solution and the mixture was stirred at room temperature for 24 h. The solvent was distilled off *in vacuo* to give the title compound **53** (97 mg, 54%) as a brown oil. ¹H NMR (DMSO-*d*₆, 400 MHz) δ (ppm) = 6.36 (d, 2H, biotin-NH, *J* = 12.3 Hz), 4.30 – 4.25 (m, 1H, 27-H), 4.13 – 4.07 (m, 1H, 26-H), 3.09 – 3.02 (m, 3H, 24-H, 6-H), 2.96 – 2.93 (m, 1H, 4-H), 2.76 – 2.65 (m, 4H, 25-H, 18-H), 2.60 – 2.54 (m, 2H, 20-H), 2.47 – 2.45 (m, 6H, 8-H, 3-H, 2-H), 1.64 – 1.24 (m, 12H, 23-H, 22-H, 21-H, 17-H, 16-H, 9-H), 1.21 – 1.10 (m, 12H, 15-H, 14-H, 13-H, 12-H, 11-H, 10-H); ¹³C NMR (DMSO-*d*₆, 100 MHz) δ (ppm) = 204.7 (C7), 172.8 (C1), 170.2 (C19), 170.0 (C5), 162.8 (C28), 65.4 (C2), 61.1 (C26), 59.3 (C27), 55.2 (C24), 45.7 (C6), 42.7 (C20), 40.3 (C4), 30.0, 29.6, 29.1, 28.7, 28.5, 28.4, 28.2, 28.0, 27.97, 27.9, 27.5, 26.4 (C23, C22, C21, C17, C16, C15, C14, C13, C12, C11, C10, C9), 25.4, 25.3, 25.25, 25.2 (C25, C18, C8, C3); HRMS (ESI) *m/z* calcd for C₂₈H₄₆N₄NaO₆S [M+Na]⁺ 589.3030, found 589.3038; [α]_D²⁰ = -11.9° (*c* = 0.8, DMSO); IR: (film, cm⁻¹) 2925, 2850, 2522.

AHL-derivative 69

According to general procedure 1, the title compound AHL-derivative **69** (324 mg, 75%) was obtained from oleic acid (0.30 mL, 1.06 mmol), DMAP (130 mg, 1.06 mmol), DCC (219 mg, 1.06 mmol), Meldrum's acid (153 mg, 1.06 mmol) and (*S*)- α -amino- γ -butyrolactone hydrobromide (194 mg, 1.06 mmol) as a colourless solid.

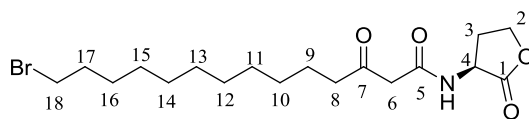
¹H NMR (CDCl₃, 400 MHz) δ (ppm) = 7.69 – 7.63 (m, 1H, N-H), 5.38 – 5.29 (m, 2H, 16-H, 15-H), 4.62 – 4.54 (m, 1H, 4-H), 4.47 (m, 1H, 2-H), 4.31 – 4.24 (m, 1H, 2-H), 3.46 (s, 2H, 6-H), 2.52 (t, 2H, 8-H, $J = 7.1$ Hz), 2.31 – 2.13 (m, 1H, 3-H), 2.03 – 1.99 (m, 4H, 17-H, 14-H), 1.72 – 1.54 (m, 3H, 9-H, 3-H), 1.38 – 1.19 (m, 20H, 23-H, 22-H, 21-H, 20-H, 19-H, 18-H, 13-H, 12-H, 11-H, 10-H), 0.88 (t, 3H, 24-H, $J = 7.1$ Hz); **¹³C NMR** (CDCl₃, 100 MHz) δ (ppm) = 206.7 (C7), 174.8 (C1), 166.3 (C5), 130.1, 129.4 (C16, C15), 65.7 (C3), 48.8 (C4), 48.1 (C6), 43.9 (C8), 34.0, 31.7 (C17, C14), 29.9, 29.7, 29.56, 29.5, 29.3, 29.2, 28.98, 27.2, 25.6, 24.8, 23.3 (C22, C21, C20, C19, C18, C13, C12, C11, C10, C9, C3), 22.6 (C23), 14.2 (C24); **HRMS** (ESI) m/z calcd for C₂₄H₄₁NNaO₄ [M+Na]⁺ 430.2928, found 430.2937; $[\alpha]_D^{20} = -14.0^\circ$ ($c = 0.3$, MeOH); **Mp.**: 75.4 °C; **IR** (KBr, cm⁻¹): 3305, 2924, 2852, 1776, 1708, 1649; **CHN** calcd. for C₂₄H₄₁NO₄: C, 70.72%; H, 10.14%; N, 3.44%. Found: C, 68.44%; H, 10.05%; N, 3.64%.

Azide 58



12-bromododecanoic acid (0.50 g, 1.79 mmol) and NaN₃ (1.17 g, 17.9 mmol, 10 equiv.) were dissolved in DMF (60 mL) and stirred at 60 °C for 24 h. The solvent was evaporated *in vacuo* and the crude residue was dissolved in CH₂Cl₂ (60 mL). The organic phase was washed twice with 1 M aqueous HCl and brine. The solvent was distilled off to give the desired product as a colourless solid (408 mg, 94%). **¹H NMR** (CDCl₃, 400 MHz) δ (ppm) = 11.23 (br, 1H, O-H), 3.23 (t, 2H, 12-H, $J = 6.6$ Hz), 2.32 (t, 2H, 2-H, $J = 7.4$ Hz), 1.64 – 1.53 (m, 4H, 11-H, 3-H), 1.35 – 1.22 (m, 14H, 10-H, 9-H, 8-H, 7-H, 6-H, 5-H, 4-H); **MS** (ESI) m/z 264.2 (M+Na⁺, 100%).

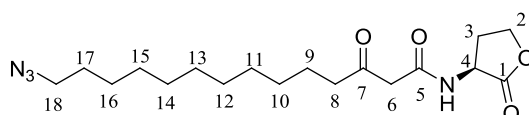
The compound was synthesised according to a route depicted by Amara *et al.*³¹

AHL-derivative 59

According to general procedure 1, the title compound AHL-derivative **59** (300 mg, 69%) was obtained from 12-bromododecanoic acid (300 mg, 1.08 mmol), DMAP (132 mg, 1.08 mmol), DCC (222 mg, 1.08 mmol), Meldrum's acid (155 mg, 1.08 mmol) and (*S*)- α -amino- γ -butyrolactone hydrobromide (196 mg, 1.08 mmol) as a colourless solid. The crude product was purified by flash chromatography PE/EtOAc (9:1, R_f =0.2, cerium stain).

$^1\text{H NMR}$ (CD_3OD , 400 MHz, COCH_2CO signal is hidden under solvent peak) δ (ppm) = 4.63 (dd, 1H, 4-H, $J = 10.7$ Hz), 4.46 (ddd, 1H, 2-H, $J = 9.3$ Hz, 8.7 Hz, 2.1 Hz), 4.35 – 4.29 (m, 1H, 2-H), 3.45 (t, 2H, 8-H, $J = 6.6$ Hz), 2.60 (t, 2H, 18-H, $J = 7.7$ Hz), 2.37 – 2.56 (m, 1H, 3-H), 1.77 – 1.56 (m, 5H, 17-H, 9-H, 3-H), 1.37 – 1.30 (m, 14H, 16-H, 15-H, 14-H, 13-H, 12-H, 11-H, 10-H).

Compound is literature known²³⁴ but was synthesised according to general procedure 1.

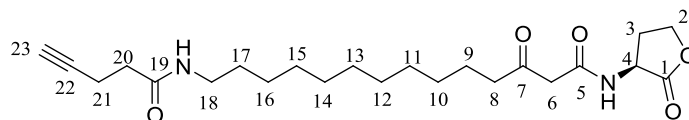
AHL-derivative 60

Method 1: According to general procedure 1, the title compound **60** (480 mg, 77%) was obtained from carboxylic acid **58** (408 mg, 1.69 mmol), DMAP (207 mg, 1.69 mmol), DCC (349 mg, 1.69 mmol), Meldrum's acid (244 mg, 1.69 mmol) and (*S*)- α -amino- γ -butyrolactone hydrobromide (308 mg, 1.69 mmol) as a colourless solid after flash chromatography (EtOAc/MeOH 9:1, $R_f = 0.3$, cerium stain). **$^1\text{H NMR}$** (CD_3OD , 400 MHz, COCH_2CO signal is hidden under solvent peak) δ (ppm) = 4.61 (dd, 1H, 4-H, $J = 9.3$ Hz, 9.3 Hz), 4.44 (ddd, 1H, 2-H, $J = 9.8$ Hz, 8.8 Hz, 2.2 Hz), 4.33 – 4.27 (m, 1H, 2-H), 3.27 (t, 2H, 18-H, $J = 5.9$ Hz), 2.57 (t, 2H, 8-H, $J = 8.0$ Hz), 2.34 – 2.23 (m, 1H, 3-H), 1.673– 1.67 (m, 1H, 3-H), 1.63 – 1.53 (m, 4H, 17-H, 9-H), 1.38 – 1.28 (m, 14H, 16-H, 15-H, 14-H, 13-H, 12-H, 11-H, 10-H); **$^{13}\text{C NMR}$** (CD_3OD , 100 MHz) δ (ppm) = 206.5 (C7), 171.2 (C5), 169.4 (C1), 67.1 (C2), 52.5 (C6), 50.0 (C4), 43.9 (C8), 34.8 (C18), 30.9, 30.7, 30.6, 30.5, 30.2, 30.0, 29.7, 27.9, 26.8, 24.5 (C17, C16, C15, C14, C13, C12, C11 C10, C9, C3);

HRMS (ESI) m/z calcd for $C_{18}H_{30}N_4NaO_4$ $[M+Na]^+$ 389.2160, found 389.2160; $[\alpha]_D^{20} = -8.0^\circ$ ($c=0.1$, MeOH); **Mp.**: 67.5 °C; **IR** (KBr, cm^{-1}): 3306, 2915, 2859, 2089, 1725, 1647; **CHN** calcd. for $C_{18}H_{30}N_4O_4$: C, 59.00%; H, 8.25%; N, 15.29%. Found: C, 59.25%; H, 8.49%; N, 14.42%.

Method 2: AHL-derivative **59** (292 mg, 0.72 mmol) and NaN_3 (471 mg, 7.20 mmol, 10 equiv.), were dissolved in DMF (80 mL) and stirred at 60 °C for 24 h. The solvent was distilled off and the residue was dissolved in EtOAc (30 mL). The organic phase was washed twice with 1 M aqueous $KHSO_4$ -solution (30 mL), saturated aqueous $NaHCO_3$ -solution (30 mL) and brine. The organic phase was dried over Na_2SO_4 . After filtration the solvent was evaporated *in vacuo* to give the title compound as a colourless solid (135 mg, 51%).

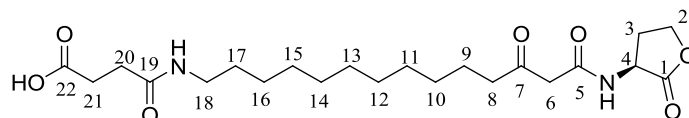
AHL-derivative 63



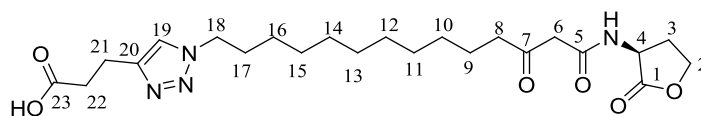
Method 1: According to general procedure 7, the title compound **63** (94 mg, 76%) was obtained as a brown oil from NHS-ester **61** (57 mg, 0.29 mmol) and AHL-derivative **51** (100 mg, 0.29 mmol). The crude product was purified by flash chromatography $CH_2Cl_2/MeOH$ (8:1, $R_f = 0.7$, cerium stain); 1H NMR ($DMSO-d_6$, 400 MHz) δ (ppm) = 4.57 – 4.52 (m, 1H, 4-H), 4.35 (m, 1H, 2-H, $J = 6.4$ Hz), 4.22 – 4.18 (m, 1H, 2-H) 3.31 (s, 2H, 6-H), 3.01 (t, 2H, 18-H, $J = 6.7$ Hz), 2.43 – 2.37 (m, 2H, 8-H), 2.36 – 2.31 (m, 2H, 21-H), 2.23 (t, 2H, 20-H, $J = 6.1$ Hz), 2.19 – 2.08 (m, 1H, 3-H), 2.06 (s, 1H, 23-H), 1.74 – 1.58 (m, 1H, 3-H), 1.47 – 1.33 (m, 4H, 17-H, 9-H), 1.26 – 1.19 (m, 14H, 16-H, 15-H, 14-H, 13-H, 12-H, 11-H, 10-H); ^{13}C NMR (CD_3OD , 100 MHz) δ (ppm) = 204.6 (C7), 175.0 (C19), 170.5 (C1), 166.4 (C5), 83.6 (C22), 70.9 (C23), 65.4 (C2), 50.1 (C6), 48.1 (C4), 41.9 (C8), 34.3 (C18), 28.9 (C20), 28.9, 28.86, 28.8, 28.7, 28.66, 28.5, 28.3, 27.9, 26.2 (C17, C16, C15, C14, C13, C12, C11, C10, C3), 22.7 (C9), 14.3 (C21); **HRMS** (ESI) m/z calcd for $C_{23}H_{36}N_2NaO_5$ $[M+Na]^+$ 443.2516, found 443.2510; $[\alpha]_D^{20} = -10.6^\circ$ ($c=0.4$, MeOH); **IR** (film, cm^{-1}): 3298, 2919, 2850, 1778, 1636, 1546.

Method 2: 4-pentynoic acid (15 mg, 0.15 mmol) was dissolved in DMF (20 mL) and Et₃N (0.06 mL, 0.46 mmol, 3 equiv.) was added to the solution. The reaction was stirred for 5 min, cooled to 0 °C and EDC·HCl (42 mg, 0.22 mmol) and HOBT (30 mg, 0.22 mmol) were added. AHL-derivative **51** (50 mg, 0.15 mmol) was added after 15 min and the solution was stirred at room temperature for 3 days. The solvent was evaporated *in vacuo* and the residue was solved in EtOAc (30 mL). The organic phase was washed twice with 1 M aqueous KHSO₄-solution (30 mL), saturated aqueous NaHCO₃-solution (30 mL) and brine. The solution was dried over Na₂SO₄. After filtration the solvent was evaporated *in vacuo* to give the title compound as a colourless solid (22 mg, 35%).

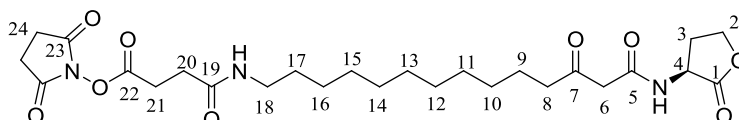
AHL-derivative 65



AHL-derivative **51** (150 mg, 0.44 mmol) and succinic anhydride (44 mg, 0.44 mmol) were dissolved in DMSO (30 mL). Et₃N (0.08 mL, 0.57 mmol, 1.3 equiv.) was added and the solution was stirred for 48 h at room temperature. The solvent was distilled off *in vacuo* and the residue was dissolved in 1 M aqueous HCl. The solution was extracted three times with EtOAc (20 mL) to give the desired product (72 mg, 37%) as a colourless solid. ¹H NMR (CD₃OD, 400 MHz, COCH₂CO signal is hidden under solvent peak) δ (ppm) = 4.65 – 4.54 (m, 1H, 4-H), 4.45 (ddd, 1H, 2-H, J = 9.0 Hz, 8.9 Hz, 2.1 Hz), 4.34 – 4.26 (m, 1H, 2-H), 3.15 (t, 2H, 18-H, J = 7.4 Hz), 2.62 – 2.55 (m, 4H, 21-H, 8-H), 2.48 – 2.43 (m, 2H, 20-H), 2.35 – 2.24 (m, 1H, 3-H), 1.63 – 1.45 (m, 5H, 17-H, 9-H, 3-H), 1.40 – 1.25 (m, 14H, 16-H, 15-H, 14-H, 13-H, 12-H, 11-H, 10-H); ¹³C NMR (CD₃OD, 100 MHz) δ (ppm) = 206.2 (C7), 176.7 (C22), 176.1 (C19), 174.4 (C1), 166.4 (C5), 67.4 (C2), 50.2 (C4), 49.6 (C6), 44.3 (C8), 43.7 (C18), 40.5 (C21), 34.8 (C20), 31.7, 31.4, 30.6, 30.4, 30.1, 29.7, 28.0, 26.8, 26.1 (C17, C16, C15, C14, C13, C12, C11, C10, C3), 24.5 (C9); HRMS (ESI) m/z calcd for C₂₂H₃₆N₂NaO₇ [M+Na]⁺ 463.2415, found 463.2416; [α]_D²⁰ = -14.0 ° (c = 0.3, MeOH); Mp.: 90.2 °C; IR (KBr, cm⁻¹): 3309, 2918, 2849, 1630, 1557.

AHL-derivative 67

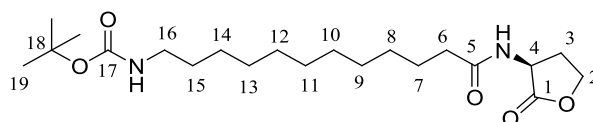
According to general procedure 8, the title compound (283 mg, 56%) was obtained as a colourless solid from the azide **60** (400 mg, 1.09 mmol), the alkyne **62** (107 mg, 1.09 mmol), CuSO₄ (17 mg, 0.11 mmol) and sodium ascorbate (22 mg, 0.11 mmol); ¹H NMR (CDCl₃, 400 MHz) δ (ppm) = 7.59 (s, 1H, 19-H), 4.58 (dd, 1H, 4-H, J = 9.0 Hz, 9.0 Hz), 4.45 (ddd, 1H, 2-H, J = 9.6 Hz, 9.3 Hz, 2.5 Hz), 4.33 – 4.26 (m, 3H, 18-H, 2-H), 2.98 (t, 2H, 21-H, J = 7.2 Hz), 2.67 (t, 2H, 8-H, J = 8.3 Hz), 2.56 (t, 2H, 22-H, J = 7.6 Hz), 2.34 – 2.22 (m, 1H, 3-H), 1.91 – 1.80 (m, 2H, 17-H), 1.73 – 1.64 (m, 1H, 3-H), 1.60 – 1.52 (m, 2H, 9-H), 1.36 – 1.20 (m, 14H, 16-H, 15-H, 14-H, 13-H, 12-H, 11-H, 10-H); ¹³C NMR (CDCl₃, 100 MHz) δ (ppm) = 204.8 (C7), 177.1 (C23), 176.0 (C1), 172.5 (C5), 147.8 (C20), 123.2 (C19), 67.6 (C2), 51.8 (C6), 50.1 (C4), 44.0 (C18), 35.0 (C8), 34.6 (C22), 31.5, 30.7, 30.6, 30.3, 30.2, 30.0, 27.6, 26.9, 26.2 (C17, C16, C15, C14, C13, C12, C11, C10, C3), 24.6 (C21), 22.0 (C9); HRMS (ESI) m/z calcd for C₂₃H₃₆N₄NaO₆ [M+Na]⁺ 487.2527, found 487.2522; [α]_D²⁰ = -15.6° (c = 0.3, MeOH); Mp.: 108.5 °C; IR (KBr, cm⁻¹): 2918, 2849, 1703.

AHL-derivative 66

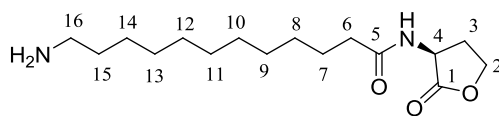
AHL-derivative **65** (503 mg, 1.14 mmol), *N*-hydroxysuccinimide (197 mg, 1.71 mmol) and EDC·HCl (329 mg, 1.71 mmol) were dissolved in DMF (40 mL) and stirred for 48 h at room temperature. The solvent was distilled off *in vacuo* and the residue was dissolved in EtOAc (30 mL). The organic phase was washed three times with 1 M aqueous KHSO₄-solution (30 mL) and saturated aqueous NaHCO₃-solution (30 mL). The organic phase was dried over Na₂SO₄. After filtration the solvent was distilled off *in vacuo* to give the crude product (381 mg, 52%) which was purified by column chromatography CH₂Cl₂/MeOH (9:1, R_f = 0.3, cerium stain).

¹H NMR (CD₃OD, 400 MHz COCH₂CO signal is hidden under solvent peak) δ (ppm) = 4.51 (dd, 1H, 4-H, J = 9.3 Hz, 9.3 Hz), 4.35 (ddd, 1H, 2-H, J = 9.3 Hz, 9.3 Hz, 1.8 Hz), 4.24 – 4.18 (m, 1H, 2-H), 3.36 (t, 2H, 18-H, J = 7.8 Hz), 2.76 – 2.74 (m, 4H, 21-H, 8-H), 2.60 (s, 4H, 23-H), 2.54 – 2.46 (m, 2H, 20-H), 2.26 – 2.15 (1H, 3-H), 1.50 – 1.36 (m, 5H, 17-H, 9-H, 3-H), 1.24 – 1.16 (m, 14H, 16-H, 15-H, 14-H, 13-H, 12-H, 11-H, 10-H); **¹³C NMR** (CD₃OD, 100 MHz) δ (ppm) = 208.1 (C7), 179.9 (C22), 179.8 (C19), 174.8 (C1), 173.1 (C5), 167.9 (C24), 67.3 (C2), 59.3 (C6), 51.5 (C4), 44.3 (C8), 40.1 (C18), 35.4 (C21), 31.7 (C22), 30.8, 30.7, 30.5, 30.2, 29.9, 29.3, 28.9, 28.0, 26.8, 26.6 (C23, C17, C16, C15, C14, C13, C12, C11, C10, C3), 24.6 (C9); **HRMS** (ESI) m/z calcd for C₂₆H₃₉N₃O₉ [M+Na]⁺ 560.2579, found 560.2583; $[\alpha]_D^{20}$ = -31.5 ° (c = 0.6, MeOH); **Mp.**: 50.1 °C; **CHN** calcd. for C₂₆H₃₉N₃O₉: C, 58.09%; H, 7.31%; N, 7.82%. Found: C, 55.55%; H, 7.20%; N, 7.19%.

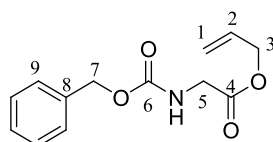
AHL-derivative 71



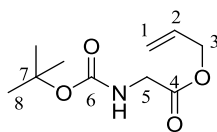
The title compound (562 mg, 89%) was obtained from carboxylic acid **70** (500 mg, 1.59 mmol), DMAP (194 mg, 1.59 mmol), DCC (327 mg, 1.59 mmol) and (*S*)- α -amino- γ -butyrolactone hydrobromide (289 mg, 1.59 mmol) after 24 h at 60 °C in DMF (100 mL). The crude product was purified by flash chromatography (PE/EtOAc 6:4, R_f = 0.4, cerium stain); **¹H NMR** (CDCl₃, 400 MHz) δ (ppm) = 6.20 (s, 1H, N-H), 4.58 – 4.51 (m, 1H, 4-H), 4.71 – 4.2 (m, 1H, 2-H), 4.30 – 4.23 (m, 1H, 2-H), 3.11 – 3.04 (m, 2H, 16-H), 2.23 (t, 2H, 6-H, J = 7.5 Hz), 2.18 – 2.07 (m, 1H, 3-H), 1.69 – 1.58 (m, 3H, 15-H, 3-H), 1.46 – 1.40 (m, 11H, 19-H, 7-H), 1.35 – 1.22 (m, 14H, 14-H, 13-H, 11-H, 10-H, 9-H, 8-H); **¹³C NMR** (CDCl₃, 100 MHz) δ (ppm) = 175.6 (C1), 173.7 (C5), 156.1 (C17), 78.9 (C18), 66.0 (C2), 49.2 (C4), 40.4 (C6), 36.3 (C16), 33.7 (C3), 30.6, 30.1, 29.5, 29.4, 29.3, 29.2, 28.4, 26.7, 25.4, 24.9 (C19, C15, C14, C13, C12, C11, C10, C9, C8, C7); **HRMS** (ESI) m/z calcd for C₂₁H₃₈N₂O₅ [M+Na]⁺ 421.2673, found 421.2688; $[\alpha]_D^{20}$ = -44 ° (c = 0.5, MeOH); **Mp.**: 108.6 °C; **IR** (KBr, cm⁻¹): 2850, 1800, 1700, 1650, 1550, 1180; **CHN** calcd. for C₂₁H₃₈N₂O₅: C, 63.29%; H, 9.61%; N, 7.03%. Found: C, 63.26%; H, 9.69%; N, 6.71%.

AHL-derivative 72

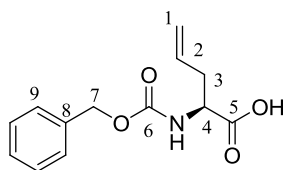
According to general procedure 2, the desired product (383 mg, 91%) was obtained as a brown solid from AHL derivative **71** (562 mg, 1.41 mmol) and purified by flash chromatography (EtOAc/EtOH 9:1, $R_f = 0.4$, cerium stain); $^1\text{H NMR}$ (CD_3OD , 600 MHz) δ (ppm) = 4.57 (dd, 1H, 4-H, $J = 9.0$ Hz, 9.0 Hz), 4.46 – 4.42 (m, 1H, 2-H), 4.31 – 4.27 (m, 1H, 2-H), 2.91 (t, 2H, 16-H, $J = 8.3$ Hz), 2.55 – 2.51 (m, 1H, 3-H), 2.32 – 2.26 (m, 1H, 3-H), 2.24 (t, 2H, 6-H, $J = 7.2$ Hz), 1.67 – 1.59 (m, 4H, 15-H, 7-H), 1.41 – 1.30 (m, 14H, 14-H, 13-H, 12-H, 11-H, 10-H, 9-H, 8-H); $^{13}\text{C NMR}$ (CD_3OD , 100 MHz) δ (ppm) = 176.2 (C1), 175.0 (C5), 65.8 (C2), 48.7 (C4), 39.5 (C6), 35.2 (C16), 29.09, 29.08, 29.04, 29.0, 28.9, 28.8, 28.7, 28.1, 27.1, 26.0 (C15, C14, C13, C12, C11, C10, C9, C8, C7, C3); **HRMS** (ESI) m/z calcd for $\text{C}_{16}\text{H}_{30}\text{N}_2\text{O}_3$ $[\text{M}+\text{H}]^+$ 299.2329, found 299.2326; $[\alpha]_{\text{D}}^{20} = -9^\circ$ ($c = 0.2$, MeOH); **Mp.**: 72.4 °C; **IR** (KBr, cm^{-1}): 3000, 1800, 1650, 1510, 1200.

8.4 Lactone ring modified AHL-derivatives**Cbz-glycine allylester 74b**

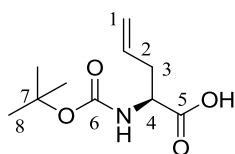
According to general procedure 3, the title compound **74b** (458 mg, 64%) was obtained from Cbz-glycine (600 mg, 2.87 mmol), allylic alcohol (0.2 mL, 2.87 mmol), DMAP (35.0 mg, 0.29 mmol) and DCC (591 mg, 2.87 mmol). The crude product was purified by flash chromatography $\text{CH}_2\text{Cl}_2/\text{MeOH}$ (10:0.2, $R_f = 0.6$, cerium stain) to give the product as a colourless oil. $^1\text{H NMR}$ (CDCl_3 , 400 MHz) δ (ppm) = 7.12 – 7.05 (m, 5H, 9-H), 5.70 – 5.60 (m, 1H, 2-H), 5.09 – 4.99 (m, 2H, 1-H), 4.87 (s, 2H, 7-H), 4.39 (d, 2H, 3-H, $J = 6.0$ Hz), 3.75 (d, 2H, 5-H, $J = 6.0$ Hz); $^{13}\text{C NMR}$ (CDCl_3 , 100 MHz) δ (ppm) = 169.7 (C4), 156.3 (C6), 136.2 (C8), 131.5 (C2), 128.54, 128.51, 128.21, 128.15, 128.1 (C9), 119.0 (C1), 67.1 (C7), 66.0 (C3), 42.8 (C5).

Boc-glycine ester 74c

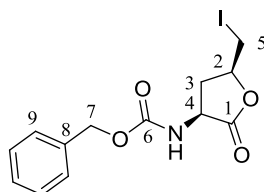
According to general procedure 3, the title compound **74c** (893 mg, 73%) was obtained as a colourless oil from Boc-glycine (1.0 g, 5.71 mmol), allylic alcohol (0.39 mL, 5.71 mmol), DMAP (697 mg, 0.57 mmol) and DCC (1.18 g, 5.71 mmol). $^1\text{H NMR}$ (CDCl_3 , 400 MHz) δ (ppm) = 5.89 – 5.70 (m, 1H, 2-H), 5.28 – 5.17 (m, 3H, NH, 1-H), 4.57 (d, 2H, 3-H, $J = 6.7$ Hz), 3.87 – 3.85 (m, 2H, 5-H), 1.39 (s, 9H, 8-H); $^{13}\text{C NMR}$ (CDCl_3 , 100 MHz) δ (ppm) = 170.5 (C4), 155.7 (C6), 131.7 (C2), 118.6 (C1), 79.9 (C7), 65.8 (C3), 42.2 (C5), 28.2 (C8).

Cbz-protected allyl glycine 75b

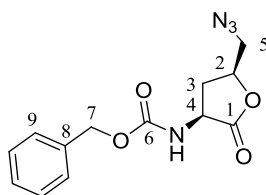
According to general procedure 4, the title compound **75b** (263 mg, 88%) was obtained as a brown oil. LHMDS solution was prepared freshly from hexamethyldisilazane (1.5 mL, 6.96 mmol) in abs THF (5.0 mL) with *n*-BuLi (5.0 mL, 6.00 mmol). Cbz-glycine allylester **74b** (300 mg, 1.20 mmol), $\text{Al}(\text{OPr-}i)_3$ (269 mg, 1.32 mmol) and quinidine (972 mg, 3.00 mmol) were dissolved in abs THF (50 mL). The LHMDS-solution was added slowly to the reaction mixture. $^1\text{H NMR}$ (CDCl_3 , 400 MHz) δ (ppm) = 7.38 – 7.29 (m, 5H, 9-H), 5.78 – 5.67 (m, 1H, 2-H), 5.18 – 5.09 (m, 4H, 7-H, 1-H), 4.51 – 4.46 (m, 1H, 4-H), 2.67 – 2.52 (m, 2H, 3-H); $^{13}\text{C NMR}$ (CDCl_3 , 100 MHz) δ (ppm) = 175.0 (C5), 154.9 (C6), 135.2 (C8), 130.9 (C2), 127.5, 127.4, 127.3, 127.2, 127.1 (C9), 118.5 (C1), 65.9 (C7), 52.3 (C4), 35.3 (C3).

Boc-protected allyl glycine 75c

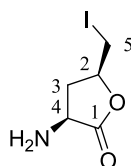
According to general procedure 4, the title compound **75c** (300 mg, quant.) was obtained as a brown oil. LHMDS solution was prepared freshly from hexamethyldisilazane (1.7 mL, 8.12 mmol) in abs THF (5.0 mL) with *n*-BuLi (7.0 mL, 7.00 mmol). Boc-glycine allylester **74c** (300 mg, 1.40 mmol), Al(OPr-*i*)₃ (314 mg, 1.54 mmol) and quinidine (1.13 g, 3.50 mmol) were dissolved in abs THF (50 mL). The LHMDS-solution was added slowly to the reaction mixture. ¹H NMR (CDCl₃, 400 MHz) δ (ppm) = 5.78 – 5.67 (m, 1H, 2-H), 5.18 – 5.02 (m, 2H, 1-H), 4.94 (1H, NH), 4.41 – 4.32 (m, 1H, 4-H), 2.62 – 2.41 (m, 2H, 3-H), 1.42 (s, 9H, 8-H); ¹³C NMR (CDCl₃, 100 MHz) δ (ppm) = 208.2 (C5), 179.2 (C6), 155.7 (C7), 132.0 (C2), 119.5 (C1), 53.0 (C4), 36.3 (C3), 28.4 (C8).

Cbz-protected iodolactone 76b

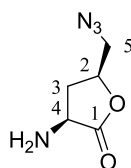
According to general procedure 5, the title compound **76b** (330 mg, 83%) was obtained from Cbz-protected allyl glycine **75b** (264 mg, 1.06 mmol) and I₂ (536 mg, 2.12 mmol). The crude product was purified by flash chromatography PE/EtOAc (1:1, *R*_f = 0.4, cerium stain) to give **76b** as a brown oil. ¹H NMR (DMSO-*d*₆, 400 MHz) δ (ppm) = 7.41 – 7.32 (m, 5H, 9-H), 5.06 (s, 2H, 7-H), 4.67 – 4.56 (m, 1H, 4-H), 4.45 – 4.44 (m, 1H, 2-H), 3.55 - 3.24 (m, 2H, 5-H), 2.63 – 2.56 (m, 1H, 3-H), 1.92 – 1.77 (m, 1H, 3-H); ¹³C NMR (DMSO-*d*₆, 100 MHz) δ (ppm) = 174.2 (C1), 155.9 (C6), 136.9 (C8), 128.4, 128.3, 127.9, 127.8, 127.6 (C9), 75.4 (C4), 65.8 (C7), 51.4 (C2), 34.7 (C3), 9.7 (C5), 7.8 (C3); HRMS (ESI) *m/z* calcd for C₁₃H₁₄INNaO₄ [M+Na]⁺ 397.9860, found 397.9861.

Cbz-protected azide 79b

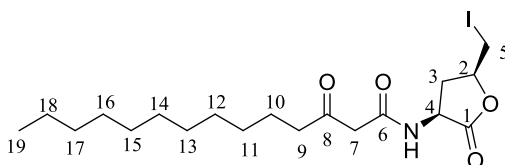
According to general procedure 6, the title compound **79b** (296 mg, 95%) was obtained from lactone **76b** (400 mg, 1.07 mmol) and NaN_3 (347 mg, 5.34 mmol). The crude product was purified by flash chromatography PE/EtOAc (1:1, $R_f = 0.3$, cerium stain) to give **79b** as a brown oil. $^1\text{H NMR}$ (DMSO- d_6 , 400 MHz) δ (ppm) = 7.37 – 7.29 (m, 5H, 9-H), 5.03 (s, 2H, 7-H), 4.65 – 4.41 (m, 2H, 4-H, 2-H), 3.80 – 3.61 (m, 2H, 5-H), 2.48 – 2.40 (m, 1H, 3-H), 2.07 – 1.93 (m, 1H, 3-H); $^{13}\text{C NMR}$ (DMSO- d_6 , 100 MHz) δ (ppm) = 174.5 (C1), 155.5 (C6), 136.8 (C8), 128.4, 128.35, 127.9, 127.8, 127.7 (C9), 75.4 (C4), 65.7 (C7), 52.9 (C2), 52.9 (C5), 50.5 (C3), 30.4 (C3); **HRMS** (ESI) m/z calcd for $\text{C}_{13}\text{H}_{14}\text{N}_4\text{O}_4$ $[\text{M}+\text{Na}]^+$ 313.0907, found 313.0907.

Iodolactone 77

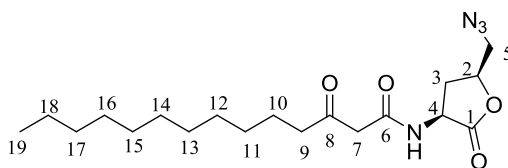
Deprotection of the Boc-group was performed according to general procedure 2. Boc-protected iodolactone **76c** (209 mg, 0.61 mmol) was dissolved in TFA/ CH_2Cl_2 (30 mL, 1:1) to give the crude product which was used in the next step without further purification. **HRMS** (ESI) m/z calcd for $\text{C}_5\text{H}_8\text{INO}_2$ $[\text{M}+\text{H}]^+$ 241.9672, found 241.9668.

Azide lactone 80

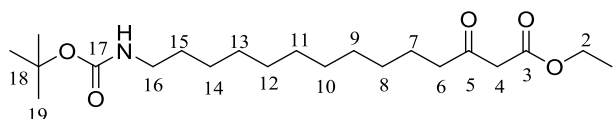
Deprotection of the Boc-group was performed according to general procedure 2. Boc-protected Azide **79c** (129 mg, 0.50 mmol) was dissolved in TFA/CH₂Cl₂ (30 mL, 1:1). The product was not isolated and used in the next step without further purification.

AHL-derivative 78

According to general procedure 1, the title compound **78** (120 mg, 43% over 2 steps) was obtained from lauric acid (119 mg, 0.60 mmol), DMAP (73 mg, 0.60 mmol), DCC (124 mg, 0.60 mmol), Meldrum's acid (86 mg, 0.60 mmol) and iodolactone **77** (143 mg, 0.60 mmol). The crude product was purified by flash chromatography (PE/EtOAc 9:1, $R_f = 0.2$, cerium stain); ¹H NMR (CDCl₃, 400 MHz) δ (ppm) = 4.80 – 4.46 (m, 2H, 4-H, 2-H), 3.49 – 3.44 (m, 3H, 7-H, 5-H), 3.38 – 3.30 (m, 1H, 5-H), 3.00 – 2.93 (m, 1H, 3-H), 2.54 – 2.44 (m, 2H, 9-H), 1.98 – 1.89 (m, 1H, 3-H), 1.71 – 1.55 (m, 2H, 10-H), 1.35 – 1.19 (m, 16H, 18-H, 17-H, 16-H, 15-H, 14-H, 13-H, 12-H, 11-H), 0.87 (t, 3H, 19-H, $J = 8.1$ Hz). ¹³C NMR (CDCl₃, 100 MHz) δ (ppm) = 206.8 (C8), 173.6 (C6), 166.3 (C1), 76.3 (C4), 50.7 (C2), 48.2 (C9), 44.1 (C7), 36.1 (C3), 34.1 (C17), 32.1 (C13), 29.6, 29.4, 29.3, 29.0 (C16, C15, C14, C12), 25.5 (C11), 23.36 (C10), 22.65 (C18), 14.1 (C19), 7.9 (C5); HRMS (ESI) m/z calcd C₁₉H₃₂INO₄ [M+Na]⁺ 488.1268, found 488.1256.

AHL-derivative 81

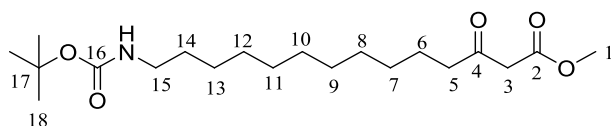
According to general procedure 1, the title compound **81** (106 mg, 35% over 2 steps) was obtained from lauric acid (163 mg, 0.82 mmol), DMAP (99.4 mg, 0.82 mmol), DCC (168 mg, 0.82 mmol), Meldrum's acid (117 mg, 0.82 mmol) and azide **80** (127 mg, 0.82 mmol) as a colourless solid. The crude product was purified by flash chromatography (PE/EtOAc 1:1, $R_f = 0.2$, cerium stain). $^1\text{H NMR}$ (CDCl_3 , 400 MHz) δ (ppm) = 4.76 – 4.55 (m, 2H, 4-H, 2-H), 3.67 – 3.43 (m, 2H, 7-H), 2.65 – 2.55 (m, 2H, 9-H), 2.15 – 2.06 (m, 1H, 3-H), 1.88 – 1.82 (m, 1H, 3-H), 1.74 – 1.67 (m, 1H, 10-H), 1.53 – 1.64 (m, 3H, 10-H, 5-H), 1.24 – 1.36 (m, 16H, 18-H, 17-H, 16-H, 15-H, 14-H, 13-H, 12-H, 11-H), 0.89 (t, 3H, 19-H, $J = 8.1$ Hz); $^{13}\text{C NMR}$ (CDCl_3 , 100 MHz) δ (ppm) = 206.4 (C8), 175.7 (C6), 169.7 (C1), 79.3 (C4), 54.8 (C2), 51.0 (C9), 43.6 (C7), 34.9 (C3), 33.1 (C17), 32.1 (C13), 30.9, 30.8, 30.5, 30.2, 26.9, 26.1, 24.6, 23.9 (C18, C16, C15, C14, C12, C11, C10, C5), 14.6 (C19); **HRMS** (ESI) m/z $\text{C}_{19}\text{H}_{32}\text{N}_4\text{O}_4$ $[\text{M}+\text{Na}]^+$ 403.2316, found: 403.2329; **Mp.**: 89.2 °C; **IR** (KBr): 2915, 2848, 2089, 1653, 1630 cm^{-1} .

8.5 Synthesis of a bifunctional AHL mimic **β -ketoester 101**

Boc-protected aminododecanoic acid **49** (197 mg, 0.63 mmol), DMAP (76 mg, 0.63 mmol), DCC (129 mg, 0.63 mmol) and Meldrum's acid (92 mg, 0.63 mmol) were dissolved in CH_2Cl_2 (50 mL) and stirred for 24 h at room temperature. After filtration of the *N,N*-dicyclohexyl urea formed in the reaction, the solvent was distilled off *in vacuo*. The residue was dissolved in EtOH (50 mL) and stirred under reflux for 3 h. After evaporation of the alcohol, the crude product was purified by flash chromatography PE/EtOAc (7:3, $R_f = 0.4$, cerium stain) to give the title compound (217 mg, 90%) as a colourless solid.

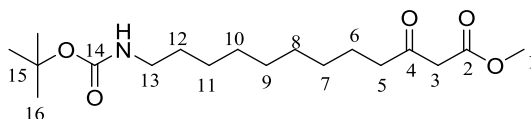
¹H NMR (CDCl₃, 400 MHz) δ (ppm) = 4.58 (br, 1H, N-H), 4.13 (q, 2H, 2-H, J = 7.7 Hz), 3.36 (s, 2H, 4-H), 3.06 – 3.00 (m, 2H, 16-H), 2.47 (t, 2H, 6-H, J = 8.0 Hz), 1.55 – 1.49 (m, 2H, 7-H), 1.38 (s, 11H, 19-H, 15-H), 1.24 – 1.20 (m, 17H, 14-H, 13-H, 12-H, 11-H, 10-H, 9-H, 8-H, 1-H); **¹³C NMR** (CDCl₃, 100 MHz) δ (ppm) = 203.1 (C5), 167.4 (C3), 155.8 (C17), 78.8 (C18), 61.1 (C2), 49.5 (C4), 43.0 (C6), 34.9 (C16), 30.0, 29.4, 29.3, 29.2, 28.9, 28.4, 26.7, 25.4, 24.6, 23.4 (C19, C15, C14, C13, C12, C11, C10, C9, C8, C7), 14.3 (C1); **HRMS** (ESI) m/z C₂₁H₃₉NO₅ [M+Na]⁺ 408.2736, found: 408.2720; **Mp.**: 68.3 °C; **CHN** calcd. for C₂₁H₃₉NO₅: C, 65.40%; H, 10.20%; N, 3.63%. Found: C, 66.03%; H, 10.01%; N, 4.21%.

β -ketoester 100



Boc-protected aminododecanoic acid **49** (300 mg, 0.95 mmol), DMAP (166 mg, 0.95 mmol), DCC (196 mg, 0.95 mmol) and Meldrum's acid (137 mg, 0.95 mmol) were dissolved in CH₂Cl₂ (50 mL) and stirred for 24 h at room temperature. After filtration of the *N,N*-dicyclohexyl urea formed in the reaction the solvent was distilled off. The residue was dissolved in MeOH (50 mL) and the reaction was stirred 3 h under reflux to give the crude product as a yellow solid (211 mg, 60%) which was directly used for the next reaction. **HRMS** (ESI) m/z C₂₀H₃₇NO₅ [M+Na]⁺ 394.2564, found: 394.2571.

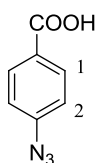
β -ketoester 105c



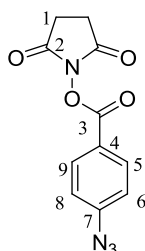
N-boc-protected carboxylic acid (200 mg, 0.70 mmol), DMAP (85 mg, 0.70 mmol), DCC (144 mg, 0.70 mmol) and Meldrum's acid (100 mg, 0.70 mmol) were dissolved in CH₂Cl₂ (70 mL) and stirred for 24 h at room temperature. After filtration of the *N,N*-dicyclohexyl urea formed in the reaction the solvent was distilled off. The residue was dissolved in MeOH (50 mL) and the reaction was stirred 24 h under reflux.

The solvent was evaporated *in vacuo* and the crude product was purified by flash chromatography PE/EtOAc (7:3, $R_f = 0.3$, cerium stain) to give the title compound as a colourless solid (202 mg, 85%). $^1\text{H NMR}$ (CD_3OD , 400 MHz) δ (ppm) = 4.77 (s, 2H, 3-H), 3.72 (s, 3H, 1-H), 3.04 (t, 2H, 13-H, $J = 7.4$ Hz), 2.58 (t, 2H, 5-H, $J = 8.1$ Hz), 1.62 – 1.54 (m, 2H, 6-H), 1.54 – 1.42 (m, 11H, 16-H, 12-H), 1.37 – 1.29 (m, 10H, 11-H, 10-H, 9-H, 8-H, 7-H); $^{13}\text{C NMR}$ (CD_3OD , 100 MHz) δ (ppm) = 205.3 (C4), 169.7 (C2), 158.5 (C14), 79.8 (C15), 52.7 (C1), 51.7 (C3), 43.9 (C5), 41.4 (C13), 31.0, 30.6, 30.5, 30.4, 30.1, 29.0, 27.9 (C16, C12, C11, C10, C9, C8, C7), 24.5 (C6); **HRMS** (ESI) m/z $\text{C}_{18}\text{H}_{33}\text{NO}_5$ $[\text{M}+\text{Na}]^+$ 366.2251, found: 366.2241; **Mp.**: 42.2 °C; **IR** (KBr, cm^{-1}): 3370, 2920, 2853, 1753, 1720, 1697; **CHN** calcd. for $\text{C}_{18}\text{H}_{33}\text{NO}_5$: C, 62.95%; H, 9.68%; N, 4.08%. Found: C, 62.83%; H, 9.80%; N, 3.88%.

Azide 110¹⁷⁵

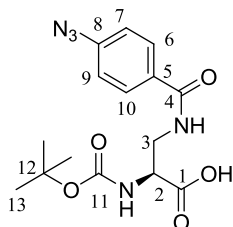


4-Aminobenzoic acid (1.50 g, 10.9 mmol) was dissolved in H_2O (100 mL) and conc. HCl (2.3 mL) was added. The mixture was cooled to 0 °C and a solution of NaNO_2 (0.91 g, 13.1 mmol) in H_2O (30 mL) was added slowly. In the next step NaN_3 (0.85 g, 13.1 mmol) was added and the ice bath was removed. The solution was stirred for 1 h at room temperature and then extracted four times with EtOAc (60 mL). The organic phase was extracted three times with aqueous NaOH-solution (3 M, 30 mL). Conc. HCl was added carefully to the combined basic solution until a pH value of 2 was reached. Afterwards the mixture was extracted four times with EtOAc (40 mL) and the combined organic phases were dried over Na_2SO_4 . After filtration the solvent was evaporated *in vacuo* to give the title compound (1.78 g, quant., EtOAc impurities) as a brown solid. $^1\text{H NMR}$ (DMSO-d_6 , 400 MHz) δ (ppm) = 7.99 (d, 2H, 1-H, $J = 8.1$ Hz), 7.04 (d, 2H, 2-H, $J = 7.3$ Hz).

NHS-ester 112²³⁵

Azide **110** (1.78 g, 10.9 mmol), *N*-hydroxysuccinimide (1.88 g, 16.4 mmol) and EDC·HCl (3.15 g, 16.4 mmol) were dissolved in DMF (90 mL) and stirred for 48 h at room temperature. The solvent was distilled off *in vacuo* and the residue was dissolved in EtOAc (60 mL). The organic phase was washed twice with 1 M aqueous KHSO₄-solution (30 mL), saturated aqueous NaHCO₃-solution (30 mL) and brine. After filtration the solvent was distilled off to give product (2.63 g, 93%) as a brown oil. **MS** (ESI) *m/z* 283.1 (M+Na⁺, 100%).

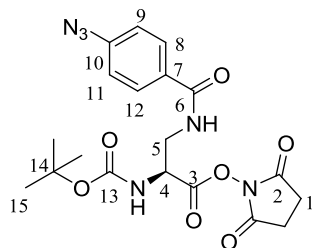
Compound is literature known but was synthesised according to general NHS ester procedure used in this thesis.

Carboxylic acid 109

Boc-Dap-OH (250 mg, 1.23 mmol), NHS-ester **112** (319 mg, 1.23 mmol) and Et₃N (0.3 mL, 2.45 mmol) were dissolved in DMSO (40 mL) and stirred for three days at room temperature. The solvent was distilled off *in vacuo* to give the crude product (363 mg, 85%) as a colourless solid. **¹H NMR** (CD₃OD, 400 MHz) δ (ppm) = 7.84 – (d, 2H, 10-H, 6-H, *J* = 8.0 Hz), 7.13 (d, 2H, 9-H, 7-H, *J* = 7.4 Hz), 4.41 – 4.38 (m, 1H, 2-H), 3.80 – 3.65 (m, 2H, 3-H), 1.40 (s, 9H, 13-H); **¹³C NMR** (CDCl₃, 100 MHz) δ (ppm) = 173.3 (C1), 166.3 (C4), 155.5 (C11), 142.2 (C8), 129.4 (C5), 127.9 (C10, C6), 117.8 (C9, C8), 78.8 (C12), 53.8 (C2), 44.8 (C3), 27.2 (C13);

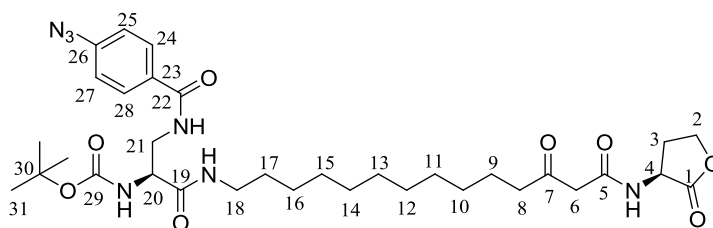
HRMS (ESI) m/z calcd for $C_{15}H_{19}N_5O_5$ $[M+Na]^+$ 372.1278, found 372.1280; **Mp.:** 93.8 °C; $[\alpha]_D^{20} = +33.0^\circ$ ($c = 0.4$, MeOH); **IR** (KBr, cm^{-1}): 3363, 2920, 2119; **CHN** calcd. for $C_{15}H_{19}N_5O_5$: C, 51.57%; H, 5.48%; N, 20.05%, found: C, 51.03%; H, 5.53%; N, 19.09%.

NHS-ester **114**



Amino acid **109** (1.41 g, 4.05 mmol), *N*-hydroxysuccinimide (0.67 g, 6.07 mmol, 1.5 equiv.) and DCC (1.25 mg, 6.07 mmol, 1.5 equiv.) were dissolved in DMF (100 mL) and stirred 48 h at room temperature. The DCU which was formed during the reaction was filtered off and the solvent was evaporated *in vacuo*. The crude residue was purified by flash chromatography PE/EtOAc (6:4, $R_f = 0.4$, cerium stain) to give the title compound (1.35 g, 75%). **1H NMR** (CD_3OD , 400 MHz) δ (ppm) = 7.91 – 7.83 (m, 2H, 12-H, 8-H), 7.15 (d, 2H, 11-H, 9-H, $J = 8.6$ Hz), 3.01 – 2.89 (m, 1H, 4-H), 2.89 – 2.85 (m, 2H, 5-H), 2.70 (s, 4H, 1-H), 1.43 (s, 9H, 15-H); **^{13}C NMR** (CD_3OD , 100 MHz) δ (ppm) = 174.9 (C3), 173.0 (C2), 169.8 (C6), 157.9 (C13), 144.9 (C10), 131.9 (C7), 130.4 (C12, C8), 120.1 (C11, C9), 81.1 (C14), 55.2 (C4), 42.1 (C5), 34.8 (C5), 28.7 (C15), 26.4 (C1); **HRMS** (ESI) m/z calcd for $C_{19}H_{22}N_6O_7$ $[M+Na]^+$ 469.1442, found 469.1451; **Mp.:** 98.6 °C; $[\alpha]_D^{20} = +24.3^\circ$ ($c = 0.4$, MeOH); **IR** (KBr, cm^{-1}): 3412, 2933, 2127, 1701, 1286.

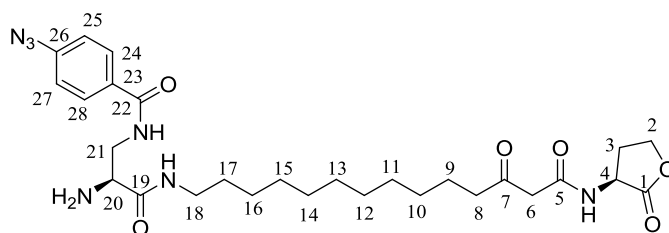
AHL-derivative 108



Method 1: NHS-ester **114** (366 mg, 0.82 mmol), AHL-derivative **51** (279 mg, 0.82 mmol) and Et₃N (0.14 mL, 1.07 mmol, 1.3 equiv.) were dissolved in DMSO (40 mL) and stirred 3 d at room temperature. The solvent was distilled off *in vacuo* and the crude residue was purified by flash chromatography CH₂Cl₂/MeOH (9.5:0.5, *R_f* = 0.5, cerium stain) to give the title compound as a colourless solid (268 mg, 49%). ¹H NMR (CD₃OD, 400 MHz, COCH₂CO signal is hidden under solvent peak) δ (ppm) = 7.86 (d, 2H, 28-H, 24-H, *J* = 8.4 Hz), 7.14 (d, 2H, 27-H, 25-H, *J* = 8.4 Hz), 4.62 (dd, 1H, 4-H, *J* = 9.3 Hz, 9.3 Hz), 4.44 (ddd, 1H, 2-H, *J* = 10.1 Hz, 8.9 Hz, 2.0 Hz), 4.33 – 4.27 (m, 1H, 2-H), 3.69 – 3.56 (m, 2H, 18-H), 3.52 – 3.40 (m, 1H, 20-H), 3.24 – 3.06 (m, 2H, 21-H), 2.58 (t, 2H, 8-H, *J* = 6.8 Hz), 2.34 – 2.23 (m, 1H, 3-H), 1.88 – 1.82 (m, 1H, 3-H), 1.75 – 1.53 (m, 4H, 17-H, 9-H), 1.41 (s, 9H, 31-H), 1.33 – 1.22 (14H, 16-H, 15-H, 14-H, 13-H, 12-H, 11-H, 10-H); ¹³C NMR (DMSO-*d*₆, 150 MHz) δ (ppm) = 205.2 (C7), 175.4 (C1), 170.4 (C5), 166.8 (C19), 165.9 (C29), 155.8 (C26), 142.8 (C22), 131.2 (C23), 129.6 (C28, C24), 119.4 (C27, C25), 78.6 (C30), 65.7 (C2), 55.1 (C6), 50.7 (C20), 48.5 (C4), 42.4 (C8), 39.1 (C21), 29.5 (C18), 29.44, 29.40, 29.35, 29.31, 29.2, 28.9, 28.6, 28.58, 28.55, 26.8 (C31, C17, C16, C15, C14, C13, C12, C11, C10, C3), 23.3 (C9); HRMS (ESI) *m/z* calcd for C₃₃H₄₉N₇O₈ [M+Na]⁺ 694.3535, found 694.3533; **Mp.**: 123.2 °C; [α]_D²⁰ = -23.0 ° (*c* = 0.3, MeOH); **IR** (KBr, cm⁻¹): 3334, 2926, 2850, 2123, 2090, 1772, 1629, 1527.

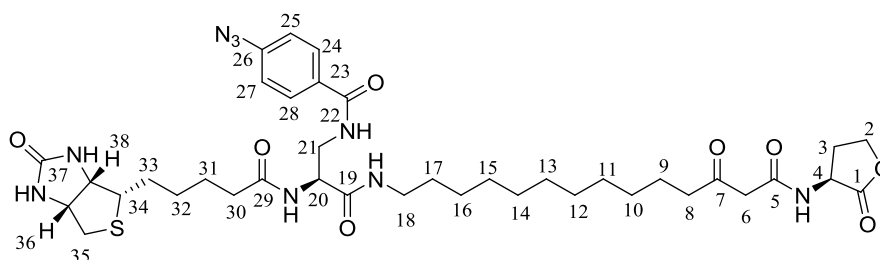
Method 2: Carboxylic acid **109** (417 mg, 1.19 mmol) was dissolved in DMF (20 mL) and Et₃N (0.28 mL, 2.03 mmol, 1.7 equiv.) was added to the solution. The reaction was stirred for 5 min, cooled to 0 °C and EDC·HCl (320 mg, 1.67 mmol) and HOBt (225 mg, 1.67 mmol) were added. AHL-derivative **51** (406 mg, 1.19 mmol) was added after 15 min and the solution was stirred at room temperature for 3 days. The solvent was evaporated *in vacuo* and the residue was solved in EtOAc (30 mL). The organic phase was washed twice with 1 M aqueous KHSO₄-solution (30 mL), saturated aqueous NaHCO₃-solution (30 mL) and brine. The solution was dried over Na₂SO₄. After filtration the solvent was evaporated *in vacuo* to give the title compound as a colourless solid (653 mg, 82%).

AHL-derivative 115



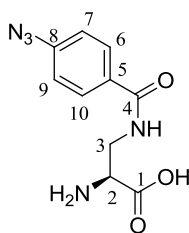
According to general procedure 2, AHL-derivative **115** (330 mg, 68%) was obtained as a brown solid from AHL-derivative **108** (573 mg, 0.85 mmol), $^1\text{H NMR}$ (CD_3OD , 400 MHz, COCH_2CO signal is hidden under solvent peak) δ (ppm) = 7.90 (d, 2H, 28-H, 24-H, $J = 8.6$ Hz), 7.14 (d, 2H, 27-H, 25-H, $J = 8.6$ Hz), 4.61 (dd, 1H, 4-H, $J = 9.4$ Hz, 9.4 Hz), 4.44 (ddd, 1H, 2-H, $J = 8.9$ Hz, 8.7 Hz, 3.1 Hz), 4.33 – 4.26 (m, 1H, 2-H), 3.81 (t, 2H, 18-H, $J = 6.2$ Hz), 3.28 – 3.17 (m, 2H, 21-H), 2.68 – 2.58 (m, 1H, 20-H), 2.57 (t, 2H, 8-H, $J = 7.3$ Hz), 2.35 – 2.25 (m, 1H, 3-H), 1.74 – 1.45 (m, 5H, 17-H, 9-H, 3-H), 1.34 – 1.21 (m, 14H, 16-H, 15-H, 14-H, 13-H, 12-H, 11-H, 10-H); $^{13}\text{C NMR}$ (CD_3OD , 100 MHz) δ (ppm) = 206.4 (C7), 177.3 (C1), 170.3 (C19), 169.4 (C5), 167.9 (C22), 145.5 (C26), 131.4 (C23), 130.7 (C28, C24), 120.0 (C27, C25), 67.4 (C2), 54.6 (C20), 50.2 (C6), 43.9 (C4), 42.0 (C21), 40.8 (C8), 40.4 (C18), 34.8, 30.7, 30.6, 30.5, 30.3, 30.1, 27.8, 26.3 (C16, C15, C14, C13, C12, C11, C10, C3), 26.0 (C17), 24.3 (C9); **HRMS** (ESI) m/z calcd for $\text{C}_{28}\text{H}_{41}\text{N}_7\text{O}_6$ $[\text{M}+\text{Na}]^+$ 594.3011, found 594.3020; **Mp.**: 81.6 °C; $[\alpha]_{\text{D}}^{20} = -28.0^\circ$ ($c = 0.1$, MeOH); **IR** (KBr, cm^{-1}): 1800, 1650, 1550, 1300, 1180.

AHL-derivative 107



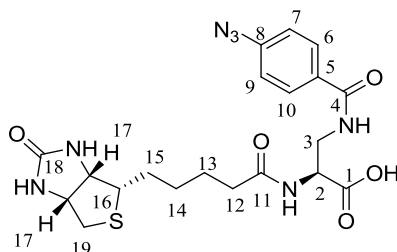
AHL-derivative **115** (177 mg, 0.31 mmol), biotin NHS-ester (105 mg, 0.31 mmol) and Et_3N (0.06 mL, 0.40 mmol, 1.3 eq.) were dissolved in DMSO (20 mL) and stirred for 3 days at room temperature. The solvent was distilled off *in vacuo* to give the crude product. Only traces of the product could be detected. **HRMS** (ESI) m/z calcd for $\text{C}_{38}\text{H}_{55}\text{N}_9\text{O}_8\text{S}$ $[\text{M}+\text{Na}]^+$ 820.3787, found 820.3783;

Deprotected photoactive linker 116



According to general procedure 2, the product (355 mg, 89%) was obtained as a brown solid from the educt **109** (559 mg, 1.60 mmol); $^1\text{H NMR}$ (DMSO- d_6 , 600 MHz) δ (ppm) = 8.86 (br, 1H, O-H), 8.51 (br, 2H, N-H₂), 7.94 (d, 2H, 10-H, 6-H, $J = 8.2$ Hz), 7.21 (d, 2H, 9-H, 7-H, $J = 8.7$ Hz), 4.09 – 4.03 (m, 1H, 2-H), 3.78 – 3.72 (m, 2H, 3-H); $^{13}\text{C NMR}$ (DMSO- d_6 , 100 MHz) δ (ppm) = 169.7 (C1), 166.5 (C4), 142.9 (C5), 130.7 (C8), 129.8 (C10, C6), 119.3 (C9, C7), 52.6 (C2), 25.6 (C3); **HRMS** (ESI) m/z calcd for C₁₀H₁₂N₅O₃ [M+H]⁺ 250.0935, found 250.0948; **Mp.**: 129.5 °C; $[\alpha]_{\text{D}}^{20} = +141.0^\circ$ ($c = 0.1$, MeOH); **IR** (KBr, cm⁻¹): 2000, 1650, 1600, 1500, 1280, 1200, 1150.

Biotin derivative 117

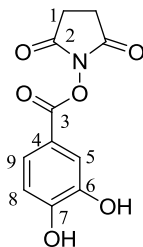


Method 1: Biotin NHS ester (166 mg, 0.49 mmol), the free amine **116** (110 mg, 0.44 mmol) and Et₃N (0.1 mL, 0.66 mmol) were dissolved in DMSO (20 mL) and stirred for 3 d at room temperature to give the crude product; $^1\text{H NMR}$ (DMSO- d_6 , 600 MHz, impurities) δ (ppm) = 7.88 (d, 2H, 10-H, 6-H, $J = 8.1$ Hz), 7.21 (d, 2H, 9-H, 7-H, $J = 8.4$ Hz), 6.44 – 6.38 (2H, biotin N-H), 4.46 – 4.42 (m, 1H, 17-H), 4.34 – 4.27 (m, 1H, 17-H), 4.12 – 4.07 (m, 1H, 16-H), 3.13 – 3.03 (m, 5H, 19-H, 3-H, 2-H), 2.13 (t, 2H, 12-H, $J = 7.3$ Hz), 1.67 – 1.25 (6H, 15-H, 14-H, 13-H).

Method 2: Biotin NHS ester (166 mg, 0.49 mmol), the free amine **116** (110 mg, 0.44 mmol) and abs Et₃N (0.2 mL, 1.46 mmol) were dissolved in abs DMSO (20 mL) under Ar atmosphere and stirred for 3 d at room temperature to give the crude product.

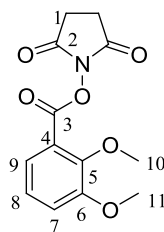
8.6 Catechol derivatives

Dihydroxybenzoic acid NHS-ester 122²³⁶



3,4-Dihydroxybenzoic acid (350 mg, 2.27 mmol), *N*-hydroxysuccinimide (261 mg, 2.26 mmol) and DCC (468 mg, 2.27 mmol) were dissolved in DMF (40 mL). After stirring for 48 h at room temperature the solvent was distilled off *in vacuo* and H₂O (20 mL) was added. DCU was filtered off and the solvent was evaporated *in vacuo* to give the crude product as colourless oil, which was used without further purification. MS (ESI) *m/z* 274.1 (M+Na⁺, 100%).

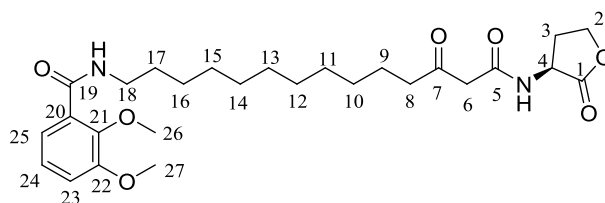
Dimethoxybenzoic acid NHS-ester 119



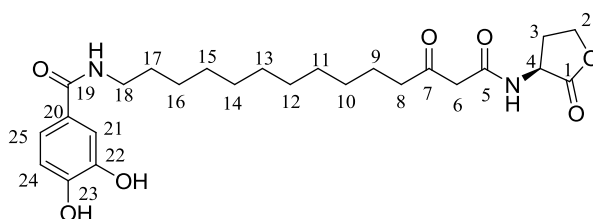
2,3-Dimethoxybenzoic acid (300 mg, 1.65 mmol), *N*-hydroxysuccinimide (303 mg, 2.63 mmol) and EDC·HCl (503 mg, 2.63 mmol) were dissolved in DMF (50 mL). After stirring for 24 h at room temperature the solvent was distilled off *in vacuo* and EtOAc (20 mL) was added. The organic phase was washed three times with 20 mL 1 M aqueous KHSO₄ solution, saturated aqueous NaHCO₃ solution and saturated aqueous NaCl-solution. The organic layer was then dried over Na₂SO₄, filtered and the solvent evaporated *in vacuo* to give the title compound (373 mg, 81%) as a colourless solid.

¹H NMR (CDCl₃, 400 MHz) δ (ppm) = 7.53 (d, 1H, 9-H, J = 4.7 Hz), 7.19 – 7.11 (m, 2H, 8-H, 7-H), 3.93 (s, 3H, 10-H), 3.89 (s, 3H, 11-H), 2.88 (s, 4H, 1-H); **¹³C NMR** (CDCl₃, 100 MHz) δ (ppm) = 169.2 (C2), 161.0 (C3), 153.8 (C6), 150.7 (C5), 124.2 (C9), 122.9 (C8), 120.4 (C7), 118.1 (C4), 61.9 (C10), 56.4 (C11), 25.9 (C1); **HRMS** (ESI) m/z C₁₃H₁₃NO₆ [M+Na]⁺ 302.0635, found: 302.0635; **Mp.**: 80.0 °C; **IR** (KBr, cm⁻¹): 2940, 1731, 1262, 1215, 1066; **CHN** calcd. for C₁₃H₁₃NO₆: C, 55.09%; H, 4.69%; N, 5.02%. Found: C, 54.63%; H, 4.69%; N, 5.76%.

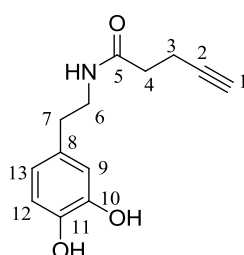
AHL-derivative 120



According to general procedure **7**, the title compound **120** (127 mg, 39%) was obtained as colourless oil from Dimethoxybenzoic acid NHS-ester **119** (178 mg, 0.64 mmol), **51** (217 mg, 0.64 mmol) and Et₃N (0.11 mL, 0.83 mmol). The crude product was purified by flash chromatography (EtOAc 100%, R_f = 0.2, cerium stain). **¹H NMR** (CD₃OD, 400 MHz, COCH₂CO signal is hidden under solvent peak) δ (ppm) = 7.32 (dd, 1H, 25-H J = 2.9 Hz, 2.9 Hz), 7.17 – 7.11 (m, 2H, 24-H, 23-H), 4.61 (dd, 1H, 4-H, J = 9.1 Hz, 9.1 Hz), 4.44 (ddd, 1H, 2-H, J = 9.8 Hz, 9.0 Hz, 2.8 Hz), 4.43 – 4.26 (m, 1H, 2-H), 3.89 (s, 3H, 26-H), 3.87 (s, 3H, 27-H), 3.38 (t, 2H, 18-H, J = 6.8 Hz), 2.57 (t, 2H, 8-H, J = 7.8 Hz), 2.34 – 2.27 (m, 1H, 3-H), 1.74 – 1.51 (m, 5H, 17-H, 9-H, 3-H), 1.60 – 1.45 (m, 14H, 16-H, 15-H, 14-H, 13-H, 12-H, 11-H, 10-H); **¹³C NMR** (CD₃OD, 100 MHz) δ (ppm) = 205.2 (C7), 175.8 (C1), 173.6 (C5), 166.9 (C19), 153.1 (C22), 147.0 (C21), 128.1 (C20), 123.9 (C24), 120.9 (C25), 115.2 (C23), 65.8 (C2), 60.3 (C26), 55.1 (C27), 48.7 (C4), 42.3 (C6), 39.3, 33.3, 29.2, 29.1, 29.03, 29.0, 28.9, 28.6, 28.2, 26.6, 24.9 (C18, C17, C16, C15, C14, C13, C12, C11, C10, C8, C3), 23.0 (C9); **HRMS** (ESI) m/z C₂₇H₄₀N₂O₇ [M+Na]⁺ 527.2728, found: 527.2735; $[\alpha]_D^{20}$ = -10.9 ° (c = 0.4, MeOH); **IR** (film, cm⁻¹): 3274, 2927, 2852, 1221, 1185.

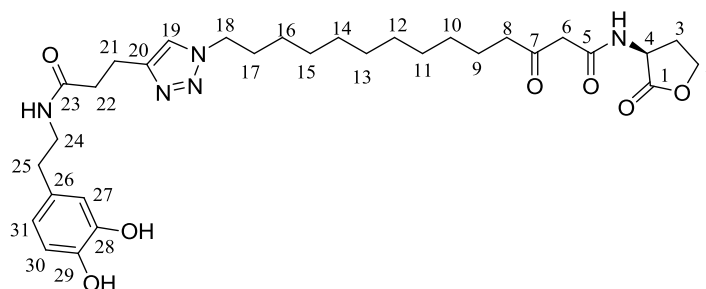
AHL-derivative 39

According to general procedure 7, the title compound **39** (180 mg, 88% over 2 steps) was obtained as a colourless oil from Dihydroxybenzoic acid NHS-ester **122** (147 mg, 0.59 mmol), **51** (200 mg, 0.59 mmol) and Et₃N (0.11 mL, 0.76 mmol); ¹H NMR (CD₃OD, 400 MHz) δ (ppm) = 7.48 – 7.20 (m, 2H, 25-H, 24-H), 6.83 (d, 1H, 21-H, J = 7.4 Hz), 4.62 – 4.58 (m, 1H, 4-H), 4.47 – 4.44 (m, 1H, 2-H), 4.35 – 4.28 (m, 1H, 2-H) 3.22 – 3.17 (m, 2H, 18-H), 2.93 (t, 1H, 8-H, J = 11.0 Hz), 2.71 (s, 2H, 6-H), 2.61 – 2.57 (m, 2H, 8-H, 3-H), 2.40 – 2.26 (m, 1H, 3-H), 1.72 – 1.53 (m, 4H, 17-H, 9-H), 1.43 – 1.26 (m, 14H, 16-H, 15-H, 14-H, 13-H, 12-H, 11-H, 10-H); ¹³C NMR (CD₃OD, 100 MHz) δ (ppm) = 206.7 (C7), 177.2 (C1), 175.1 (C5), 170.5 (C19), 151.4 (C23), 150.0 (C22), 146.0 (C20), 124.0 (C25), 117.6 (C24), 115.7 (C21), 67.1 (C2), 50.2 (C18), 47.9 (C8), 40.8 (C4), 30.6, 30.5, 30.4, 30.2, 30.1, 29.6, 28.6, 27.4, 26.3, 24.5, 24.4 (C17, C16, C15, C14, C13, C12, C11, C10, C9, C6, C3); HRMS (ESI) m/z calcd for C₂₅H₃₆N₂O₇ [M+H]⁺ 499.2415, found 499.2396; [α]_D²⁰ = -57.0 ° (c = 0.3, MeOH); IR (film, cm⁻¹): 3195, 2928, 2854, 1767, 1708, 1676, 1600, 1292, 1201.

Alkyne 124²³⁷

Dopamine·HCl (306 mg, 2.00 mmol), NHS-alkyne **61** (390 mg, 2.00 mmol), Et₃N (0.36 mL, 2.60 mmol, 1.3 equiv.) were dissolved in DMSO (30 mL) and stirred at room temperature for 48 h. The solvent was distilled off *in vacuo* and the residue was solved in EtOAc (30 mL). The organic phase was washed twice with H₂O (20 mL) and dried over Na₂SO₃. After filtration the solvent was evaporated *in vacuo* to give the title compound as a colourless oil (310 mg, 67%). MS (ESI) m/z 256.1 (M+Na⁺, 100%).

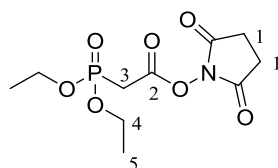
AHL-derivative 125



According to general procedure **8**, the title compound (162 mg, 62%) was obtained as a colourless solid from the azide **60** (160 mg, 0.44 mmol), the alkyne **124** (102 mg, 0.44 mmol), CuSO₄ (7 mg, 0.04 mmol) and sodium ascorbate (9 mg, 0.04 mmol). The crude product was purified by flash chromatography CH₂Cl₂/MeOH (9:1, *R_f* = 0.2, cerium stain); **¹H NMR** (CDCl₃, 400 MHz) δ (ppm) = 7.91 – 7.77 (m, 1H, 19-H), 7.35 (s, 1H, 27-H), 6.75 – 6.38 (m, 2H, 31-H, 30-H), 4.61 – 4.53 (m, 1H, 4-H), 4.46 – 4.40 (m, 1H, 2-H), 4.28 – 4.20 (m, 3H, 18-H, 2-H), 3.44 (s, 2H, 6-H), 3.23 (t, 2H, 8-H, *J* = 7.6 Hz), 3.02 – 2.90 (m, 2H, 21-H), 2.50 – 2.47 (m, 4H, 24-H, 22-H), 2.31 – 2.17 (m, 1H, 3-H), 1.90 – 1.80 (m, 2H, 25-H), 1.71 – 1.48 (m, 5H, 17-H, 9-H, 3-H), 1.36 – 1.16 (m, 14H, 16-H, 15-H, 14-H, 13-H, 12-H, 11-H, 10-H); **¹³C NMR** (CDCl₃, 100 MHz) δ (ppm) = 206.5 (C7), 175.3 (C23), 172.5 (C1), 166.4 (C5), 146.5 (C28), 144.1 (C29), 143.3 (C20), 130.7 (C26), 121.9 (C19), 120.3 (C31), 115.9 (C30), 115.3 (C27), 65.9 (C2), 51.5 (C6), 50.5 (C18), 49.2 (C4), 48.3 (C8), 43.9 (C22), 41.1 (C24), 33.9 (C25), 29.6, 29.4, 29.3, 29.28, 29.1, 28.8, 26.7, 25.6, 24.9 (C17, C16, C15, C14, C13, C12, C11, C10, C3), 23.4 (C21), 21.3 (C9); **HRMS** (ESI) *m/z* calcd for C₃₁H₄₅N₅O₇ [M+Na]⁺ 622.3211, found 622.3210; **[α]_D²⁰** = -18.7° (*c* = 0.5, MeOH); **Mp.**: 74.0 °C; **IR** (KBr, cm⁻¹): 3327, 2927, 2850, 2098, 1776, 1653; **CHN** calcd. for C₁₈H₃₂N₂O₄: C, 62.08%; H, 7.56%; N, 11.68%. Found: C, 60.89%; H, 8.41%; N, 11.65%.

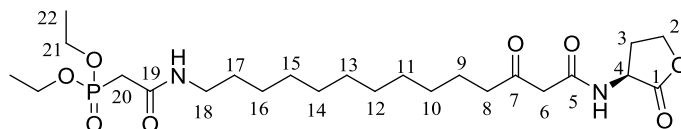
8.7 Phosphonate derivatives

NHS-ester **146**²³⁸



Diethyl phosphonoacetic acid (0.12 mL, 0.77 mmol), *N*-hydroxysuccinimide (114 mg, 0.99 mmol) and DCC (158 mg, 0.77 mmol) were dissolved in DMF (30 mL) and stirred for 48 h at room temperature. In the next step, the DCU was filtered off and the solvent was evaporated *in vacuo* to give the crude product which was used for the next step without further purification.

AHL-derivative **148**

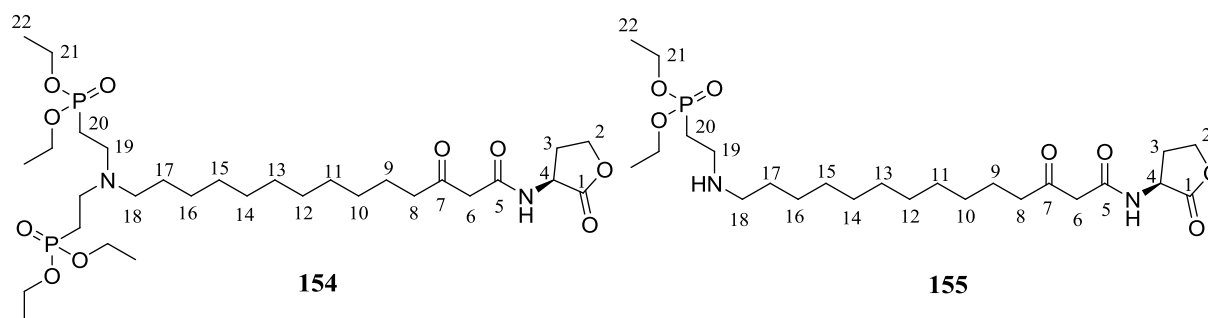


Method 1: According to general procedure 7, the title compound (76 mg, 49%) was obtained from NHS-ester **146** (86 mg, 0.29 mmol), AHL-derivative **51** (100 mg, 0.29 mmol) and Et₂N (0.05 mL, 0.38 mmol, 1.3 equiv) as a colourless oil. The crude residue was purified by flash chromatography CH₂Cl₂/MeOH (9:1, *R_f* = 0.3, cerium stain).

Method 2: Diethylphosphonoacetic acid (119 mg, 0.61 mmol) and Et₃N (0.25 mL, 1.82 mmol, 3 equiv.) were dissolved in DMF (20 mL). After 5 min the solution was cooled to 0 °C and EDC·HCl (163 mg, 0.85 mmol, 1.4 equiv.) and HOBt (115 mg, 0.85 mmol, 1.4 equiv.) were added. The mixture was stirred for 15 min and AHL-derivative **51** (206 mg, 0.61 mmol) was added. The solution was stirred at room temperature for 3 d and the solvent was evaporated *in vacuo*. The crude residue was solved in EtOAc (30 mL) and washed twice with 20 mL 1 M aqueous KHSO₄ solution, saturated aqueous NaHCO₃ solution and saturated aqueous NaCl-solution. The organic layer was then dried over Na₂SO₄, filtered and the solvent evaporated *in vacuo*. The crude product was purified by flash chromatography CH₂Cl₂/MeOH (9:1, *R_f* = 0.3, cerium stain) to give the title compound as a colourless oil (114 mg, 36%);

^1H NMR (CD_3CD , 500 MHz, minor impurities) δ (ppm) = 4.61 (dd, 1H, 4-H, J = 9.6 Hz, 9.6 Hz), 4.45 (ddd, 1H, 2-H, J = 9.3 Hz, 9.0 Hz, 2.8 Hz), 4.17 (quin, 4H, 21-H, J = 7.1 Hz, 14.0 Hz), 3.24 – 3.18 (m, 4H, 20-H, 6-H), 2.91 (t, 2H, 18-H, J = 8.0 Hz, 2.58 (t, 2H, 8-H, J = 7.4 Hz), 2.36 – 2.26 (m, 1H, 3-H), 1.69 – 1.52 (m, 4H, 17-H, 9-H), 1.35 – 1.29 (m, 21H, 22-H, 16-H, 15-H, 14-H, 13-H, 12-H, 11-H, 10-H, 3-H); **^{13}C NMR** (CD_3CD , 100 MHz) δ (ppm) = 206.4 (C7), 177.3 (C1), 169.5 (C5), 166.6 (C19), 67.4 (C2), 64.2 (C21), 50.1 (C6), 44.32 (C4), 43.8 (C18), 40.9 (C8), 30.7, 30.6, 30.5, 30.4, 30.3, 30.2, 30.1, 29.8, 29.7, 27.9, 24.5 (C20, C17, C16, C15, C14, C13, C12, C11, C10, C9, C3), 16.7 (C22); **^{31}P NMR** (CD_3CD , 100 MHz) δ (ppm) = 23.2; **HRMS** (ESI) m/z calcd for $\text{C}_{24}\text{H}_{43}\text{N}_2\text{O}_8\text{P}$ $[\text{M}+\text{Na}]^+$ 541.2649, found 541.2679; $[\alpha]_{\text{D}}^{20}$ = -18.7° (c = 0.4, MeOH); **IR** (film, cm^{-1}): 3400, 2800, 1700, 1200.

AHL-derivatives 154 and 155



Method 1: AHL-derivative **51** (150 mg, 0.44 mmol), diethylvinylphosphonate (0.14 mL, 0.88 mmol) and Et_3N (0.06 mL, 0.44 mmol) were dissolved in $\text{EtOH}/\text{H}_2\text{O}$ (9:1) and stirred for 5 min. The pH value was adjusted to 7-8 by adding 1 M aqueous HCl and the solution was stirred for 48 h under reflux. The solvent was evaporated *in vacuo* and the crude residue was purified by flash chromatography $\text{CH}_2\text{Cl}_2/\text{MeOH}$ (8:2) to give a mixture of diethylvinyl phosphonate, the mono substituted product **155** and the double substituted product **154**.

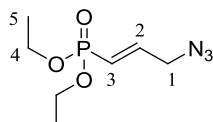
Mono substituted product 155: **HRMS** (ESI) m/z calcd for $\text{C}_{24}\text{H}_{45}\text{N}_2\text{O}_7\text{P}$ $[\text{M}+\text{H}]^+$ 505.3037, found 505.3045; **Double substituted product 154:** **HRMS** (ESI) m/z calcd for $\text{C}_{30}\text{H}_{58}\text{N}_2\text{O}_{10}\text{P}$ $[\text{M}+\text{H}]^+$ 669.3639, found 669.3640

Method 2: AHL-derivative **51** (200 mg, 0.59 mmol), diethylvinylphosphonate (0.2 mL, 1.2 mmol) and Et₃N (0.08 mL, 0.59 mmol) were dissolved in EtOH and stirred for 5 min. The pH value was adjusted to 7-8 by adding 1 M aqueous HCl and the solution was stirred for 48 h under reflux followed by a mass analysis of the crude mixture. The mono substituted **155** as well as the double substituted product **154** were detectable. The reaction mixture was stirred under reflux for additional 3 d. The solvent was evaporated *in vacuo* and the residue was analysed by mass spectrometry. Only the mono substituted product **155** (263 mg, 89%) could be detected and was purified by column chromatography CH₂Cl₂/MeOH (9:1, *R_f* = 0.2, cerium stain) to give a colourless oil; ¹H NMR (CD₃OD, 400 MHz) δ (ppm) = 4.62 – 4.52 (m, 1H, 4-H), 4.48 – 4.46 (m, 1H, 2-H), 4.33 – 4.27 (m, 1H, 2-H), 3.72 – 3.60 (m, 2H, 6-H), 3.21 – 3.16 (m, 10H, 21-H, 20-H, 19-H, 18-H), 2.89 (t, 2H, 8-H, *J* = 8.9 Hz), 2.38 – 2.25 (m, 1H, 3-H), 1.93 – 1.82 (m, 1H, 3-H), 1.69 – 1.51 (m, 4H, 17-H, 9-H), 1.37 – 1.25 (m, 20H, 22-H, 16-H, 15-H, 14-H, 13-H, 12-H, 11-H, 10-H); ¹³C NMR (CD₃OD, 100 MHz) δ (ppm) = 67.6 (C2), 62.7 (C21), 59.3 (C6), 51.6 (C4), 47.9 (C19), 44.2 (C18), 41.0 (C8), 35.5, 30.6, 30.56, 30.55, 30.5, 30.3, 30.1, 29.7, 28.7, 27.7 (C20, C17, C16, C15, C14, C13, C12, C11, C10, C3), 24.7 (C9), 9.7 (C22); ³¹P NMR (CD₃OD, 400 MHz) δ (ppm) = 25.69; HRMS (ESI) *m/z* calcd for C₂₄H₄₅N₂O₇P [M+H]⁺ 505.3037, found 505.3045; [α]_D²⁰ = -30.4 ° (*c* = 0.4, MeOH).

Signals of the quaternary C1, C5 and C7 cannot be seen in the ¹³C NMR.

NMR: slight impurities with diethylvinyl phosphonate

Azide **150**²³⁹

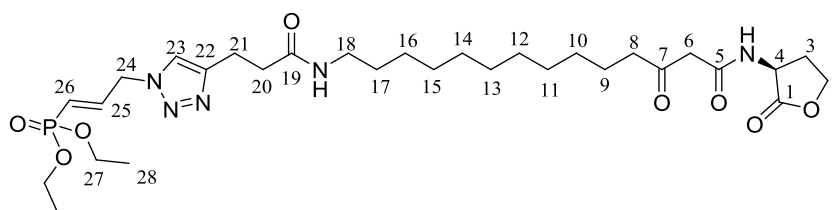


3-bromo-1-propen-phosphonic acid diethylester (0.3 mL, 1.57 mmol) and NaN₃ (1.020 g, 15.69 mmol) were dissolved in DMF (100 mL) and stirred at 60 °C for 24 h. The solvent was evaporated *in vacuo* and the residue was dissolved in EtOAc (40 mL). The organic phase was washed twice with 1 M aqueous KHSO₄-solution (30 mL) and brine (30 mL). The organic phase was dried over Na₂SO₄. After filtration the solvent was distilled off *in vacuo* and the residue was purified by column chromatography CH₂Cl₂/MeOH (9:1, *R_f* = 0.7, cerium stain) to give the product as a brown oil (342 mg, quant).

$^1\text{H NMR}$ (CDCl_3 , 400 MHz) δ (ppm) = 6.23 – 6.21 (m, 1H, 2-H), 4.78 – 4.76 (m, 1H, 3-H), 4.00 – 3.91 (m, 4H, 4-H), 2.52 – 2.45 (m, 2H, 1-H), 1.23 – 1.04 (m, 6H, 5-H); **MS** (ESI) m/z 242.1 ($\text{M}+\text{Na}^+$, 100%).

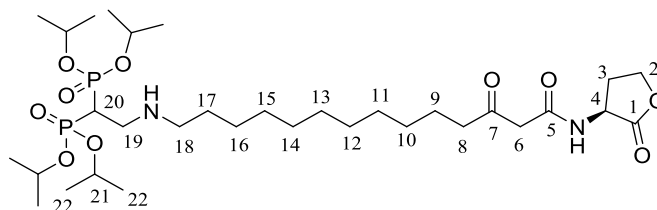
Compound is literature known but was synthesised using a different approach.

AHL-derivative 151



Method 1: According to general procedure 8, traces of the title compound were obtained as a brown oil from the azide **150** (205 mg, 0.94 mmol), the alkyne **63** (394 mg, 0.94 mmol), CuSO_4 (15 mg, 0.094 mmol) and sodium ascorbate (19 mg, 0.094 mmol). The crude residue was purified by flash chromatography $\text{CH}_2\text{Cl}_2/\text{MeOH}$ (8:2, $R_f = 0.3$, cerium stain) but it was impossible to get rid of the impurities.

Method 2: According to general procedure 8, but TBTA was added to the reaction. The title compound (222 mg, 73%) was obtained as a yellow oil from the azide **150** (100 mg, 0.47 mmol), the alkyne **63** (200 mg, 0.48 mmol), CuSO_4 (10 mg, 0.06 mmol) and TBTA (12 mg, 0.02 mmol). The crude product was purified by flash chromatography $\text{CH}_2\text{Cl}_2/\text{MeOH}$ (8:2, $R_f = 0.3$, cerium stain); $^1\text{H NMR}$ (CD_3OD , 400 MHz, minor impurities) δ (ppm) = 7.23 – 7.18 (m, 1H, 23-H), 5.70 – 5.61 (m, 1H, 26-H), 5.25 – 5.61 (m, 1H, 25-H), 4.67 – 4.63 (m, 1H, 4-H), 4.60 – 4.49 (m, 1H, 2-H), 4.36 – 4.29 (m, 1H, 3-H), 4.26 – 4.05 (m, 6H, 27-H, 24-H), 3.20 – 3.13 (m, 2H, 18-H), 3.07 – 3.00 (m, 2H, 8-H), 2.62 – 2.56 (m, 3H, 21-H, 20-H), 2.39 – 2.32 (m, 1H, 3-H), 1.76 – 1.59 (m, 5H, 17-H, 9-H, 3-H), 1.41 – 1.27 (m, 20H, 28-H, 16-H, 15-H, 14-H, 13-H, 12-H, 11-H, 10-H), $^{13}\text{C NMR}$ (CD_3OD , 100 MHz) δ (ppm) = 205.1 (C7), 173.0 (C1), 168.1 (C5), 145.8 (C22), 125.2 (C25), 122.9 (C23), 113.8 (C26), 68.8 (C27), 65.8 (C2), 62.6 (C24), 48.7 (C4), 48.3 (C6), 42.3 (C20), 38.9 (C21), 34.8 (C18), 33.4 (c8), 29.2, 29.0, 28.9, 28.7, 28.3, 26.5, 25.4, 24.6, 23.1 (C17, C16, C15, C14, C13, C12, C11, C10, C3), 21.00 (C9), 15.3 (C28); $^{31}\text{P NMR}$ (CD_3OD , 400 MHz) δ (ppm) = 26.5; **HRMS** (ESI) m/z calcd for $\text{C}_{30}\text{H}_{50}\text{N}_5\text{O}_8\text{P}$ [$\text{M}+\text{Na}$] $^+$ 662.3287, found 662.3289; $[\alpha]_D^{20} = -163.4^\circ$ ($c = 0.1$ MeOH); **IR** (film, cm^{-1}): 2000, 1650, 1500, 1450, 1280, 1900, 1000.

Bis-phosphonate AHL-derivative 157

Method 1: Tetraisopropyl vinylidene diphosphonate (0.14 mL, 0.44 mmol), AHL-derivative **51** (150 mg, 0.44 mmol) and Et₃N (0.07 mL, 0.53 mmol) were dissolved in H₂O (30 mL) and stirred for 48 h under reflux to give traces of the desired product.

Method 2: Tetraisopropyl vinylidene diphosphonate (0.13 mL, 0.39 mmol), AHL-derivative **51** (120 mg, 0.35 mmol) and cat. DMAP (12 mg, 0.098) were dissolved in dry CH₂Cl₂ (30 mL) and stirred for 3 d at room temperature. The solvent was distilled off *in vacuo* and the crude product was solved in EtOAc and washed three times with saturated aqueous NaHCO₃ solution, 1 M aqueous KHSO₄ and brine to give the title compound as a brown oil which was purified by flash chromatography CH₂Cl₂/MeOH (9:1, R_f = 0.2, cerium stain). However, the product could not be purified; **HRMS** (ESI) *m/z* calcd for C₃₂H₆₂N₂O₁₀P₂ [M+H]⁺ 697.3952, found 697.3955

8.8 Nanoparticles**Coating Procedures****Method A**

AHL derivative **39** was solved in MeOH/H₂O (1:9) and the nanoparticles were added to the mixture. The pH value was adjusted to 8 with 1 M aqueous NaOH. After 24 h of ultrasonic treatment the nanoparticles were separated from the solution by centrifugation. Thereafter, the particles were washed twice with H₂O and separated from the solvent by centrifugation each time. In the end the TiO₂-nanoparticles were dried by lyophilisation.

Method B

The particles were treated as described in method 1, but the pH value was adjusted to 9. After ultrasonic treatment the particles were washed four times with H₂O.

Calculation

The following calculation describes how to determine the appropriate amount of AHL **39** needed for a total coverage of the nanoparticles' surface.

Example: AHL immobilisation on 50 mg TiO₂ (P25) nanoparticles

Specific surface area A: 51.2708 m²/g

$$A = m^2/g \quad (2)$$

Amount of TiO₂ P25: 50 mg

$$0.050 \text{ g} * 51.271 \text{ m}^2/\text{g} = 2.564 \text{ m}^2 \quad (3)$$

$$2.564 \text{ m}^2 = 2.564 * 10^{18} \text{ nm}^2 \quad (4)$$

Assumption: For a full coverage of the particles' surface an area of 24 Å² per molecule (about four molecules per nm²) is assumed. This assumption is commonly used in literature.¹⁸⁶

$$4 \text{ molecules} = 1 \text{ nm}^2 \quad (5)$$

$$2.564 * 10^{18} \text{ nm}^2 * 4 \rightarrow 1.026 * 10^{19} \text{ molecules} \quad (6)$$

Assumption: A 5-fold excess of AHL **39** is used to guarantee a full coverage of the surface:

$$1.026 * 10^{19} \text{ molecules} * 5 = 5.130 * 10^{19} \text{ molecules} \quad (7)$$

The Avogadro constant N_A is defined as the number of constituent particles N per mol n :

$$N_A = N/n = 6.022 * 10^{23} \text{ mol}^{-1} \quad (8)$$

$$N = 5.130 * 10^{19} \quad (9)$$

$$n = \frac{N}{N_A} = \frac{5.130 * 10^{19}}{6.022 * 10^{23} \text{ mol}^{-1}} = 0.000085 \text{ mol} \quad (10)$$

The molar mass (M) of the catechol-AHL is 476 g/mol:

$$m = n * M \quad (11)$$

$$m = 0.000085 \text{ mol} * 476 \text{ g/mol} = 0.041 \text{ g} \quad (12)$$

For a total coverage of 50 mg TiO₂ P25 nanoparticles 41 mg AHL derivative **39** are needed, taking a huge excess into account.

Calculation for the Thermo gravimetric Analysis (TGA):

Expected mass loss in % for a fully covered surface of the nanoparticle:

Specific surface area:

$$A = 51.271 \text{ m}^2/\text{g} \quad (13)$$

$$1 \text{ g} = 51.271 \text{ m}^2 \quad (13)$$

$$51.271 \text{ m}^2 = 5.127 * 10^{19} \text{ nm}^2 \quad (14)$$

Assumption: Four molecules per nm^2

$$5.127 * 10^{19} \text{ nm}^2 * 4 = 2.051 * 10^{20} \text{ molecules} \quad (15)$$

$$n = \frac{N}{N_A} = \frac{2.051 * 10^{20}}{6.022 * 10^{23} \text{ mol}^{-1}} = 0.00034 \text{ mol} \quad (16)$$

Molecular Mass (M) of the catechol-AHL derivative is 476 g/mol:

$$m = n * M \quad (17)$$

$$m = 0.00034 \text{ mol} * 476 \text{ g/mol} = 0.162 \text{ g} \quad (18)$$

Weight loss in percent in regard to the total mass:

$$\left(\frac{m}{1 \text{ g} + m} \right) * 100\% \quad (20)$$

$$\left(\frac{0.162 \text{ g}}{1 \text{ g} + 0.162 \text{ g}} \right) * 100\% = 13.9\% \quad (19)$$

9 Hazardous Materials

Chemical	Hazard Statement	H-Statement	P-Statement
Acetic anhydride	Danger	226-332-302-314	280-301+330+331-305+351+338-309+310
Acetone	Danger	225-319-336	210-233-305+351+338
Acetonitrile (MeCN)	Danger	225-332-302-312-319	210-305+351+338-403+235
Allylic alcohol	Danger	225-331-311-301-319-335-315-400	210-261-273-280-301+310-305+351+338
Aluminiumisopropoxide Al(OPr- <i>i</i>) ₃	Warning	228	210
4-Aminobenzoic acid	-	-	260
(<i>S</i>)- α -aminobutyrolactone hydrobromide	Warning	315-319-335	261-280-301+312-302+352-305+351+338
12-Aminododecanoic acid	-	-	-
(<i>S</i>)-3-Amino-2-(<i>tert</i> - butoxycarbonylamino)propanoic acid (Boc-Dap-OH)	Warning	302-315-319-335	264-302+352-304+340-305+351+338-332+313-337+313
Ammonium hydroxide	Warning	314-400	273-280-305+351+338-309+310
Ammonium molybdate	Warning	315-319-335	261-305+351 + 338
Benzylamine	Danger	314-302-312	280-305+351+338-310

Benzyloxycarbonyl chloride (Cbz-Cl)	Danger	314-410	273-501
Benzyloxocarbonyl glycine	Warning	315-319-335	264-302+352- 304+340- 305+351+338- 332+313-337+313
Biotin	-	-	-
Brine	-	-	-
12-bromododecanoic acid	-	-	-
<i>n</i> -butanol	Danger	226-302-318- 315-335-336	280-302+352- 305+351+338-313
<i>tert</i> -butanol	Danger	225-332-319-335	210- 305+351+338- 403+233
<i>tert</i> -butyl acrylate	Danger	225-302-312- 315-317-332- 335-411	210-261-273-280
<i>n</i> -butyllithium	Danger	225-250-304- 314-336-361- 373-411	210-222-231-261- 273-422
Celite	Warning	373	260-314-501
Cerium (IV) sulfate	Warning	315-319-335	261-305+351+338
Chloroform	Warning	302-315-351-373	302+352-314
Copper sulfate	Warning	302-319-315-410	273- 305+351+338- 302+352
Cyclohexane	Danger	225-304-315- 336-410	210-240-273- 301+310-331- 403+235

Dichloromethane	Warning	351	281-308+313
Dicyclohexylcarbodiimide (DCC)	Danger	311-302-318-317	280-305+351+338
Diethyl ether	Danger	224-302-336	210-240-403+235
Diethyl phosphono acetic acid	Warning	315-319-335	261-280-305+351+338-304+340-405-501A
Diethyl vinyl phosphonate	Warning	302	273
3,4-dihydroxybenzoic acid	Warning	315-319-335	261-305+351+338
2,3-dimethoxy benzoic acid	Warning	315-319-335	261-280-305+351+338-304+340-405-501A
4-(Dimethylamino)pyridine (DMAP)	Danger	310-301-315-319	302+352-305+351+338
2,2-dimethyl-1,3-dioxane-4,6-dione	-	-	-
Dimethylformamide	Danger	360D-226-332-312-319	201-302+352-305+351+338-308+313
Dimethyl sulfoxide	-	-	-
1,4-dioxane	Danger	225-351-319-335	210-261-281-305+351+338
Dopamine	Warning	302-400	273
Disodium hydrogen phosphate	-	-	-
Di- <i>tert</i> -butyl dicarbonate (Boc ₂ O)	Danger	226-330-315-319-317	210-280-309-310-304+340-305+351+338-302+352
Ethyl acetate (EtOAc)	Danger	225-319-336	210-240-305+351+338

Ethylenediaminetetraacetic acid (EDTA)	Warning	319	305+351+338
<i>N</i> -Ethyl- <i>N'</i> -(3-dimethylamino-propyl)carbodiimide (EDC)	Danger	314	280-305+351+338-310
Hexane	Danger	225-361f-304-373-315-336-411	210-240-273-301+310-331-302+352-403+235
Hexamethyldisilazane	Danger	225-311+331-302-314	210-280-301+330+331-302+352-304+340-305+351+338-309-310-403+235
Hydroxybenzotriazole (HOBt)	Danger	203	370+380-501
Hydrochloric acid (conc.)	Danger	314-335	260-301+330+331-303+361+353-305+351+338-405-501
<i>N</i> -hydroxysuccinimide	-	-	-
Iodide	Warning	332-312-400	273-302+352
Iron(III) chloride	Danger	302-315-318-290	280-302+352-305+351+338-313
Lauric acid	Warning	319	305+351+338
Lithium hydroxide	Danger	301+331-314	261-280-305+351+338-301+310
Methanol (MeOH)	Danger	225-331-311-301-370	210-233-280-302+352
4-Morpholinopropanesulfonic-acid (MOPS)	Warning	315-319-335	261-305+351+338
Ninhydrin	Warning	302-315-319-335	261-305+351+338

Oleic acid	-	-	-
Pamidronate	Warning	302	264-270-301+312-330-501
4-Pentynoic acid	Danger	314-318	260-303+361+353-305+351+338-301+330+331-405-501A
Petrol ether 50-70	Danger	225-304-315-336-361-373-411	210-261-273-281-301+310-331
Potassium carbonate	Warning	315-319-335	302+352-305+351+338
Potassium hydrogen carbonate	-	-	-
Potassium dihydrogen phosphate	-	-	-
Potassium hydrogen sulfate	Danger	314-335	280-301+330+331-305+351+338-309-310
Potassium sulfate	-	-	-
Pyridine	Danger	225-332-312-302	210-233-302+352
Quinidine	Danger	301	301+310
Sodium azide	Danger	300-400-410	273-309-310
Sodium ascorbate	-	-	-
Sodium hydrogen carbonate	-	-	-
Sodium nitrite	Danger	272-301-400	273-309+310
Sodium sulfate	-	-	-
Succinic anhydride	Warning	302-319-335	305+351+338

Sulphuric acid (conc.)	Danger	314	280- 301+330+331- 309-310- 305+351+338
Tetrahydrofuran (THF)	Danger	225-319-335-351	210-233-243- 305+351+338
TiO ₂ -nanoparticle	-	-	-
Triethylamine	Danger	225-331-311- 302-314	210-280- 303+361+353- 305+351+338- 310-312
Trifluoroacetic acid (TFA)	Danger	332-314-412	271-273- 301+330+331- 305+351+338- 309+310
Triphenylphosphine	Warning	302-317-413	262-273-280- 302+352

10 Curriculum Vitae

Education

- since 10/2011 **University of Hamburg, Institute of Pharmacy**
 Doctoral thesis in the research group of Prof. Dr. Wolfgang Maison
- 04/2011 – 09/2011 **Justus-Liebig-University Gießen, Institute of Organic Chemistry**
 PhD Thesis in the research group of Prof. Dr. Wolfgang Maison;
 Topic: „Synthesis of modified *N*-acyl homoserine lactones as
 chemical probes for the elucidation of plant-microbe interactions“
- 10/2008 – 11/2010 **Justus-Liebig-University Gießen, Master of Science Chemistry**
 Thesis in the research group of Prof. Dr. Wolfgang Maison; Topic:
 “Analysis of atropisomeric anilides for Pd-catalyzed natural product
 synthesis”
- 10/2005 – 10/2008 **Justus-Liebig-University Gießen, Bachelor of Science Chemistry**
 Thesis in the research group of Prof. Dr. Wolfgang Maison; Topic:
 “Stereoselective synthesis of bicyclic diketopiperazines based on
 valine”
- 08/1996 – 06/2005 **Herderschule Gießen, A-level**
 Successfully participated in the Anglo-German bilingual stream

Work Experience

- since 10/2011 Scientific Associate, University of Hamburg, Institute of Pharmacy
- 04/2011 – 09/2011 Scientific Associate, Justus-Liebig University, Institute of Organic Chemistry

- Publications** Thomanek, H., Schenk, T.S., Stein, E., Koge, K.-H., Schikora, A.,
 Maison, W., Modified *N*-acyl homoserine lactones as chemical probes
 for the elucidation of plant-microbe interactions, *Org. Biomol. Chem.*
2013, *11*, 6994.
- Deppermann, N., Thomanek, H., Prenzel, A. H. G. P., Maison, W.,
 Pd-catalysed assembly of spirooxindole natural products: a short
 synthesis of horsfiline, *J. Org. Chem.* **2010**, *7*, 5994.

Conferences

- 09/2011 Poser presentation: “Modified *N*-acyl homoserine lactones as chemical probes for the elucidation of plant receptors” at the “4th GGL CONFERENCE on LIFE SCIENCE” in Gießen
- 09/2010 Poster and oral presentation of the topic: “Pd-catalyzed assembly of spirooxindole natural products” at the ORCHEM 2010 in Weimar

Language Skills

Native language **German**

Other languages **English** (excellent), **French** (advanced knowledge), **Spanish** (basic knowledge)

Membership

04/2011 – 09/2011 Member of the GGL (International Giessen Graduate School for the Life Sciences)

Skills & Abilities Excellent proficiency in different analytical techniques (HPLC, MS, TGA, IR, XRD, NMR)

Technical Competence MS Office Software (Word, PowerPoint, Excel, very good), Windows (very good), ChemDraw (very good), Endnote (very good), Bruker Topspin (very good), SciFinder Scholar (very good)

11 Declaration

This thesis with the title “Modified *N*-acyl Homoserine Lactones for the Evaluation of Plant-Bacteria Interactions” was submitted in part fulfilment of the requirements for the degree of Doctor rer. nat. at the University of Hamburg. Unless otherwise stated the work described in this thesis is original and has not been submitted previously in whole or in part for any degree or other qualification at this, or any other university. Parts of this work have already been published:

Thomanek, H.; Schenk, S. T.; Stein, E.; Kogel, K.-H.; Schikora, A.; Maison, W. *Org. Biomol. Chem.* **2013**, *11*, 6994.

Eidesstattliche Erklärung

Hiermit erkläre ich an Eides statt, dass ich die vorliegende Dissertationsschrift mit dem Titel „Modifizierte *N*-acyl Homoserin Lactone zur Evaluierung der Interaktion von Pflanzen und Bakterien“ selbstständig und ohne fremde Hilfe verfasst habe. Andere als die angegebenen Quellen und Hilfsmittel habe ich nicht benutzt und die wörtlich oder inhaltlich übernommenen Stellen als solchen kenntlich gemacht. Ich erkläre außerdem, dass diese Dissertation weder in gleicher noch in anderer Form bereits in einem anderen Prüfungsverfahren vorgelegen hat. Ich habe früher, außer mit den im Zulassungsversuch urkundlich vorgelegten Graden, keine weiteren akademischen Grade erworben oder zu erwerben versucht.

Teile dieser Arbeit sind bereits in einer wissenschaftlichen Fachzeitschrift publiziert worden:

Thomanek, H.; Schenk, S. T.; Stein, E.; Kogel, K.-H.; Schikora, A.; Maison, W. *Org. Biomol. Chem.* **2013**, *11*, 6994.

(Ort, Datum)

(Unterschrift)

12 Literature

- (1) Obst, U. *Anal. Bioanal. Chem.* **2007**, 387, 369.
- (2) Doudoroff, M. *J. Bacteriol.* **1942**, 44, 451.
- (3) Churchill, M. E. A.; Chen, L. *Chem. Rev.* **2010**, 111, 68.
- (4) Jacob, E. B.; Becker, I.; Shapira, Y.; Levine, H. *Trends Microbiol.* **2004**, 12, 366.
- (5) Tomasz, A. *Nature* **1965**, 208, 155.
- (6) Nealson, K. H.; Platt, T.; Hastings, J. W. *J. Bacteriol.* **1970**, 104, 313.
- (7) Bainton, N. J.; Stead, P.; Chhabra, S. R.; Bycroft, B. W.; Salmond, G. P.; Stewart, G. S.; Williams, P. *Biochem. J.* **1992**, 288, 997.
- (8) Fuqua, W. C.; Winans, S. C.; Greenberg, E. P. *J. Bacteriol.* **1994**, 176, 269.
- (9) Gambello, M. J.; Iglewski, B. H. *J. Bacteriol.* **1991**, 173, 3000.
- (10) Amara, N.; Krom, B. P.; Kaufmann, G. F.; Meijler, M. M. *Chem. Rev.* **2010**, 111, 195.
- (11) Blackwell, H. E.; Fuqua, C. *Chem. Rev.* **2011**, 111, 1.
- (12) González, J. E.; Keshavan, N. D. *Microbiol. Mol. Biol. Rev.* **2006**, 70, 859.
- (13) Rice, S. A.; Koh, K. S.; Queck, S. Y.; Labbate, M.; Lam, K. W.; Kjelleberg, S. J. *Bacteriol.* **2005**, 187, 3477.
- (14) Boyer, M.; Wisniewski-Dyé, F. *FEMS Microbiol. Ecol.* **2009**, 70, 1.
- (15) Waters, C. M.; Bassler, B. L. *Annu. Rev. Cell Dev. Biol.* **2005**, 21, 319.
- (16) Dickschat, J. S. *Nat. Prod. Rep.* **2010**, 27, 343.
- (17) Flickinger, S. T.; Copeland, M. F.; Downes, E. M.; Braasch, A. T.; Tuson, H. H.; Eun, Y.-J.; Weibel, D. B. *J. Am. Chem. Soc.* **2011**, 133, 5966.
- (18) Geske, G. D.; Wezeman, R. J.; Siegel, A. P.; Blackwell, H. E. *J. Am. Chem. Soc.* **2005**, 127, 12762.
- (19) Hentzer, M.; Givskov, M. *J. Clin. Invest.* **2003**, 112, 1300.
- (20) Parsek, M. R.; Greenberg, E. P. *Trends Microbiol.* **2005**, 13, 27.
- (21) Walker, T. S.; Bais, H. P.; Déziel, E.; Schweizer, H. P.; Rahme, L. G.; Fall, R.; Vivanco, J. M. *Plant Physiol.* **2004**, 134, 320.
- (22) Mattmann, M. E.; Blackwell, H. E. *J. Org. Chem.* **2010**, 75, 6737.
- (23) Davies, D. G.; Parsek, M. R.; Pearson, J. P.; Iglewski, B. H.; Costerton, J. W.; Greenberg, E. P. *Science* **1998**, 280, 295.
- (24) Galloway, W. R. J. D.; Hodgkinson, J. T.; Bowden, S. D.; Welch, M.; Spring, D. R. *Chem. Rev.* **2010**, 111, 28.
- (25) Bassler, B. L. *Cell* **2002**, 109, 421.

- (26) Bassler, B. L.; Losick, R. *Cell* **2006**, *125*, 237.
- (27) Henke, J. M.; Bassler, B. L. *Trends Cell Biol.* **2004**, *14*, 648.
- (28) Ji, G.; Beavis, R.; Novick, R. P. *Science* **1997**, *276*, 2027.
- (29) Otto, M.; Süßmuth, R.; Jung, G.; Götz, F. *FEBS Lett.* **1998**, *424*, 89.
- (30) Hakenbeck, R.; Stock, J. B. In *Methods Enzymol.*; Sankar, A., Ed.; Academic Press: 1996; Vol. Volume 273, p 281.
- (31) Amara, N.; Mashiach, R.; Amar, D.; Krief, P.; Spieser, S. p. A. H.; Bottomley, M. J.; Aharoni, A.; Meijler, M. M. *J. Am. Chem. Soc.* **2009**, *131*, 10610.
- (32) Chhabra, S.; Philipp, B.; Eberl, L.; Givskov, M.; Williams, P.; Cámara, M. In *The Chemistry of Pheromones and Other Semiochemicals II*; Schulz, S., Ed.; Springer Berlin / Heidelberg: 2005; Vol. 240, p 117.
- (33) Decho, A. W.; Norman, R. S.; Visscher, P. T. *Trends Microbiol.* **2010**, *18*, 73.
- (34) Bassler, B. L.; Wright, M.; Showalter, R. E.; Silverman, M. R. *Mol. Microbiol.* **1993**, *9*, 773.
- (35) Bassler, B. L.; Wright, M.; Silverman, M. R. *Mol. Microbiol.* **1994**, *13*, 273.
- (36) Cao, J. G.; Meighen, E. A. *J. Biol. Chem.* **1989**, *264*, 21670.
- (37) Chen, X.; Schauder, S.; Potier, N.; Van Dorsselaer, A.; Pelczer, I.; Bassler, B. L.; Hughson, F. M. *Nature* **2002**, *415*, 545.
- (38) Bassler, B. L.; Greenberg, E. P.; Stevens, A. M. *J. Bacteriol.* **1997**, *179*, 4043.
- (39) Boettcher, K. J.; Ruby, E. G. *J. Bacteriol.* **1995**, *177*, 1053.
- (40) Fuqua, C.; Greenberg, E. P. *Nat. Rev. Mol. Cell Biol.* **2002**, *3*, 685.
- (41) Eberhard, A.; Burlingame, A. L.; Eberhard, C.; Kenyon, G. L.; Nealson, K. H.; Oppenheimer, N. J. *Biochemistry* **1981**, *20*, 2444.
- (42) Geske, G. D.; O'Neill, J. C.; Blackwell, H. E. *Chem. Soc. Rev.* **2008**, *37*, 1432.
- (43) Lupp, C.; Urbanowski, M.; Greenberg, E. P.; Ruby, E. G. *Mol. Microbiol.* **2003**, *50*, 319.
- (44) Swift, S.; Throup, J. P.; Williams, P.; Salmond, G. P. C.; Stewart, G. S. A. B. *Trends Biochem. Sci.* **1996**, *21*, 214.
- (45) Whitehead, N. A.; Barnard, A. M. L.; Slater, H.; Simpson, N. J. L.; Salmond, G. P. C. *FEMS Microbiol. Rev.* **2001**, *25*, 365.
- (46) Engebrecht, J.; Nealson, K.; Silverman, M. *Cell* **1983**, *32*, 773.
- (47) Engebrecht, J.; Silverman, M. *P. Natl. Acad. Sci.* **1984**, *81*, 4154.
- (48) Hanzelka, B. L.; Greenberg, E. P. *J. Bacteriol.* **1996**, *178*, 5291.
- (49) Shadel, G. S.; Young, R.; Baldwin, T. O. *J. Bacteriol.* **1990**, *172*, 3980.

- (50) Slock, J.; VanRiet, D.; Kolibachuk, D.; Greenberg, E. P. *J. Bacteriol.* **1990**, *172*, 3974.
- (51) Evans, K.; Passador, L.; Srikumar, R.; Tsang, E.; Nezezson, J.; Poole, K. *J. Bacteriol.* **1998**, *180*, 5443.
- (52) Kaplan, H. B.; Greenberg, E. P. *J. Bacteriol.* **1985**, *163*, 1210.
- (53) Pearson, J. P.; Passador, L.; Iglewski, B. H.; Greenberg, E. P. *P. Natl. Acad. Sci.* **1995**, *92*, 1490.
- (54) Welch, M.; Todd, D. E.; Whitehead, N. A.; McGowan, S. J.; Bycroft, B. W.; Salmond, G. P. C. *EMBO J.* **2000**, *19*, 631.
- (55) Miller, M. B.; Bassler, B. L. *Annu. Rev. Microbiol.* **2001**, *55*, 165.
- (56) Devine, J. H.; Shadel, G. S.; Baldwin, T. O. *P. Natl. Acad. Sci.* **1989**, *86*, 5688.
- (57) Egland, K. A.; Greenberg, E. P. *Mol. Microbiol.* **1999**, *31*, 1197.
- (58) Gray, K. M.; Garey, J. R. *Microbiology* **2001**, *147*, 2379.
- (59) Borlee, B. R.; Geske, G. D.; Blackwell, H. E.; Handelsman, J. *Appl. Environ. Microbiol.* **2010**, *76*, 8255.
- (60) Bottomley, M. J.; Muraglia, E.; Bazzo, R.; Carfi, A. *J. Biol. Chem.* **2007**, *282*, 13592.
- (61) Whiteley, M.; Lee, K. M.; Greenberg, E. P. *P. Natl. Acad. Sci.* **1999**, *96*, 13904.
- (62) O'Toole, G. A.; Kolter, R. *Mol. Microbiol.* **1998**, *30*, 295.
- (63) O'Toole, G. A.; Kolter, R. *Mol. Microbiol.* **1998**, *28*, 449.
- (64) Nasser, W.; Reverchon, S. *Anal. Bioanal. Chem.* **2007**, *387*, 381.
- (65) Case, R. J.; Labbate, M.; Kjelleberg, S. *ISME J.* **2008**, *2*, 345.
- (66) Williams, P. *Microbiology* **2007**, *153*, 3923.
- (67) Frommberger, M.; Hertkorn, N.; Englmann, M.; Jakoby, S.; Hartmann, A.; Kettrup, A.; Schmitt-Kopplin, P. *Electrophoresis* **2005**, *26*, 1523.
- (68) Englmann, M.; Fekete, A.; Kuttler, C.; Frommberger, M.; Li, X.; Gebefügi, I.; Fekete, J.; Schmitt-Kopplin, P. *J. Chromatogr. A* **2007**, *1160*, 184.
- (69) Yates, E. A.; Philipp, B.; Buckley, C.; Atkinson, S.; Chhabra, S. R.; Sockett, R. E.; Goldner, M.; Dessaux, Y.; Cámara, M.; Smith, H.; Williams, P. *Infect. Immun.* **2002**, *70*, 5635.
- (70) Laue, B. E.; Jiang, Y.; Chhabra, S. R.; Jacob, S.; Stewart, G. S. A. B.; Hardman, A.; Downie, J. A.; O'Gara, F.; Williams, P. *Microbiology* **2000**, *146*, 2469.
- (71) Schripsema, J.; de Rudder, K. E.; van Vliet, T. B.; Lankhorst, P. P.; de Vroom, E.; Kijne, J. W.; van Brussel, A. A. *J. Bacteriol.* **1996**, *178*, 366.
- (72) Chhabra, S. R.; Harty, C.; Hooi, D. S. W.; Daykin, M.; Williams, P.; Telford, G.; Pritchard, D. I.; Bycroft, B. W. *J. Med. Chem.* **2002**, *46*, 97.

- (73) Holden, M. T. G.; Ram Chhabra, S.; De Nys, R.; Stead, P.; Bainton, N. J.; Hill, P. J.; Manefield, M.; Kumar, N.; Labatte, M.; England, D.; Rice, S.; Givskov, M.; Salmond, G. P. C.; Stewart, G. S. A. B.; Bycroft, B. W.; Kjelleberg, S.; Williams, P. *Mol. Microbiol.* **1999**, *33*, 1254.
- (74) Degrassi, G.; Aguilar, C.; Bosco, M.; Zahariev, S.; Pongor, S.; Venturi, V. *Curr. Microbiol.* **2002**, *45*, 250.
- (75) Pesci, E. C.; Milbank, J. B. J.; Pearson, J. P.; McKnight, S.; Kende, A. S.; Greenberg, E. P.; Iglewski, B. H. *P. Natl. Acad. Sci.* **1999**, *96*, 11229.
- (76) Loh, J.; Carlson, R. W.; York, W. S.; Stacey, G. *P. Natl. Acad. Sci.* **2002**, *99*, 14446.
- (77) Loh, J.; Lohar, D. P.; Andersen, B.; Stacey, G. *J. Bacteriol.* **2002**, *184*, 1759.
- (78) Loh, J. T.; Yuen-Tsai, J. P. Y.; Stacey, M. G.; Lohar, D.; Welborn, A.; Stacey, G. *Mol. Microbiol.* **2001**, *42*, 37.
- (79) Withers, H.; Swift, S.; Williams, P. *Curr. Opin. Microbiol.* **2001**, *4*, 186.
- (80) Moré, M. I.; Finger, L. D.; Stryker, J. L.; Fuqua, C.; Eberhard, A.; Winans, S. C. *Science* **1996**, *272*, 1655.
- (81) Schaefer, A. L.; Val, D. L.; Hanzelka, B. L.; Cronan, J. E.; Greenberg, E. P. *P. Natl. Acad. Sci.* **1996**, *93*, 9505.
- (82) Khan, S. R.; Mavrodi, D. V.; Jog, G. J.; Suga, H.; Thomashow, L. S.; Farrand, S. K. *J. Bacteriol.* **2005**, *187*, 6517.
- (83) Labbate, M.; Queck, S. Y.; Koh, K. S.; Rice, S. A.; Givskov, M.; Kjelleberg, S. *J. Bacteriol.* **2004**, *186*, 692.
- (84) Parsek, M. R.; Val, D. L.; Hanzelka, B. L.; Cronan, J. E.; Greenberg, E. P. *P. Natl. Acad. Sci.* **1999**, *96*, 4360.
- (85) Watson, W. T.; Minogue, T. D.; Val, D. L.; von Bodman, S. B.; Churchill, M. E. A. *Mol. Cell* **2002**, *9*, 685.
- (86) Parsek, M. R.; Schaefer, A. L.; Greenberg, E. P. *Mol. Microbiol.* **1997**, *26*, 301.
- (87) Teplitski, M.; Mathesius, U.; Rumbaugh, K. P. *Chem. Rev.* **2010**, *111*, 100.
- (88) Cao, H.; Baldini, R. L.; Rahme, L. G. *Annu. Rev. Phytopathol.* **2001**, *39*, 259.
- (89) von Bodman, S. B.; Bauer, W. D.; Coplin, D. L. *Annu. Rev. Phytopathol.* **2003**, *41*, 455.
- (90) Meyers, B. R.; Bottone, E.; Hirschman, S. Z.; Schneier, S. S. *Ann. Intern. Med.* **1972**, *76*, 9.
- (91) Fan, H.; Dong, Y.; Wu, D.; Bowler, M. W.; Zhang, L.; Song, H. *P. Natl. Acad. Sci.* **2013**, *110*, 20765.

- (92) Filloux, A. P. *Natl. Acad. Sci.* **2013**, *110*, 20360.
- (93) Shiner, E. K.; Rumbaugh, K. P.; Williams, S. C. *FEMS Microbiol. Rev.* **2005**, *29*, 935.
- (94) Smith, R. S.; Harris, S. G.; Phipps, R.; Iglewski, B. J. *Bacteriol.* **2002**, *184*, 1132.
- (95) Thomas, G. L.; Bohner, C. M.; Williams, H. E.; Walsh, C. M.; Ladlow, M.; Welch, M.; Bryant, C. E.; Spring, D. R. *Mol. BioSyst.* **2006**, *2*, 132.
- (96) Schuster, M.; Lostroh, C. P.; Ogi, T.; Greenberg, E. P. *J. Bacteriol.* **2003**, *185*, 2066.
- (97) Wagner, V. E.; Bushnell, D.; Passador, L.; Brooks, A. I.; Iglewski, B. H. *J. Bacteriol.* **2003**, *185*, 2080.
- (98) Chen, Z.; Kloek, A. P.; Boch, J.; Katagiri, F.; Kunkel, B. N. *Mol. Plant-Microbe Interact.* **2000**, *13*, 1312.
- (99) Dumenyo, C.; Mukherjee, A.; Chun, W.; Chatterjee, A. *Eur. J. Plant Pathol.* **1998**, *104*, 569.
- (100) Bonkowski, M.; Villenave, C.; Griffiths, B. *Plant Soil* **2009**, *321*, 213.
- (101) Goddard, V. J.; Bailey, M. J.; Darrah, P.; Lilley, A. K.; Thompson, I. P. *Plant Soil* **2001**, *232*, 181.
- (102) Whipps, J. M. *J. Exp. Bot.* **2001**, *52*, 487.
- (103) Gantner, S.; Schmid, M.; Dürr, C.; Schuegger, R.; Steidle, A.; Hutzler, P.; Langebartels, C.; Eberl, L.; Hartmann, A.; Dazzo, F. B. *FEMS Microbiol. Ecol.* **2006**, *56*, 188.
- (104) Schuegger, R.; Ihring, A.; Gantner, S.; Bahnweg, G.; Knappe, C.; Vogg, G.; Hutzler, P.; Schmid, M.; Van Breusegem, F.; Eberl, L. E. O.; Hartmann, A.; Langebartels, C. *Plant Cell Environ.* **2006**, *29*, 909.
- (105) Gonzalez, J. E.; Marketon, M. M. *Microbiol. Mol. Biol. Rev.* **2003**, *67*, 574.
- (106) Sanchez-Contreras, M.; Bauer, W. D.; Gao, M.; Robinson, J. B.; Allan Downie, J. *Philos. T. Roy. Soc. B* **2007**, *362*, 1149.
- (107) Barnard, A. L.; Salmond, G. C. *Anal. Bioanal. Chem.* **2007**, *387*, 415.
- (108) Morohoshi, T.; Nakamura, Y.; Yamazaki, G.; Ishida, A.; Kato, N.; Ikeda, T. *J. Bacteriol.* **2007**, *189*, 8333.
- (109) White, C. E.; Winans, S. C. *Philos. T. Roy. Soc. B* **2007**, *362*, 1135.
- (110) Escobar, M. A.; Dandekar, A. M. *Trends Plant Sci.* **2003**, *8*, 380.
- (111) Bakker, P. H. M.; Raaijmakers, J.; Bloemberg, G.; Höfte, M.; Lemanceau, P.; Cooke, M. *Eur. J. Plant Pathol.* **2007**, *119*, 241.
- (112) Ramamoorthy, V.; Viswanathan, R.; Raguchander, T.; Prakasam, V.; Samiyappan, R. *Crop Prot.* **2001**, *20*, 1.

- (113) Steindler, L.; Bertani, I.; De Sordi, L.; Schwager, S.; Eberl, L.; Venturi, V. *Appl. Environ. Microbiol.* **2009**, *75*, 5131.
- (114) Hong, Y.; Pasternak, J. J.; Glick, B. R. *Can. J. Microbiol.* **1991**, *37*, 796.
- (115) Burd, G. I.; Dixon, D. G.; Glick, B. R. *Appl. Environ. Microbiol.* **1998**, *64*, 3663.
- (116) Barriuso, J.; Ramos Solano, B.; Fray, R. G.; Cámara, M.; Hartmann, A.; Gutiérrez Mañero, F. J. *Plant Biotechnol. J.* **2008**, *6*, 442.
- (117) Bloemberg, G. V.; Lugtenberg, B. J. J. *Curr. Opin. Plant Biol.* **2001**, *4*, 343.
- (118) Persello-Cartieaux, F.; Nussaume, L.; Robaglia, C. *Plant, Cell Environ.* **2003**, *26*, 189.
- (119) Zehnder, G.; Murphy, J.; Sikora, E.; Kloepper, J. *Eur. J. Plant Pathol.* **2001**, *107*, 39.
- (120) Cronin, D.; Moëgne-Loccoz, Y.; Fenton, A.; Dunne, C.; Dowling, D. N.; O'Gara, F. *FEMS Microbiol. Ecol.* **1997**, *23*, 95.
- (121) Buysens, S.; Heungens, K.; Poppe, J.; Hofte, M. *Appl. Environ. Microbiol.* **1996**, *62*, 865.
- (122) Kalbe, C.; Marten, P.; Berg, G. *Microbiol. Res.* **1996**, *151*, 433.
- (123) van Loon, L. C.; Bakker, P. A. H. M.; Pieterse, C. M. J. *Annu. Rev. Phytopathol.* **1998**, *36*, 453.
- (124) Audenaert, K.; Pattery, T.; Cornelis, P.; Höfte, M. *Mol. Plant-Microbe Interact.* **2002**, *15*, 1147.
- (125) De Meyer, G.; Capieau, K.; Audenaert, K.; Buchala, A.; Métraux, J.-P.; Höfte, M. *Mol. Plant-Microbe Interact.* **1999**, *12*, 450.
- (126) De Meyer, G.; Höfte, M. *Phytopathology* **1997**, *87*, 588.
- (127) Pieterse, C. J.; Van Pelt, J.; Van Wees, S. M.; Ton, J.; Léon-Kloosterziel, K.; Keurentjes, J. B.; Verhagen, B. M.; Knoester, M.; Van der Sluis, I.; Bakker, P. H. M.; Van Loon, L. C. *Eur. J. Plant Pathol.* **2001**, *107*, 51.
- (128) Glick, B. R.; Penrose, D. M.; Li, J. J. *Theor. Biol.* **1998**, *190*, 63.
- (129) Okon, Y.; Kapulnik, Y. In *Nitrogen Fixation with Non-Legumes*; Skinner, F. A., Uomala, P., Eds.; Springer Netherlands: 1986; Vol. 21, p 3.
- (130) Vessey, J. K. *Plant Soil* **2003**, *255*, 571.
- (131) Johnson, P. R.; Ecker, J. R. *Annu. Rev. Genet.* **1998**, *32*, 227.
- (132) Uroz, S.; Dessaux, Y.; Oger, P. *ChemBioChem* **2009**, *10*, 205.
- (133) Manefield, M.; de Nys, R.; Naresh, K.; Roger, R.; Givskov, M.; Peter, S.; Kjelleberg, S. *Microbiology* **1999**, *145*, 283.
- (134) Manefield, M.; Rasmussen, T. B.; Henzter, M.; Andersen, J. B.; Steinberg, P.; Kjelleberg, S.; Givskov, M. *Microbiology* **2002**, *148*, 1119.

- (135) Delalande, L.; Faure, D.; Raffoux, A.; Uroz, S.; D'Angelo-Picard, C.; Elasri, M.; Carlier, A.; Berruyer, R.; Petit, A.; Williams, P.; Dessaux, Y. *FEMS Microbiol. Ecol.* **2005**, *52*, 13.
- (136) Horswill, A.; Stoodley, P.; Stewart, P.; Parsek, M. *Anal. Bioanal. Chem.* **2007**, *387*, 371.
- (137) Dong, Y. H.; Zhang, L. H. *J. Microbiol.* **2005**, *43*, 101.
- (138) Götz, C.; Fekete, A.; Gebefuegi, I.; Forczek, S.; Fuksová, K.; Li, X.; Englmann, M.; Gryndler, M.; Hartmann, A.; Matucha, M.; Schmitt-Kopplin, P.; Schröder, P. *Anal. Bioanal. Chem.* **2007**, *389*, 1447.
- (139) Gould, T. A.; Watson, W. T.; Choi, K.-H.; Schweizer, H. P.; Churchill, M. E. A. *Acta Crystallogr. Sect. D* **2004**, *60*, 518.
- (140) Vannini, A.; Volpari, C.; Gargioli, C.; Muraglia, E.; Cortese, R.; De Francesco, R.; Neddermann, P.; Di Marco, S. *EMBO J.* **2002**, *21*, 4393.
- (141) Gnanendra, S.; Anusuya, S.; Natarajan, J. *J. Mol. Model.* **2012**, *18*, 4709.
- (142) Eberhard, A.; Widrig, C.; McBath, P.; Schineller, J. *Arch. Microbiol.* **1986**, *146*, 35.
- (143) Schaefer, A. L.; Hanzelka, B. L.; Eberhard, A.; Greenberg, E. P. *J. Bacteriol.* **1996**, *178*, 2897.
- (144) Olsen, J. A.; Severinsen, R.; Rasmussen, T. B.; Hentzer, M.; Givskov, M.; Nielsen, J. *Bioorg. Med. Chem. Lett.* **2002**, *12*, 325.
- (145) Geske, G. D.; O'Neill, J. C.; Miller, D. M.; Mattmann, M. E.; Blackwell, H. E. *J. Am. Chem. Soc.* **2007**, *129*, 13613.
- (146) Zhu, J.; Beaber, J. W.; Moré, M. I.; Fuqua, C.; Eberhard, A.; Winans, S. C. *J. Bacteriol.* **1998**, *180*, 5398.
- (147) Reverchon, S.; Chantegrel, B.; Deshayes, C.; Doutheau, A.; Cotte-Pattat, N. *Bioorg. Med. Chem. Lett.* **2002**, *12*, 1153.
- (148) Janssens, J. C. A.; Metzger, K.; Daniels, R.; Ptacek, D.; Verhoeven, T.; Habel, L. W.; Vanderleyden, J.; De Vos, D. E.; De Keersmaecker, S. C. *J. Appl. Environ. Microbiol.* **2007**, *73*, 535.
- (149) Müh, U.; Hare, B. J.; Duerkop, B. A.; Schuster, M.; Hanzelka, B. L.; Heim, R.; Olson, E. R.; Greenberg, E. P. *Proc. Natl. Acad. Sci.* **2006**, *103*, 16948.
- (150) von Rad, U.; Klein, I.; Dobrev, P.; Kottova, J.; Zazimalova, E.; Fekete, A.; Hartmann, A.; Schmitt-Kopplin, P.; Durner, J. *Planta* **2008**, *229*, 73.
- (151) Sieper, T.; Forczek, S.; Matucha, M.; Krämer, P.; Hartmann, A.; Schröder, P. *New Phytol.* **2014**, *201*, 545.

- (152) Ortíz-Castro, R.; Martínez-Trujillo, M.; López-Bucio, J. *Plant Cell Environ.* **2008**, *31*, 1497.
- (153) Schenk, S. T.; Stein, E.; Kogel, K. H.; Schikora, A. *Plant Signal Behav.* **2012**, *7*.
- (154) Schikora, A.; Schenk, S. T.; Stein, E.; Molitor, A.; Zuccaro, A.; Kogel, K. H. *Plant Physiol.* **2011**.
- (155) Palmer, A. G.; Streng, E.; Blackwell, H. E. *ACS Chem. Biol.* **2011**, *6*, 1348.
- (156) Palmer, A. G.; Streng, E.; Jewell, K. A.; Blackwell, H. E. *ChemBioChem* **2011**, *12*, 138.
- (157) Breitbach, A. S.; Broderick, A. H.; Jewell, C. M.; Gunasekaran, S.; Lin, Q.; Lynn, D. M.; Blackwell, H. E. *Chem. Commun.* **2011**, *47*, 370.
- (158) Thomanek, H.; Schenk, S. T.; Stein, E.; Kogel, K.-H.; Schikora, A.; Maison, W. *Org. Biomol. Chem.* **2013**, *11*, 6994.
- (159) Karlsson, T.; Turkina, M. V.; Yakymenko, O.; Magnusson, K.-E.; Vikström, E. *PLoS Pathog.* **2012**, *8*, e1002953.
- (160) Spandl, R. J.; Nicholson, R. L.; Marsden, D. M.; Hodgkinson, J. T.; Su, X.; Thomas, G. L.; Salmond, G. P. C.; Welch, M.; Spring, D. R. *Synlett* **2008**, *2008*, 2122.
- (161) Gould, T. A.; Schweizer, H. P.; Churchill, M. E. A. *Mol. Microbiol.* **2004**, *53*, 1135.
- (162) Persson, T.; Hansen, T. H.; Rasmussen, T. B.; Skinderso, M. E.; Givskov, M.; Nielsen, J. *Org. Biomol. Chem.* **2005**, *3*, 253.
- (163) Stevens, A. M.; Queneau, Y.; Soulère, L.; Bodman, S. v.; Doutheau, A. *Chem. Rev.* **2010**, *111*, 4.
- (164) Mues, H.; Kazmaier, U. *Synthesis* **2001**, *2001*, 0487.
- (165) Kikuchi, H.; Sasaki, K.; Sekiya, J. i.; Maeda, Y.; Amagai, A.; Kubohara, Y.; Oshima, Y. *Bioorg. Med. Chem.* **2004**, *12*, 3203.
- (166) Svedhem, S.; Hollander, C.-Å.; Shi, J.; Konradsson, P.; Liedberg, B.; Svensson, S. C. T. *J. Org. Chem.* **2001**, *66*, 4494.
- (167) Lebeau, L.; Oudet, P.; Mioskowski, C. *Helv. Chim. Acta* **1991**, *74*, 1697.
- (168) Kotzyba-Hibert, F.; Kapfer, I.; Goeldner, M. *Angew. Chem. Int. Ed. Engl.* **1995**, *34*, 1296.
- (169) Kotzyba-Hibert, F.; Kapfer, I.; Goeldner, M. *Angew. Chem.* **1995**, *107*, 1391.
- (170) Dubinsky, L.; Jarosz, L. M.; Amara, N.; Krief, P.; Kravchenko, V. V.; Krom, B. P.; Meijler, M. M. *Chem. Commun.* **2009**, 7378.
- (171) Diamandis, E. P.; Christopoulos, T. K. *Clin. Chem.* **1991**, *37*, 625.
- (172) Dekhane, M.; Douglas, K. T.; Gilbert, P. *Tetrahedron Lett.* **1996**, *37*, 1883.

- (173) Koch, G. K.; Kop, J. M. M. *Tetrahedron Lett.* **1974**, *15*, 603.
- (174) Mander, L. N.; Sethi, S. P. *Tetrahedron Lett.* **1983**, *24*, 5425.
- (175) Bräse, S.; Gil, C.; Knepper, K.; Zimmermann, V. *Angew. Chem. Int. Ed.* **2005**, *44*, 5188.
- (176) Franzmann, E.; Khalil, F.; Weidmann, C.; Schröder, M.; Rohnke, M.; Janek, J.; Smarsly, B. M.; Maison, W. *Chem. Eur. J.* **2011**, *17*, 8596.
- (177) Gademann, K.; Kobylinska, J.; Wach, J.-Y.; Woods, T. *BioMetals* **2009**, *22*, 595.
- (178) Ye, Q.; Zhou, F.; Liu, W. *Chem. Soc. Rev.* **2011**, *40*, 4244.
- (179) Pezzella, A.; Panzella, L.; Natangelo, A.; Arzillo, M.; Napolitano, A.; d'Ischia, M. *J. Org. Chem.* **2007**, *72*, 9225.
- (180) Li, B.; Liu, W.; Jiang, Z.; Dong, X.; Wang, B.; Zhong, Y. *Langmuir* **2009**, *25*, 7368.
- (181) Ryu, J.; Ku, S. H.; Lee, H.; Park, C. B. *Adv. Funct. Mater.* **2010**, *20*, 2132.
- (182) Waite, J. H. *Nat. Mater.* **2008**, *7*, 8.
- (183) Gomes, J.; Grunau, A.; Lawrence, A. K.; Eberl, L.; Gademann, K. *Chem. Commun.* **2013**, *49*, 155.
- (184) Queffélec, C.; Petit, M.; Janvier, P.; Knight, D. A.; Bujoli, B. *Chem. Rev.* **2012**, *112*, 3777.
- (185) Szajnman, S. H.; García Liñares, G.; Moro, P.; Rodriguez, J. B. *Eur. J. Org. Chem.* **2005**, *2005*, 3687.
- (186) Guerrero, G.; Mutin, P. H.; Vioux, A. *Chem. Mater.* **2001**, *13*, 4367.
- (187) Guénin, E.; Monteil, M.; Bouchemal, N.; Prangé, T.; Lecouvey, M. *Eur. J. Org. Chem.* **2007**, *2007*, 3380.
- (188) Turhanen, P. A.; Vepsäläinen, J. J. *Beilstein J. Org. Chem.* **2008**, *4*, 7.
- (189) Berg, R.; Straub, B. F. *Beilstein J. Org. Chem.* **2013**, *9*, 2715.
- (190) Song, X.-P.; Bouillon, C.; Lescrinier, E.; Herdewijn, P. *ChemBioChem* **2011**, *12*, 1868.
- (191) Houghton, T. J.; Tanaka, K. S. E.; Kang, T.; Dietrich, E.; Lafontaine, Y.; Delorme, D.; Ferreira, S. S.; Viens, F.; Arhin, F. F.; Sarmiento, I.; Lehoux, D.; Fadhil, I.; Laquerre, K.; Liu, J.; Ostiguy, V.; Poirier, H.; Moeck, G.; Parr, T. R.; Far, A. R. *J. Med. Chem.* **2008**, *51*, 6955.
- (192) Bhushan, K. R.; Tanaka, E.; Frangioni, J. V. *Angew. Chem. Int. Ed.* **2007**, *46*, 7969.
- (193) Lipton, A.; Theriault, R. L.; Hortobagyi, G. N.; Simeone, J.; Knight, R. D.; Mellars, K.; Reitsma, D. J.; Heffernan, M.; Seaman, J. J. *Cancer* **2000**, *88*, 1082.
- (194) Demmer, C. S.; Krogsgaard-Larsen, N.; Bunch, L. *Chem. Rev.* **2011**, *111*, 7981.

- (195) Yan, F.; Moon, S.-J.; Liu, P.; Zhao, Z.; Lipscomb, J. D.; Liu, A.; Liu, H.-w. *Biochemistry* **2007**, *46*, 12628.
- (196) Steidle, A.; Sigl, K.; Schuegger, R.; Ihring, A.; Schmid, M.; Gantner, S.; Stoffels, M.; Riedel, K.; Givskov, M.; Hartmann, A.; Langebartels, C.; Eberl, L. *Appl. Environ. Microbiol.* **2001**, *67*, 5761.
- (197) Li, D. *Dissertation at the Ludwig Maximilian University München* **2010**.
- (198) Andersen, J. B.; Heydorn, A.; Hentzer, M.; Eberl, L.; Geisenberger, O.; Christensen, B. B.; Molin, S.; Givskov, M. *Appl. Environ. Microbiol.* **2001**, *67*, 575.
- (199) Praneenarat, T.; Palmer, A. G.; Blackwell, H. E. *Org. Biomol. Chem.* **2012**, *10*, 8189.
- (200) Mathesius, U.; Mulders, S.; Gao, M.; Teplitski, M.; Caetano-Anolles, G.; Rolfe, B. G.; Bauer, W. D. *Proc Natl Acad Sci U S A* **2003**, *100*, 1444.
- (201) Eulgem, T.; Rushton, P. J.; Robatzek, S.; Somssich, I. E. *Trends Plant Sci.* **2000**, *5*, 199.
- (202) Eulgem, T.; Rushton, P. J.; Schmelzer, E.; Hahlbrock, K.; Somssich, I. E. *EMBO J.* **1999**, *18*, 4689.
- (203) Rushton, P. J.; Somssich, I. E.; Ringler, P.; Shen, Q. J. *Trends Plant Sci.* **2010**, *15*, 247.
- (204) Asai, T.; Tena, G.; Plotnikova, J.; Willmann, M. R.; Chiu, W.-L.; Gomez-Gomez, L.; Boller, T.; Ausubel, F. M.; Sheen, J. *Nature* **2002**, *415*, 977.
- (205) Murray, S. L.; Ingle, R. A.; Petersen, L. N.; Denby, K. J. *Mol. Plant Microbe Interact.* **2007**, *20*, 1431.
- (206) Xu, X.; Chen, C.; Fan, B.; Chen, Z. *Plant Cell* **2006**, *18*, 1310.
- (207) Zheng, Z.; Qamar, S. A.; Chen, Z.; Mengiste, T. *Plant J.* **2006**, *48*, 592.
- (208) Jones, J. D. G.; Dangl, J. L. *Nature* **2006**, *444*, 323.
- (209) Waite, J. H. *Int. J. Adhes. Adhes.* **1987**, *7*, 9.
- (210) Waite, J. H.; Tanzer, M. L. *Science* **1981**, *212*, 1038.
- (211) Brown, C. H. *Q. J. Microsc. Sci.* **1952**, *s3-93*, 487.
- (212) Lee, H.; Scherer, N. F.; Messersmith, P. B. *P. Natl. Acad. Sci.* **2006**, *103*, 12999.
- (213) Wilker, J. J. *Angew. Chem.* **2010**, *122*, 8252.
- (214) Moser, J.; Punchihewa, S.; Infelta, P. P.; Graetzel, M. *Langmuir* **1991**, *7*, 3012.
- (215) Dalsin, J. L.; Lin, L.; Tosatti, S.; Vörös, J.; Textor, M.; Messersmith, P. B. *Langmuir* **2004**, *21*, 640.
- (216) Rodriguez, R.; Blesa, M. A.; Regazzoni, A. E. *J. Colloid Interf. Sci.* **1996**, *177*, 122.

- (217) Kurepa, J.; Paunesku, T.; Vogt, S.; Arora, H.; Rabatic, B. M.; Lu, J.; Wanzer, M. B.; Woloschak, G. E.; Smalle, J. A. *Nano Lett.* **2010**, *10*, 2296.
- (218) Ramamoorthy, M.; Vanderbilt, D.; King-Smith, R. D. *Phys. Rev. B* **1994**, *49*, 16721.
- (219) Sun, C.; Liu, L.-M.; Selloni, A.; Lu, G. Q.; Smith, S. C. *J. Mater. Chem.* **2010**, *20*, 10319.
- (220) Wang, X.; Li, Z.; Shi, J.; Yu, Y. *Chem. Rev.* **2014**.
- (221) Atkins, P. W. *Physikalische Chemie*; Wiley-VCH: Weinheim, Germany, 1990.
- (222) Brunauer, S.; Emmett, P. H.; Teller, E. *J. Am. Chem. Soc.* **1938**, *60*, 309.
- (223) Zhou, K.; Zhu, Y.; Yang, X.; Jiang, X.; Li, C. *New J. Chem.* **2011**, *35*, 353.
- (224) Geiseler, B.; Fruk, L. *J. Mater. Chem.* **2012**, *22*, 735.
- (225) Jankovic, I.; Saponjic, Z.; Dzunuzovic, E.; Nedeljkovic, J. *Nanoscale Res. Lett.* **2009**, *5*, 81
- (226) Yoon, G.; Zabriskie, T. M.; Cheon, S. H. *J. Labelled Compd. Rad.* **2009**, *52*, 53.
- (227) Kazmaier, U. *Angew. Chem.* **1994**, *106*, 1046.
- (228) Kazmaier, U. *Angew. Chem. Int. Ed. Engl.* **1994**, *33*, 998.
- (229) Galibert, M.; Dumy, P.; Boturyn, D. *Angew. Chem. Int. Ed. Engl.* **2009**, *48*, 2576.
- (230) Butler, J. D.; Coffman, K. C.; Ziebart, K. T.; Toney, M. D.; Kurth, M. J. *Chem. Eur. J.* **2010**, *16*, 9002.
- (231) Werz, O. K., A.; Troschuetz, R.; Karg, E. M.; In *PCT Int. Appl.* 2009; Vol. WO2009146696 A120091210.
- (232) Praneenararat, T.; Beary, T. M. J.; Breitbach, A. S.; Blackwell, H. E. *Bioorg. Med. Chem. Lett.* **2011**, *21*, 5054.
- (233) Hoegl, A.; Darabi, H.; Tran, E.; Awuah, E.; Kerdo, E. S. C.; Habib, E.; Saliba, K. J.; Auclair, K. *Bioorg. Med. Chem. Lett.* **2014**, *24*, 3274.
- (234) Bycroft, B. W. P., D. W.; Chhabra, S. R.; Hooi, D. In *PCT Int. Appl.* 2001; Vol. WO 2001074801 A1 20011011.
- (235) Li, G.; Liu, Y.; Yu, X.; Li, X. *Bioconjugate Chem.* **2014**, *25*, 1172.
- (236) Guo, Z.-F.; Sun, Y.; Zheng, S.; Guo, Z. *Biochemistry* **2009**, *48*, 1712.
- (237) Goldmann, A. S.; Schödel, C.; Walther, A.; Yuan, J.; Loos, K.; Müller, A. H. E. *Macromol. Rapid Commun.* **2010**, *31*, 1608.
- (238) Pirrung, M. C.; Biswas, G.; Ibarra-Rivera, T. R. *Org. Lett.* **2010**, *12*, 2402.
- (239) Lu, X.; Sun, J.; Zhu, J. *Heteroat. Chem.* **1992**, *3*, 551.
- (240) Zhang, B.; Zou, W.; Zhang, J. *Res. Chem. Intermed.* **2013**, *1*.

13 Appendix

X-ray diffraction

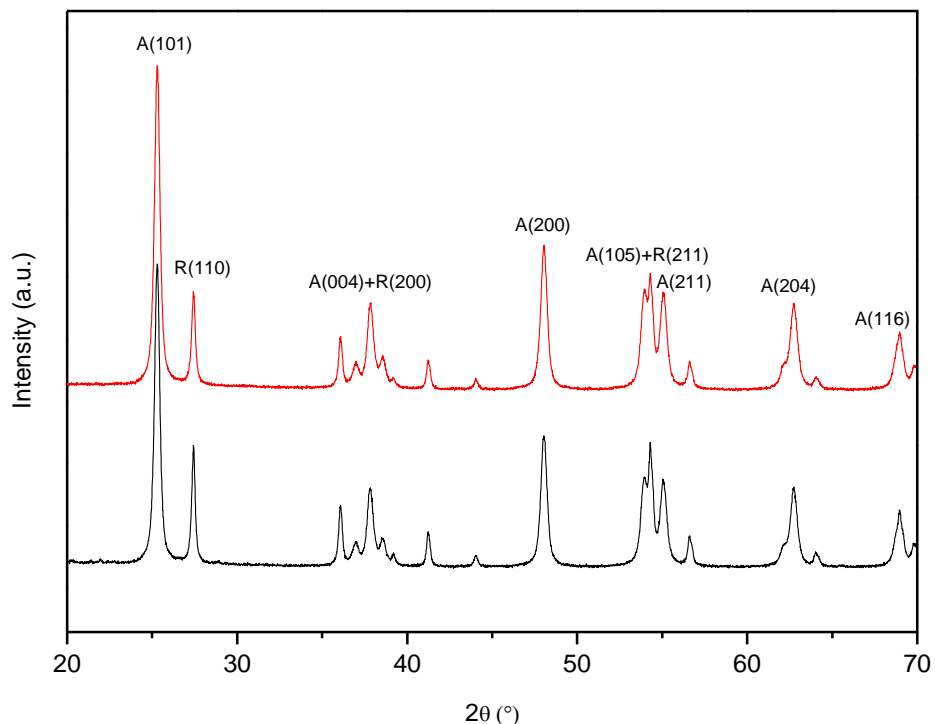


Figure 74: Wide-angle XRD of the pure TiO_2 (black curve) and the functionalised particles (red curve). Miller indices are labelled A (anatase) and R (rutile).

The main peaks of pure TiO_2 can be collated to the anatase and rutile phases (Figure 74). There is no difference between the XRD pattern of the pure nanoparticles (black curve) and the modified ones (red curve). As expected the modification does not have an effect on the crystallisation and phase characteristics of TiO_2 . This outcome correlates with experiments done by other research groups.²⁴⁰